Runners as Biomechanical Systems: New Approaches with the Spring-Mass Model

by

Geoffrey T. Burns

A dissertation submitted in partial fulfillment
of the requirements for the degree of
Doctor of Philosophy
(Kinesiology)
in the University of Michigan
2020

Doctoral Committee:

Professor Ronald F. Zernicke, Chair
Professor Richard Gonzalez
Associate Professor Riann Palmieri-Smith
Adjunct Research Assistant Professor Jessica M. Deneweth Zendler

Geoffrey T. Burns

gtburns@umich.edu

ORCID iD: 0000-0001-5225-588X

Dedication

This work is dedicated to my parents, Bryan and Kristy. They cultivated in me an abundant quantity of the ingredient that was essential to seeing this through:

a passion for the subject matter.

Acknowledgements

This body of work is a body of teamwork. It is a product of a substantial network of individuals – friends, mentors, and collaborators. For their guidance, feedback, and inspiration, both direct and indirect, I am profoundly grateful.

I'd like to thank principally my research advisor, committee chair, and mentor, Dr. Ron Zernicke. Working and researching with you has been an absolute joy. You trusted me to pursue new ideas, provided thoughtful and constructive critiques, gave kindly subtle redirection when necessary, and always empowered me to explore my passions. You modeled what great leadership looks like, and I hope this work is just the first volume in a long series of co-opted scientific endeavors. I'd also like to thank Dr. Rich Gonzalez. Your direction and intuition guided me to explore the methods presented here. More importantly, your disposition, outlook, and shared analytical enthusiasm left me feeling excited and invigorated after every one of our conversations. Similarly, I hope this is just the beginning of many fun collaborations.

To Dr. Jess Zendler, you brought me into this process and helped get me off the ground. You provided both friendship and mentorship and helped me make invaluable connections with other researchers. Without your trust, insight, feedback, and support, we could have never started these projects. Finally, I'd also like to thank Dr. Riann Palmieri-Smith. Your support and willingness through this entire process, from qualifying exams, proposals, and ultimately, the defense of this work, has been exceedingly appreciated. Your clinical expertise balanced its direction, and your flexibility and kindness made it happen. Thank you, all.

This work could not have happened without collaboration from a fantastic group of researchers at the Sport Science Institute of South Africa at the University of Cape Town. To Dr. Nicolas Tam, I cannot thank you enough for your willingness to teach and share. You've served not only as a great mentor, but also a great friend. Many thanks to Dr. Jordan Santos-Concejero and Dr. Ross Tucker, as your willingness to collaborate created a fantastic opportunity for our investigation. And finally, a big thank you to Dr. Rob Lamberts. You not only took me in to share your facilities and your science, but you also kept me warm and well-fed in the Cape Town winter.

I'd also like to thank Dr. Richard Hughes. You've served as an early mentor during my Master's studies and helped me fall in love with academic pursuits. You brought me back to the University of Michigan after graduation to begin working in biomechanics, and your service on my qualifying exam committee taught me, among other things, how to talk about optimality. Thank you for inspiring me and challenging me to grow as a scientist.

These studies would have been impossible without all the help from members of the Michigan Performance Research Laboratory, past and present. To Dr. Ken Kozloff, Dr. Adam Lepley, Dr. Cristine Agresta, Mason Ferlic, Jillian Peacock, and Lisa Rabaut – thank you for all the work you've done to facilitate and help me move through my research efforts. Thank you to all the students who have come through the lab as well – Kevin, Tyler, Seraphina, Cassie – your help with testing sessions was invaluable. I'd also like to thank Dr. Grant Goulet, as you were the original catalyst who brought me into the lab and set my studies in motion.

I'm also enormously indebted to Ron Warhurst. You brought me into a new world of the sport that I love so dearly, and you taught me so much about it. You contributed to my deeper understanding of what makes runners tick, and your magnetism directly facilitated large sections of this work. My development as a running scientist was profoundly broadened by the lessons you imparted as the artist-in-chief.

Finally, I could not have finished this without the love from my three sisters, Kaitlyn, Maire, and Rachel. You guys powered me through all of this. Kaitlyn, I cherished your frequent calls and unconditional support. You kept me grounded and sane these past few years, and you nursed my happiness when necessary. For that, I am thankful.

Preface

Long learning alone
can build stamina and strength.
By instruction only
can limbs learn to live their movement
without thinking.

-W.H. Auden, from *Runner* (*Runner*, 1962)

Table of Contents

List of Tables

List of Figures

Abstract

Running is fundamentally a simple activity, but the physical realization of it is complex. The gait patterns of a runner are the product of ever-changing systems and interactions of biomechanical components, and as such, the study of these mechanical characteristics is challenging. Traditional methods have focused on discrete components of gait and thus struggle to contextualize observations. Systemic analyses have been limited to simple descriptive models, often with exclusive or restrictive assumptions. This dissertation sought to develop novel methods for the systemic analyses using an established canonical model of the running gait – the spring-mass model – as a template. It further sought to conduct a series of biomechanical studies using this template-based approach as a framework to interpret the observations. Specifically, a method is first presented to estimate the system-level spring-mass characteristics of a runner using nonlinear regression with only the vertical ground reaction force time series of the runner. To facilitate this method, a novel parameterized form of the sinusoidal vGRF approximation was derived and validated. This NLR-based analyses yielded leg stiffness estimates that were consistent with traditional methods and further suggested that additional systemic parameters do not behave as traditional methods assume. Next, two investigations are presented that explore this method along with new methods for spring-mass dynamics comparisons and with established methods for spring-mass parameter analysis. These investigations included a cohort comparison of elite Kenyan distance runners against a cohort of non-elite recreational runners and a paired comparison of subjects before and after an ultramarathon. It was shown that the Kenyan runners

behaved more like the simple elastic system than the recreational runners and that the ultra-marathon runners demonstrated consistent systemic patterns but greater overall template dissimilarity following the race. Finally, traditional methods of spring-mass analyses were applied with a more comprehensive mixed-model experimental design to fully characterize the system-level behavior of elite middle distance runners across a spectrum of speeds. The mixed-model template-based analysis revealed that the elite runners ran as stiffer systems than their sub-elite counterparts and that their mechanical behavior was more persistent across speeds. Together, this series of investigations established and validated new methods and improved upon the implementation of existing methods with which to assess running gait holistically and analyze it as a system. It is hoped that this work will provide useful tools, new frameworks, and fresh inspiration for scientists, coaches, and athletes to assess and interpret the movements of runners.

Chapter 1 Background, Motivation, and Aims

Running is simple. Forward motion, a flight phase, and a single-support stance phase are the essential ingredients. Yet, within these limited dynamic requirements, enormous complexity emerges. Those ingredients, limited as they may be, are a constantly inconstant orchestration of mechanical interactions, metabolic processes, psychological mediations, and perhaps even unquantifiable ephemera. The symphony is played out across the animal kingdom in various forms, from the bipedalism of humans to the polypedalism of insects, and broadly, it is an efficient means for a body to cover ground quickly. This body of work will investigate that mechanism, and it will seek to add new knowledge to our collective understanding of those three ingredients.

1.1 Thesis Structure

The following pages contain four primary investigations. The first is a development of a new method, the second and third are applications of that method, with the second containing another new analytical metric. These two investigations are coupled with traditional analytical methods for context, comparison, and more complete phenomenological exploration. The final investigation leverages a distinct experimental and analytical design with traditional quantifications. Each of the four corresponding chapters are presented and written so to be standalone documents, with their respective backgrounds, contexts, and discussions presented and assuming as much. As such, this introductory chapter serves to present background for the topic and identify gaps, but does not contain an exhaustive literature review for each study, as the relevant work will be explored and reviewed in greater detail in each chapter. The final chapter includes a summary and discussion of the collective findings with thoughts and aspirations for extensions of the work.

1.2 Introduction

Apart from being a common form of terrestrial locomotion, running is an enormously popular form of sport and exercise in humans. In the United States alone, over 50 million people participate each year (Outdoor Foundation, 2018). Across this population of runners, there is a vast range of involvement and motivation, spanning from competitive aspirations to recreational participation, but at all levels, the individual and societal health benefits of participation in the sport are tremendous (Hespanhol Junior et al., 2015; Lavie et al., 2015; Lee et al., 2017; Oja et al., 2015; Williams, 2012). Motivations shared among many runners are the desire to maintain and improve health, build speed and endurance, and relieve stress (Running USA, 2017).

Testing and improving one's own performance capacity is a common motivator for runners, with 62% of runners citing the preparation for a race as a primary cause for their running (Running USA, 2017). Indeed, marathon and road racing participation has risen exponentially over the past five decades, with the number of worldwide marathon finishers increasing from 400,000 in 2000 to over 1.6 million in 2013 (Scheerder & Breedveld, 2015). Through the parkrun program alone, over 200,000 individuals participate in 5Ks each weekend worldwide, both competitively and recreationally (Ingle, 2018). The drive to continually better oneself has mass appeal, and this coupled with the health benefits of continual participation makes running a uniquely beneficial habit.

Despite these themes of self-improvement and health driving the mass participation, running carries a high risk of musculoskeletal injury; estimations of runners afflicted by lower limb injuries range from 19% to 81% (van Gent et al., 2007). The most common reason that novice runners discontinue the activity is the development of a running-related injury (Fokkema et al., 2019). The most prevalent running-related injuries include patellofemoral pain syndrome, Achilles tendinopathy, medial tibial stress syndrome, plantar fasciitis, and iliotibial band syndrome (Francis et al., 2019; Lopes et al., 2012). Generally, running injuries occur primarily due to musculoskeletal overload, with the dosage of the running, the individual's static structure, and his or her movement patterns interacting (Davis & Futrell, 2016; Hreljac, 2004). However, the etiologies of these running-related injuries are unclear, and the only determinant that consistently predicts injury in runners has been incidence of previous injury (van der Worp et al., 2015; van Gent et al., 2007).

1.3 Running Gait Characteristics

Many people run, and many enjoy doing it. Moreover, people typically want to get better at running, and people typically do not want to get hurt while running. There are myriad broad means and fields of study devoted to addressing each of these common-yet-complex drives, and one that receives consistently considerable attention is that of the mechanical patterns of the runner. Assessment of a runner's gait has long been a source of interest for clinicians, researchers, coaches, and athletes in attempts to intervene to augment performance and avoid running-related injury (Amar, 1916; Cavanagh et al., 1985; Ferber, Hreljac, & Kendall, 2009; Heiderscheit, 2011; Malisoux et al., 2017; Saragiotto, Yamato, & Lopes, 2014). A running gait is—by definition—simple. As described above: forward locomotion with a single-legged stance phase and a flight phase. The realization of this gait by the human body, however, is complex. It is indeed a "complex dynamical system" of hundreds of variables, with the various muscles, tendons, and joints of the body all contributing and interacting with each other to produce the running gait (Alexander, 1995; Hamill et al., 1999). This complexity has challenged the biomechanics field, and there is no consensus definition on what constitutes “healthy” or “optimal” gait (Davis & Futrell, 2016; Heiderscheit, 2011; Moore, 2016).

1.3.1 Gait Characteristics Related to Injury

Given this complexity, there is limited evidence connecting individual gait components with injury (Ferber et al., 2009; Heiderscheit, 2011; Mousavi et al., 2019; van der Worp et al., 2015). Several biomechanical variables have been identified to be associated with injury: vertical loading rate (Davis, Bowser, & Mullineaux, 2016; Milner et al., 2006; Zadpoor & Nikooyan, 2011), foot-strike index (Daoud et al., 2012), and peak knee internal rotation (Mousavi et al., 2019). However, apart from one investigation implicating vertical loading rate as being predictive of injury (Davis et al., 2016), these associations have not been found to be causative. Prospective studies have failed to identify any other biomechanical determinants that predict injury (Saragiotto, Yamato, Hespanhol Junior, et al., 2014; van der Worp et al., 2015), and systematic reviews have failed to find any consistent biomechanical factors that explain injury apart from experience of a previous injury (Hulme et al., 2017; van der Worp, Vrielink, & Bredeweg, 2016; van der Worp et al., 2015; van Gent et al., 2007).

There has been a recent movement to develop strategies to “improve” or “retrain” gait in runners who have suffered injury (Davis & Futrell, 2016; Heiderscheit, 2011). Many kinetic and kinematic variables can be altered with retraining interventions, but the long-term effects of these changes on reducing musculoskeletal injury are unclear (Napier et al., 2015). Strategies targeted at reducing vertical loading rates have been successful (Crowell & Davis, 2011; Napier et al., 2019; Willy et al., 2016), and studies targeting knee and hip kinematics have been found to reduce symptoms in runners with patellofemoral pain syndrome (Dos Santos et al., 2019; Noehren, Scholz, & Davis, 2011; Roper et al., 2016; Willy, Scholz, & Davis, 2012). However, whether or not these gait patterns demonstrate long-term persistence or are protective from future injury remains unclear (Davis & Futrell, 2016). Moreover, many of these strategies target alterations in stride rate or stride frequency to achieve their kinematic outcomes, which carries a higher energetic cost to the runner (Cavanagh & Kram, 1989). Given the tendency of runners to “self-optimize” their movement patterns to those which are most economical or comfortable (Nigg et al., 2015; Williams & Cavanagh, 1987), these targeted, single-variable modifications may have consequences across several more elements of gait. The effects of these systemic responses on long-term injury status or performance are still unclear.

1.3.2 Gait Characteristics Related to Performance

Similarly, biomechanical factors linked to performance capacity have been limited (Moore, 2016; Williams & Cavanagh, 1987). The factors that have been associated with running performance and economy include vertical oscillation (Cavanagh, Pollock, & Landa, 1977; Williams, Cavanagh, & Ziff, 1987), contact time (Santos-Concejero et al., 2017), leg stiffness (Dalleau et al., 1998), center-of-pressure trajectory (Lazzer et al., 2014), and leg-axis alignment with the vertical ground reaction force (Moore, Jones, & Dixon, 2016). However, these associations have not been found to be universal or causal (Lacour & Bourdin, 2015; Lussiana et al., 2019; Moore, 2016; Nummela, Keranen, & Mikkelsson, 2007; Williams & Cavanagh, 1986), and other comprehensive kinematic and kinetic studies have failed to isolate any biomechanical determinants of performance (Williams & Cavanagh, 1987).

The challenge in identifying variables related to running economy or performance is likely due to the tendency of runners to “self-optimize” their kinetic and kinematic patterns to suit their individual anatomies and physiologies (Cavanagh et al., 1977; Williams & Cavanagh, 1986). Moore and colleagues found that beginning runners spontaneously altered their individual kinematics throughout a ten-week introduction-to-running program, resulting in improved running economy (Moore, Jones, & Dixon, 2012). After examining several dozen biomechanical parameters in runners across a spectrum of performance abilities and assessing their relation with running economy, Williams and Cavanagh concluded that no one factor was of critical importance, and that positive characteristics are likely not related to any specific set of variables but rather "the overall combined effect of a large number of variables" (Williams & Cavanagh, 1987).

The traditional focus on variables in isolation does not capture the "complex dynamical system" of mechanical and physiological interactions that ultimately produce the running gait. This complexity has prevented the biomechanics field from establishing a consensus definition of what is "good" or "healthy" gait, and has further challenged communication between laboratory investigations and clinical settings (Novacheck, 1998). Without a template against which to interpret gait, researchers and clinicians are without a target towards which to direct improvements or compare impacts of interventions.

1.4 Running Gait Templates

A strategy to tackle this challenge of the "complex, high-dimensional, non-linear, dynamically coupled interactions" in gait is to reduce the dimensionality of the system (i.e., the runner) and study the features fundamental to producing the outcome (Full & Koditschek, 1999). Alexander similarly proposed that using simple models to study gait would make it "easier to discover which of its [the model's] features are essential to the observed effect" (Alexander, 1995). By studying gait from a template perspective, the redundancies of the myriad biomechanical degrees-of-freedom, from the dozens of force vectors, the hundreds of joint angles and moments, and the millions of muscle cell contractions, are collapsed into a coordinated system. One is then able to study those essential features of the task and their interactions, and any deviations from the template are brought into relief for further investigation.

Many templates with varying degrees of complexity have been proposed to model the bouncing gait of running. Fenn was first to note the elastic nature of running mechanics (Fenn, 1930a, 1930b), which was later likened to a bouncing ball (Bencsik & Zelei, 2017; Cavagna, Saibene, & Margaria, 1964). Cavagna and colleagues also described the center-of-mass dynamics as those of a pendulum (Cavagna et al., 1964), and later concluded that the two mechanisms that running bodies use to minimize energy expenditure are that of pendular motion and an elastic bounce (Cavagna, Heglund, & Taylor, 1977). These two models were later combined into a single model referred to as the spring-loaded inverted pendulum (SLIP) (Blickhan, 1989; McMahon & Cheng, 1990). This two-dimensional model treats the body as a single point mass on a linearly elastic spring, and it compresses and decompresses in an inverted pendular motion during stance (Figure 1). This model was the first to capture holistically the coordinated fluctuations of gravitational and kinetic energy in running. Its center-of-mass (COM) trajectory and ground reaction force patterns are similar to those of running humans (Blickhan, 1989; Farley & Gonzalez, 1996; McMahon & Cheng, 1990; Seyfarth et al., 2002) and other running animals (Birn-Jeffery et al., 2014; Farley, Glasheen, & McMahon, 1993; Robilliard & Wilson, 2005). This SLIP template is commonly referred to as the spring-mass model of running.

This simple, passive, single-body model has been extended in many forms. Multi-body models have decoupled the lower limb masses to capture the impact peak in the ground reaction force of heel-strike running (Kim, Voloshin, & Johnson, 1994), and more elaborate multi-body spring-mass-damper models have been used to further segment energetic fluctuations of the limbs and capture surface and shoe interactions (Liu & Nigg, 2000; Nikooyan & Zadpoor, 2011).

Actuated spring-mass models have been given an energy source at each step to address the passive nature of the SLIP template (Seipel & Holmes, 2007). Lateral leg-springs have been added to extend it into three-dimensions (Seipel & Holmes, 2005), and a recent extension of the model has assigned nonlinear elastic behavior to the spring characteristics to fit more accurately ground reaction force recordings across a wide spectrum of speeds (Clark, Ryan, & Weyand, 2017).

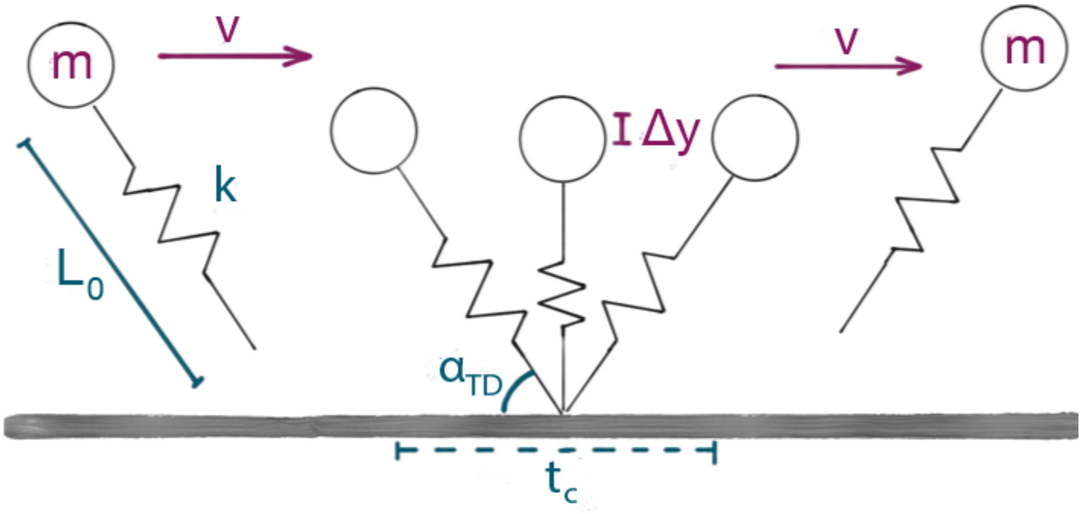

Figure 1: The Spring-Loaded Inverted Pendulum

1.5 The Spring-Loaded Inverted Pendulum as a Template

A template is "a formal reductive model that encodes parsimoniously the motion of the body with respect to the minimum number of variables and parameters" (Full & Koditschek, 1999). Thus, for the purpose of analyzing and assessing system-level behavior of running gait, the SLIP template is a natural choice. The fundamental motions that define running are those of a forward velocity with a flight phase and an elastic stance phase (Novacheck, 1998). The SLIP model describes a mass' trajectory in this fashion with the fewest possible variables and is thus the most reduced system that still captures the fundamental features of the task. Incidentally, when running systems with many more components and degrees of freedom are optimized to minimize work, they spontaneously adopt an elastic, pendular gait with COM trajectories and GRF profiles that resemble that of a SLIP system (Schultz & Mombaur, 2010; Srinivasan & Ruina, 2006).

1.5.1 SLIP Model Characteristics

The SLIP model treats the body as a two-dimensional single point mass on a massless linear elastic spring (Figure 1). For a given mass (m) and a given velocity (v) the dynamics of the system are fully described by only four parameters (Table 1) (Blickhan, 1989; Ludwig et al., 2012). During the flight phase, it follows a projectile motion subject only to gravity (g), with the x-y COM motion being described by Equations 1 and 2. During stance, the model touches down and remains fixed at x_0, and its COM motion is described by Equations 3 and 4, with Equation 5 denoting the length L of the leg spring throughout stance.

1 $$\frac{d^2x}{dt^2} = 0$$

2 $$\frac{d^2y}{dt^2} = -g$$

3 $$\frac{d^2x}{dt^2} = \frac{k}{m}(L_0 - L)\left(\frac{x-x_0}{L}\right)$$

4 $$\frac{d^2y}{dt^2} = \frac{k}{m}(L_0 - L)\left(\frac{y}{L}\right) - g$$

5 $$L = \sqrt{y^2 - (x - x_0)^2}$$

Parameter	Description
k	Leg Stiffness
α_{TD}	Touchdown Angle
L_0	Leg Length
t_c	Contact Time

Table 1 Spring-Loaded Inverted Pendulum parameters for a given mass and velocity

This results in a coordinated transfer of energy throughout the gait cycle. The horizontal GRF has an equal and opposite braking and propulsive impulse, with the cross-over of the force occurring at midstance. The vertical GRF is symmetric, with the peak also occurring at midstance (Figure 3). The vertical COM displacement inversely follows the vertical GRF and reaches its minimum at midstance. As such, the system is energy-conservative, and the changes in vertical and horizontal kinetic energy and elastic and gravitational potential energy occur in phase (Figure 2).

Though the model's dynamics are simple in description, computation and simulation are complex. The equations of motion are non-integrable through the entirety of the gait cycle, so a closed form analytic solution to fully describe the motion does not exist. Optimization and simulation techniques are commonly used to generate numeric solutions and to find stable parameter combinations that simulate SLIP running (Birn-Jeffery et al., 2014; Blickhan, 1989; Carver, Cowan, & Guckenheimer, 2009; Ludwig et al., 2012; Seyfarth et al., 2002). To more easily apply the model, approximations have been made to simplify the computation, including modeling the vertical GRF as a sinusoid (Blum, Lipfert, & Seyfarth, 2009; Morin et al., 2005; Robilliard & Wilson, 2005), assuming a small angle-sweep (Geyer, Seyfarth, & Blickhan, 2005), and isolating analysis at midstance (Farley et al., 1993; Ferris, Louie, & Farley, 1998).

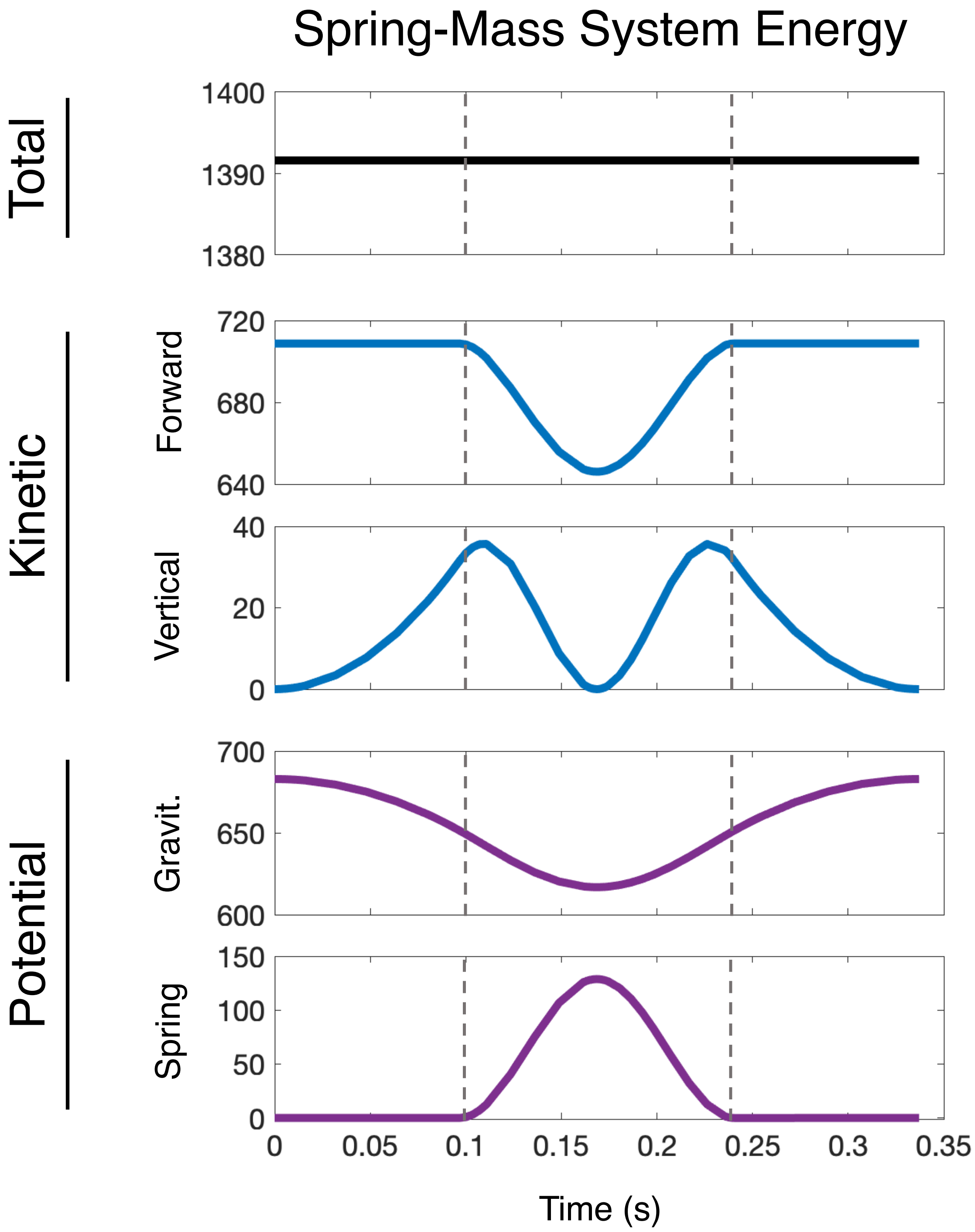

Figure 2 Energetic fluctuations of a SLIP spring-mass system through one step cycle. The dashed lines indicate landing and takeoff, and the units are Joules. The model is a 70 kg system with a 1.0 m leg moving at 4.5 m/s.

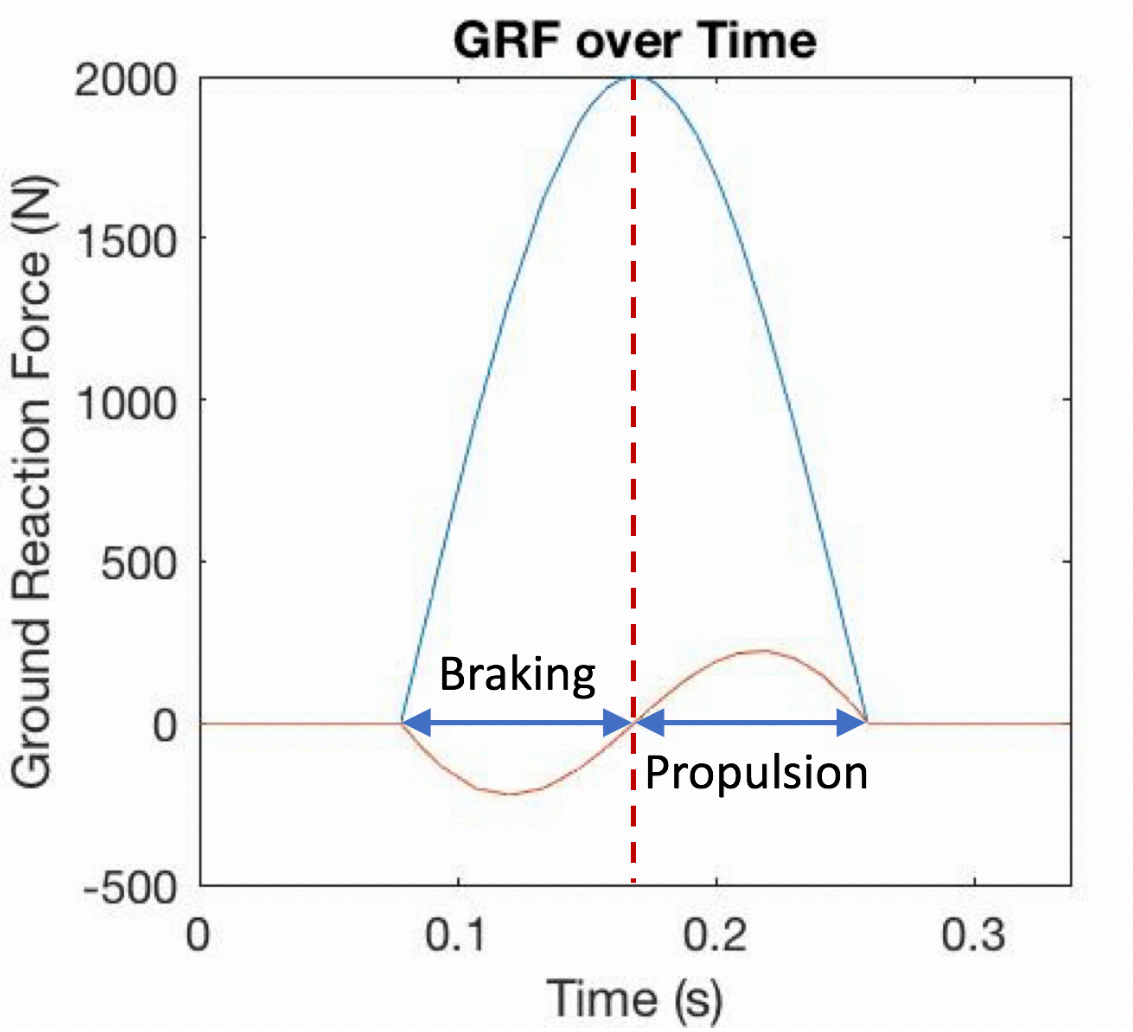

Figure 3 Vertical GRF (blue) and horizontal GRF (tan) for a SLIP step. The dashed line indicates midstance.

1.5.2 Limitations to the SLIP Template

Though the template faithfully captures the essential features of the running gait, it is imperfect. It makes several key assumptions that deviate from biological reality. The first is in assuming that the body behaves as a perfectly linear spring. The human body in motion is certainly multi-segmented, and models that include both multiple bodies and nonlinear elastic components have been shown to more faithfully recreate experimentally observed GRF and COM trajectories (Clark et al., 2017; Nikooyan & Zadpoor, 2011). The second is that the system behaves passively, which is to say that energy is perfectly conserved through the gait cycle. Energy loss during the gait cycle can occur for a multitude of musculoskeletal reasons. For example, there is a mismatch in the energy cost of braking and propulsive forces (Chang & Kram, 1999), resulting in the SLIP model overestimating a runner's horizontal impulse (Bullimore & Burn, 2007). Consequently, actuated models have been shown to re-create COM trajectories more accurately (Maus et al., 2015; Seipel & Holmes, 2007). Third, due to this passive energetic nature, the model demands symmetry in the stance phase, rendering it appropriate for steady-state running but not for cases of acceleration or unlevel terrain (Morin & Samozino, 2018). Fourth, the model is two-dimensional, representing the body exclusively in the sagittal plane. Again, models adding a mediolateral dimension to the spring exhibit greater stability (Seipel & Holmes, 2005). Finally, the model assumes a constant, invariant center-of-pressure (COP) at contact, whereas the human body's COP is forward-moving during stance (Bullimore & Burn, 2006). Despite these limitations, the model still robustly captures the kinetics of the COM and its energy fluctuations in steady, level running. With its comparative simplicity in relation to augmented models and templates, it has persisted as a valuable tool to study the overall elastic behavior of a runner.

1.6 The SLIP Template in Running Gait Analysis

The SLIP template has been widely studied and applied in gait research. It has been used to study the elastic mechanisms of running across speeds (McMahon & Cheng, 1990), stride frequencies (Farley & Gonzalez, 1996), and terrains (Ferris et al., 1998), as well as in relation to economy (Dalleau et al., 1998), fatigue (Morin, Samozino, & Millet, 2011; Morin, Tomazin, et al., 2011), and performance (Dutto & Smith, 2002). Its application has come in two chief forms: description and prediction (Bullimore & Burn, 2007).

1.6.1 The SLIP Template as a Descriptive Tool

It is most widely used as a descriptive tool to calculate the “stiffness” of the runner. There are several approaches to this calculation, and they are derived from the theoretical relation of the model’s spring stiffness to its change in spring length under maximal vertical force at midstance. The two most common methods used in gait research to calculate stiffness come from McMahon and Cheng (McMahon & Cheng, 1990) and Morin et al. (Morin et al., 2005). Both of these methods differentiate vertical stiffness (k_{vert}) and leg stiffness (k_{leg}) of the runner to characterize behavior of vertical displacement and leg length changes during the gait cycle under maximal force. As a dynamic SLIP model functions with a single linear elastic spring, the description here will be restricted to that of leg stiffness calculations. McMahon and Cheng described k_{leg} of a SLIP model as the ratio of maximal vertical force, F_{max}, and maximal spring-leg displacement, ΔL:

$$k_{leg} = \frac{F_{max}}{\Delta L} \tag{6}$$

$$\Delta L = \Delta y + L_0(1 - \sin \alpha_{TD}) \tag{7}$$

$$\alpha_{TD} = \cos^{-1} \frac{v\, t_c}{2L_0} \tag{8}$$

This method relies on recording a step with a force plate to measure F_{max} and t_c (McMahon & Cheng, 1990). The vertical force recording is also used to calculate Δy, the COM displacement, via double-integration of the vertical force (Cavagna et al., 1977). It also relies on measurement of L_0 from the runner, often taken as the distance from the greater trochanter to the floor while standing (Brughelli & Cronin, 2008; McMahon & Cheng, 1990) or as a ratio of 0.53 to the standing height of the runner (Morin et al., 2005). It estimates α_{TD} per Equation 8. McMahon and Cheng compared dynamic measures, such as stride length, duty factor, and contact time, across running speeds from a SLIP-simulation and from experimental observations of a runner. They concluded there was generally good agreement, though no systematic validation was conducted (McMahon & Cheng, 1990).

The method proposed by Morin and his colleagues does not rely on a force plate for measurement but rather approximates the vertical GRF as a sinusoid using the ratio of t_c and the flight time, t_f, to estimate F_{max} and Δy. This method requires measurement of the contact time, flight time, running speed, and resting leg length. They compared the vertical impulse, the area under the vertical GRF time curve, of their sinusoid-approximated SLIP model to that of the observed vertical impulse and found a bias of 5.33% and 2.93% in treadmill and overground running, respectively (Morin et al., 2005). Other methods have been used to estimate leg stiffness (e.g., (Arampatzis, Brüggemann, & Metzler, 1999; Cavagna et al., 1988; McMahon, Valiant, & Frederick, 1987)), but they are less commonly applied.

1.6.2 The SLIP Template as a Predictive Tool

The SLIP template has also been applied as a predictive tool for certain biomechanical parameters of gait. Stance time, aerial time, duty factor, vertical COM displacement, horizontal COM excursion during stance, vertical impulse, and horizontal impulse are all common measures that can be estimated with observed GRF recordings informing SLIP model simulations (Bullimore & Burn, 2007). Bullimore and Burn simulated SLIP running with experimentally observed GRF recordings by calculating k_{leg} from Equations 6-8 and assigning it to the model constrained to behave like a stable SLIP system (i.e., symmetric energy fluctuations). They compared ten common gait measures predicted by the simulated SLIP system with the observed values in the runners. There was generally good agreement between modeled and observed gait, with modest overestimation (%) in duty factor (6.8%), stride length (3.6%), peak vertical GRF (3.8%), t_c (2.5%), horizontal excursion during stance (5.1%), and vertical impulse (5.8%).

However, larger errors were observed in flight time (17.7%), vertical COM displacement (22.9%), horizontal impulse (43.6%), and peak mechanical energy change during stance (26.2%) (Bullimore & Burn, 2007). Rather than using single parameter comparisons, Seyfarth and colleagues evaluated the quality of SLIP model parameter combinations by assessing the number of “steps” the simulated model would take before becoming unstable (Seyfarth et al., 2002). Using this method, Blum and coworkers evaluated several methods of estimating k_{leg} across speeds of 2 – 4 m/s, using measured values of L_0, α_{TD}, and v (Blum et al., 2009). The k_{leg}-α_{TD} combinations were mapped across those of a stable SLIP system (determined as one that could take more than four consecutive steps without becoming unstable) to qualitatively compare the experimental observations. The sinusoid approximation of SLIP parameters and a duty-factor approximation of the parameters were concluded to yield generally stable gait cycles, but the effect of speed was not evaluated (Blum et al., 2009).

1.6.3 Model-Experiment Comparisons

Direct model-experiment comparison of full COM trajectories and GRF time curves has been limited. Performing this analysis from purely kinetic recordings is challenging given the aforementioned computational complexity of the model. One means that has been employed is that of assessing the force-length curve of the modeled leg spring. Günther and Blickhan demonstrated a means to do this by fitting slopes to the force-length curve during both compression and decompression (Gunther & Blickhan, 2002). The challenge of this method lies in the hysteresis in the compression and decompression, where significant deviations from linearity in early and late stance bias the fit. They attempted to resolve this by fitting a linear function with a state-shift for the compression and decompression periods, through this still underestimated leg compression. They also attempted to address the shift by fitting the force-length relation with a nonlinear term on the leg-length change, but this was similarly subjected to significant deviations driven by the distal accelerations. Importantly, this method also relied on kinematic inputs from motion capture equipment, which itself has anthropometric assumptions of the center-of-mass for marker location (taken as the hip here) and leg length compression. It is also subject to initial condition assumptions for the computation and force-length fitting. The estimates of leg stiffness from the method were thus sensitive to initial conditions of the leg coordinates as well as those of each of the velocity components (Gunther & Blickhan, 2002).

Lipfert and colleagues compared leg-force-length curves calculated directly from the GRF time curve to those of a SLIP model with estimated k_{leg} values and measured L_0 and α_{TD} values (Lipfert et al., 2012). They calculated the coefficient of determination between the model-based and experimental curves and found good agreement that was independent of running speed ($R^2 = 0.94\text{-}0.99$). However, this value was modified by the difference between simulated and experimentally observed t_c values, and the simulations were unable to produce stable gait cycles with the estimated k_{leg} and measured α_{TD} values, so α_{TD} was adjusted in the simulations to generate stable solutions (Lipfert et al., 2012). Ludwig et al. compared SLIP simulations to a single runner across several steps to evaluate the ability of a passive or actuated SLIP model to match human running gait (Ludwig et al., 2012). They estimated k_{leg}, α_{TD}, and L_0 as those which characterized a stable SLIP system that matched the observed maximal COM height, minimal COM height, and t_c. The SLIP systems and experimental observations were compared across many gait parameters, with F_{max} being slightly underestimated in the SLIP system (2.36 BW vs. 2.53 BW) and the step length being slightly overestimated (1.043m vs. 1.037m) for the first step (Ludwig et al., 2012).

1.6.4 SLIP Similarity

Similar to the challenges described above in the estimation of parameters from model experiment tracking, simply comparing the degree to which a runner behaves like a SLIP system is difficult. One way to quantify this is via the hysteresis of the compression and decompression of the leg described above. This requires kinematic recording of the assumed leg (e.g. from the hip), and it is therefore sensitive to the spatial and dynamic initial conditions assumed (Gunther & Blickhan, 2002). For simplicity, investigators sometimes choose to present force-displacement curves from the vertical component alone—i.e. the vertical compression of the leg spring. This is problematic for two reasons. The first is that the compression of the SLIP spring does not happen purely in the vertical plane—its assumption of linear elasticity occurs in dynamic, pendular motion (Blickhan, 1989). As such, modeling vertical compression as a Hookean spring is incorrect and will consequently demonstrate nonlinearity. Second, this approach is heavily biased by deviations in the early and late phases of stance where the magnitudes of center-of-mass vertical displacement are greater for relatively low magnitudes of force. A common deviation in this period is the impact peak, where its contribution results in distinct compression and decompression force-displacement curves. Dutto et al. observed several centimeters of variation between initial and final positional estimates from this (Dutto & Smith, 2002), and Hunter demonstrated that fitting a separate stiffness term for the impact peak would partially reconcile the poor fit (Hunter, 2003). Cavagna and Legramandi attempted to reconcile this by calculating the hysteresis during the period that the runner exceeded body weight, termed the “effective contact time” of stance (Cavagna & Legramandi, 2015). While this resolves the distinct nonlinearity often observed in early and late stance, and thus is less subject to bias from deviations in those periods (though not free from it), it still assumes vertical linear elasticity. When this hysteresis is assessed as a ratio or percentage of the integrated compression and decompression force-displacement periods, it does hold true that the spring-mass system will maintain a unity value of 1.0 given its conservative nature. However, because the vertical compression is not strictly linearly elastic, deviations at different points along the curve will bias the estimate non-uniformly.

Another method to calculate the degree to which a runner behaves like a spring-mass system is derived from the takeoff-landing asymmetry observations of Cavagna (Cavagna, 2006). He examined the energetic fluctuations of runners' center-of-masses through the gait cycle via force plate recordings and calculated the timing characteristics. Two quantities he noted were the braking and pushing durations, which correspond to the periods of decelerating and accelerating the center-of-mass, and the ratio of the maximal downward velocity and maximal upward velocity. In a perfectly elastic, energy-conserving system, such as the SLIP system, these two quantities should be equal (Figure 2). He and Legramandi formalized this as a metric they termed the "similarity to a symmetric bounce", where they calculated the average of the two quantities (Cavagna & Legramandi, 2015). They previously demonstrated that these two quantities peaked in teenage runners and slowly declined with age (Legramandi, Schepens, & Cavagna, 2013).

1.6.5 Challenges and Opportunities in SLIP Template Analyses

Though the SLIP template has been used for decades to describe the elastic nature of gait, there are many limitations and shortcomings in the conventional approaches to its application. The first of these is in the measurement of model parameters. With a known velocity, the dynamics of the SLIP model are determined by only four parameters (Table 1), yet in all forms of gait analysis, some of these parameters are necessarily assumed or assigned values from empirical observation. That is, the SLIP model is constrained to that specific parameter. The most common of these is the leg length, L_0, of the system. In the SLIP model, this is the distance from the center-of-mass to the point of contact on the ground. However, the parameter is nearly always assigned the value of the standing leg length (e.g., greater trochanter to the ground) (Brughelli & Cronin, 2008; Bullimore & Burn, 2007; McMahon & Cheng, 1990) or as a COM anthropometric assumption based on height, h, where $L_0 = 0.53h$ (Morin et al., 2005). In reality, a human's center-of-mass is difficult to determine statically (Clauser, McConville, & Young, 1969), and quite complex dynamically, and almost certainly not defined by the length of the human leg (Kingma et al., 1995; Maus, Seyfarth, & Grimmer, 2011; Naga, 2005; Saini et al., 1998). Clauser and colleagues measured the COM ratio to height as being 0.58, which would yield a 7–10 cm difference in L_0 estimation (Clauser et al., 1969) from the traditional 0.53 assumption. This 10% difference in L_0, based solely on which COM assumption is adopted, would yield a 7% difference in k_{leg} estimation (Morin et al., 2005). The SLIP model is highly sensitive to changes in its parameters, so small fluctuations in parameter inputs can negatively affect its stability. Indeed, different assumptions of the leg length will inevitably change estimations of the model parameters (Brughelli & Cronin, 2008; Morin et al., 2005) and affect the ability to generate stable parameter combinations (Lipfert et al., 2012). Only one investigation using a 2D SLIP template estimated L_0 from observed gait data, and it was a case study with a single subject (Ludwig et al., 2012).

Similarly, α_{TD} is frequently calculated from Equation 8 (Brughelli & Cronin, 2008; Bullimore & Burn, 2007; McMahon & Cheng, 1990; Morin et al., 2005) or measured kinematically as the angle of the leg at touchdown (Blum et al., 2009). Equation 8 necessarily underestimates the angle, as the velocity during stance must be lower than the gait cycle's average velocity (per Equations *1–4*). Kinematic measurement resolves this, but itself carries the center-of-mass positional assumption (and those associated with the motion capture processing). Even more so than with L_0 fluctuations, the SLIP template parameters vary greatly across a small range of α_{TD}

(Seyfarth et al., 2002). Fractions of a degree can yield great discrepancies in stiffness estimates and fail to enable a model to achieve stable gait (Lipfert et al., 2012).

Finally, t_c is nearly always constrained to that of the observed t_c (Brughelli & Cronin, 2008). Though this seems logical given that it is directly observable, unlike L_0 or α_{TD}, it can be problematic if one is trying to describe a SLIP system that best fits a runner. There is a tendency towards asymmetry in the stance phase of gait, with the end of the cycle often displaying a deviation from linear elasticity in the GRF curve (Cavagna, 2006; Cavagna, Legramandi, & Peyre-Tartaruga, 2008a; Clark et al., 2017). Even if this occurs in the final one or two hundredths of a second during stance, constraining the model to match this complete time course may bias description of the true elastic behavior of the runner and provide an inaccurate representation of the SLIP template. Indeed, allowing t_c to vary between model and experiment elicits more accurate predictions of COM trajectory (Lipfert et al., 2012). No investigations have attempted to estimate all four parameters simultaneously from observed data.

As such, each of these metrics as calculated are co-dependent to some degree, as leg stiffness is traditionally calculated using the leg length change approximation in Equation 7, which relies not only on the leg length assumption, but on kinematic assumptions for spring-leg position or the touchdown angle approximation in Equation 8. That itself is not only a constant-velocity approximation, but it also relies on and is constrained to the observed contact time. Errors in those assumptions can therefore be manifested in and affect all parameters. Misrepresenting contact time, for example, will propagate the error throughout the touchdown angle and the final stiffness value.

As mentioned previously, direct model-experiment comparison with the SLIP template through the full stance phase has been limited (Lipfert et al., 2012). The template is widely used to analyze the stiffness of a runner and thus relies solely upon single features of the GRF or COM time series, such as F_{max}, Δy, or t_c (Brughelli & Cronin, 2008). Apart from Lipfert and colleagues observing consistent leg-force-length curve agreement throughout the stance cycle across several speeds (Lipfert et al., 2012), the degree of model-experiment matching has not been explored in relation to intrinsic or extrinsic factors. Thus, no efforts have been made to characterize the degree to which a runner behaves like the SLIP template—that is, more or less like an energy-conserving, perfectly elastic spring.

One of the significant challenges in analyzing a runner as a SLIP system is the computational complexity of the model (Robilliard & Wilson, 2005). Optimization techniques are routinely used in biomechanics investigations to estimate model parameters from experimentally observed data (Robertson et al., 2018). However, the optimization and simulation methods required to generate stable models while tracking experimental data are computationally intensive, and model-experiment analyses have therefore been restricted to a limited number of steps or subjects (Blickhan, 1989; Bullimore & Burn, 2007; Lipfert et al., 2012; Ludwig et al., 2012; Seyfarth et al., 2002; Seyfarth, Geyer, & Herr, 2003). Moreover, numerical iteration to solve best-fit parameter combinations do not necessarily reveal mechanisms for interaction among the gait parameters. To resolve the computational complexity, the SLIP model GRF has been approximated by a sinusoidal function. These models have demonstrated good agreement in stiffness estimation and GRF impulse characterization with the traditional model (Blum et al., 2009; Morin et al., 2005; Robilliard & Wilson, 2005). However, they have not been used for simultaneous multi-parameter estimation or model-experiment comparison across the entire GRF curve or COM trajectory.

Single-subject investigations of SLIP template comparisons have revealed a high degree of within-subject, step-to-step variability in parameters (Blum et al., 2009; Lipfert et al., 2012;

Ludwig et al., 2012; McMahon & Cheng, 1990; Seyfarth et al., 2002). However, it is common across gait biomechanics studies to collapse many gait cycles to ensemble averages or analyze factors in isolation (Ferber et al., 2016). Indeed, use of the SLIP template is often reduced to calculating single leg stiffness values for subjects without consideration to covariance with the other parameters or time-variance within the analysis.

1.7 Proposed Contribution and Strategy

Establishing a method to systematically define, assess, and monitor running gait is critical to the development of interventions to decrease injury incidence and increase performance capacity in runners. Use of a gait template would reduce the complex dimensionality of the running gait and give researchers and clinicians a unified model against which to study the system-level behavior of a runner. The SLIP template is the theoretical underpinning to the canonical spring-mass model of running, and it represents the fewest degrees-of-freedom that describe the dynamics of a forward bouncing gait. It has been widely used to describe the elastic behavior of runners, and as such, it is a natural candidate for a gait template.

The SLIP model is conceptually simple, as its motion at a given speed is determined by only four parameters (Table 1). However, it is computationally complex, with its motion having no closed-form analytical description. Its application in gait research has been largely that of a tool to characterize a runner's stiffness with its other three parameters assumed from experimental measures and co-dependent. Some investigations have performed model-experiment comparisons of runners to the SLIP template, but these have been limited in scope and size, and similarly assumed parameter values.

The research described hereupon established a novel analytical and computational framework to holistically study runners against a SLIP template and presented additional applications of the method to deliver template-derived biomechanical insights. First, a means to estimate all four SLIP parameters simultaneously from experimentally observed GRF recordings was presented. A time-varying GRF function was derived from sinusoidal SLIP approximations, and nonlinear regression techniques were used to estimate the model parameters. This not only established a method for parameter estimation, but it also provided a means to describe the degree to which a runner "fits" the underlying SLIP template. It further allowed for extension of the framework to fully describe inter- and intra-subject variation in parameters with mixed-effects models.

Subsequently, this analytical method was applied to explore template characteristics in runners of different backgrounds and across conditions: first in a between-groups cohort study and second in a within-individual paired study. The first investigation examined a cohort of elite Kenyan distance runners and trained recreational runners. Their SLIP template parameters were estimated with the nonlinear regression method developed, and the mixed-effects capabilities of nonlinear regression were explored. Fixed effects were used to model template adjustments related to barefoot conditions and foot strike type, and individual subjects were modeled as random effects. The next investigation explored the intra-subject variation in SLIP template characteristics before and after a fatiguing race. Similarly, a mixed-model design with the method was employed, with a fixed effect for the race and random effects for the individuals. For each of these investigations, traditional spring-mass SLIP measures were calculated to fully characterize the spring-mass behaviors and phenomena under investigation as well as to provide context and generalizability.

This work also presented new methods of quantifying SLIP template similarity. A conceptually and computationally simple metric was presented, as well as a metric derived from the nonlinear regression method developed. For each of the two applications described above, the similarity metrics were calculated and explored in relation to the cohorts and effects under investigation. They also were compared to previously used methods for context and comparison.

Finally, the SLIP template was used with conventional calculations and a mixed-effects model design to characterize the global mechanical behavior across a spectrum speeds and within individuals in a distinct population of runners. The spatiotemporal and spring-mass characteristics of elite middle-distance runners were investigated using traditional metrics to explore how individuals with extreme performance capacity modulate their system dynamics across and within-speeds.

Together, these integrated studies presented and tested new methods for systematically assessing, analyzing, and describing running gait as a system. It brought to the SLIP template a novel, robust parameter estimation and analytical method with a limited dependency on model assumptions. It further presented a new means of comparing runners to this system to better understand elastic similarity and dissimilarity. Finally, it presented an approach to use traditional quantifications to deliver richer and more comprehensive template-based mechanical analysis and description. Along the way, each application and method explored research questions in distinct populations of runners and coupled that with traditional analyses to further advance our understanding of spring-mas behavior in runners. The ultimate aim of this work was to facilitate comprehensive characterization of the elastic dynamics of gait and to give researchers and clinicians a common framework to compare and assess the behavior of runners. The overarching goal is and will be to reveal richer insights into the movement patterns underlying running gait.

Chapter 2 Spring-Mass Analyses with Nonlinear Regression

This work has been submitted for publication as:

Geoffrey T. Burns, Richard Gonzalez, and Ronald F. Zernicke (2020). “Estimating spring-mass parameters and modeling ground reaction forces in running using nonlinear regression.”

2.1 Abstract

Runners are commonly modeled as spring-mass systems, but the traditional calculations of these models rely on discrete observations during the gait cycle (e.g., maximal vertical force) and simplifying assumptions (e.g., leg length). We present a method to model runners as spring mass systems using nonlinear regression and the full vertical ground reaction force (vGRF) time series without additional inputs or traditional parameter assumptions. We derived and validated a time-dependent function of the vGRF characterized by the four spring mass parameters: stiffness, touchdown angle, spring leg length, and contact time using a sinusoidal approximation. Next, we compared the spring mass parameters as estimated by the NLR technique to traditional calculations in runners using both independent and mixed-effects models. The mixed-effect NLR method (ME NLR) modeled the observed vGRF time series best (RMSE:155 N) compared to a conventional sinusoid approximation (RMSE: 230 N). Against the conventional methods, its estimations provided similar stiffness approximations (-0.2±0.6 kN/m) with moderately steeper touchdown angles (1.2±0.7°), longer effective leg lengths (+4.2±2.3 cm), and shorter effective contact times

(-12±4 ms). Together, these vGRF-driven system parameters more closely approximated the observed vertical impulses than traditional methods (observed: 214.8 N-s; ME NLR: 209.0 N-s; traditional: 223.6 N-s). ME NLR modeling of the vGRF in running is a useful tool to assess runners holistically as spring-mass systems with fewer measurement sources or anthropometric assumptions. Furthermore, its utility as a statistical framework lends itself to more complex mixed-effects modeling to explore research questions in running.

2.2 Introduction

Some biomechanical properties are unobservable, latent variables. That is, they represent a phenomenon, feature, or behavior of the mechanical system that cannot be measured directly. In spring mass analyses of running, the body is commonly reduced to such a mechanical system to study its elastic behavior, and the reduced parameters of this model (i.e., a runner's "stiffness") are represented as latent quantities. This stiffness parameter and the spring-mass model draw their theoretical basis from the spring-loaded inverted pendulum (SLIP) model of running (Blickhan, 1989; McMahon & Cheng, 1990). This model represents the body as a mass on a single linear leg-spring (Figure 1 and Figure 4). It is the simplest physical system that captures the salient distinguishing features of a running body: a stance and swing phase of gait with a collision and propulsion of the mass. It is conceptually simple and faithfully describes the dynamics of running with only four deterministic parameters for a given mass (m) and velocity (v): its leg-spring length (L_0), a touchdown angle (α_{TD}), a contact time (t_c), and a spring stiffness (k) (Blickhan, 1989). However, the mechanical parameters of this simple system are abstractions from the human runner, and the model itself is characterized by complex nonlinear dynamics. Thus, one is required to make assumptions and estimations of model geometry to facilitate model use in experimental situations (Brughelli & Cronin, 2008).

Figure 4: The spring-loaded inverted pendulum (SLIP) model of running as interpreted in humans

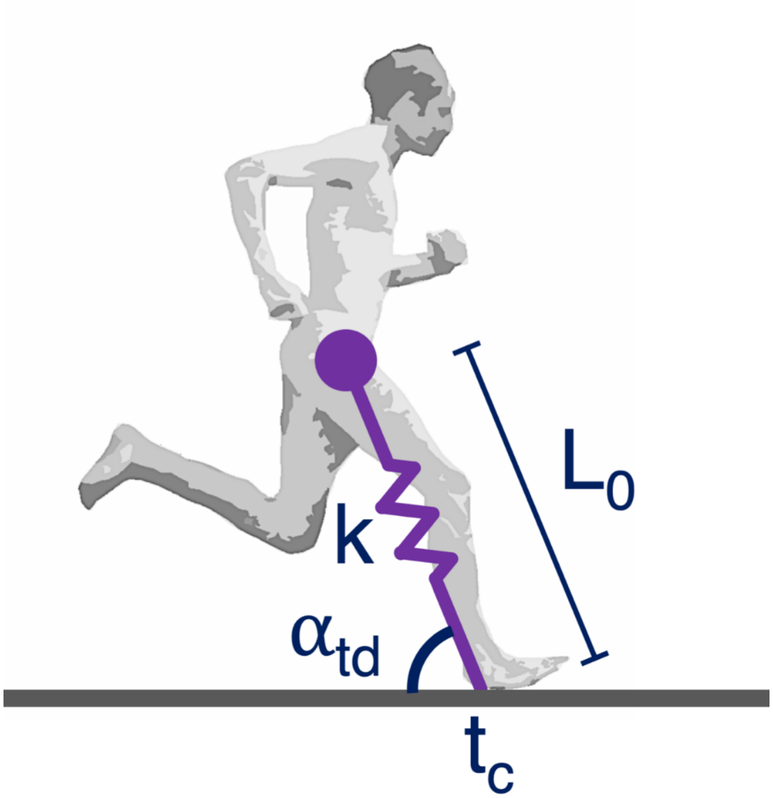

Spring-mass analyses of running are most commonly employed to describe the "stiffness" of a runner (Bullimore & Burn, 2007), and the two most common methods used in the gait literature to calculate stiffness from the spring-mass model come from McMahon and Cheng (McMahon and Cheng 1990) and Morin et al. (Morin, Dalleau et al. 2005). Both methods differentiate vertical stiffness (k_{vert}) and leg stiffness (k_{leg}) of the runner to characterize behavior of vertical displacement and leg length changes during the gait cycle under maximal force. As a dynamic SLIP model functions with a single linear elastic spring, the description here will be restricted to that of leg stiffness calculations. This stiffness is defined as the ratio of the maximal vertical force (F_{max}) to the change in the linear length of the leg spring (ΔL) (McMahon & Cheng, 1990):

9 $$k = \frac{F_{max}}{\Delta L}$$

10 $$\Delta L = \Delta y + L_0(1 - sin\,\alpha_{TD})$$

This method relies on measurement of F_{max} and t_c from a force plate, and approximates α_{TD} as:

11 $$\alpha_{TD} = cos^{-1}\frac{v\,t_c}{2L_0}$$

The spring length, L_0, of the model is assumed to be the resting leg length and is either directly measured as the height of the greater trochanter to ground (Brughelli & Cronin, 2008; McMahon & Cheng, 1990) or estimated as a ratio of 0.53 to the standing height of the runner (Morin et al., 2005; Winter, 1979). The vertical force recording is also used to calculate Δy, the COM displacement, via double-integration of the vertical force (Cavagna et al., 1977). The method of Morin et al. models the vertical ground reaction force as a sinusoid with a peak of F_{max} and a half-period of t_c (Morin et al., 2005):

12 $$F_y(t) = F_{max}\,sin\left(t\frac{t_c}{\pi}\right)$$

This method then uses measurements of contact time, flight time, and running speed to estimate F_{max} and ΔL. Similar to McMahon and Cheng, this method assumes the leg spring length to be that of the resting leg length as previously described. Blum et al. later adapted this sinusoidal method to use the observed F_{max} and a measured value of α_{TD} to estimate ΔL rather than using the flight time (Blum et al., 2009).

While the methods described above have generally been found to have good agreement in their estimation of leg stiffnesses (Blum et al., 2009; Coleman et al., 2012; Morin et al., 2005), these approaches approximate the additional parameters of the SLIP model, which may misrepresent the fundamental elastic dynamics and spring-mass characteristics of the runner. Assigning the mass and horizontal velocity of runner to the SLIP model is certainly a valid assumption, but the other parameters do not translate as analogously as they are commonly assumed. When using either of the above methods, the length of the SLIP model's spring is assumed to be the leg length of the runner. However, to model the runner as a SLIP system, this distance should be that of the runner's COM to the point of contact on the ground. A human's center of mass is difficult to determine statically (Clauser et al., 1969) and quite complex to determine dynamically, and it is almost certainly not defined by that of the human leg (Kingma et al., 1995; Maus et al., 2011; Naga, 2005; Saini et al., 1998). Clauser et al. measured the COM ratio to height as being 0.58, which would yield a 7–10 cm difference in L_0 estimation (Clauser et al., 1969) from the traditional 0.53 leg length approximation. Similarly, Blum et al. proposed using a 5% and 10% scaling factor for COM estimation from leg length measurement from Winter (Blum et al., 2009; Winter, 2005). A 10% difference in L_0, based solely on which COM approximation is adopted, would yield a 7% difference in k_{leg} estimation (Morin et al., 2005). Moreover, α_{TD}, which is the angle of the COM relative to the point of contact, is either approximated from Equation 8 or measured as the angle of the leg at touchdown, requiring additional kinematic measurements and assumptions. Given the complexity and ambiguity of the COM location, these approximations may misrepresent the underlying spring-mass dynamics. Finally, t_c is commonly assigned as that observed in the runner. While this seems like a valid assumption on the surface, it may also inaccurately model the spring-mass behavior. The final milliseconds of propulsion are often characterized by nonlinear elastic dynamics and thus exhibit a marked deviation from SLIP kinetics (Cavagna, 2006). By assigning the observed contact time to a spring-mass model, one would then bias the model towards a contact time longer than what the underlying spring-mass mechanisms would exhibit (da Rosa et al., 2019). Lipfert et al. demonstrated that by allowing t_c to vary between model and experiment, they were able to predict COM trajectories of runners more accurately from the estimated model stiffnesses (Lipfert et al., 2012).

While these differences may seem small in magnitude, stable SLIP systems and their physical realizations are highly sensitive to small parameter variations. Changes in the model's spring length by a centimeter or adjustment of the angle by a degree can demand substantial changes in stiffness or the temporal characteristics to maintain stability (Seyfarth et al., 2002). Because k is a biomechanically latent variable, and the other spring-mass model characteristics (true L_0, true α_{TD}, and SLIP t_c) are difficult, if not impossible, to precisely measure in a runner, a method to estimate these parameters simultaneously from the dynamics of a SLIP system and informed by a single high-fidelity data source such as the vertical ground reaction force may yield more accurate and useful descriptions of the spring-mass characteristics of a runner.

Due to the complex dynamics of SLIP models, direct model-experiment comparisons have been limited, and estimation of best-fit spring mass parameters from the vGRF has been restricted to iterative simulations (Lipfert et al., 2012). Nonlinear regression (NLR) is a candidate for an efficient, functional approach to the problem; it is a numerical method that allows for parameter estimation of a nonlinear function from observed data (Bates & Watts, 1988). If we model the vertical ground reaction force of a SLIP system as a time-varying function, NLR is a promising tool to estimate these SLIP parameters with fewer anatomical or mechanical assumptions and no additional measurement sources. Furthermore, as opposed to alternative optimization techniques for parameter estimation, its functional framework can reveal the nature of interactions among the parameters, allowing a description of the variance structure of the estimates and extending the models to include fixed and random effects on their estimates. Using this technique with a functional form of the SLIP GRF could yield a comprehensive description of the spring-mass behavior of a runner.

The purpose of this investigation was three-fold: (1) to derive a parameterized, time-varying functional form of the SLIP vGRF; (2) to validate the accuracy of the function in describing the actual vGRFs of SLIP models with known parameter combinations; and (3) to apply the NLR technique to analyzing the spring-mass characteristics of human runners and to compare it to the conventional methods of spring-mass analyses.

2.3 Methods

2.3.1 A Parameterized Functional Form of the Spring-Mass Vertical GRF

The time-varying vertical GRF of a SLIP system has been approximated as a half-sinusoid with an amplitude of F_{max} and a period defined by the contact time (t_c) per Equation 12 (Blum et al., 2009; Morin et al., 2005; Robilliard & Wilson, 2005). By twice-integrating this sinusoid over t_c, we obtain the vertical displacement of the COM, Δy, defined by F_{max} and t_c (Cavagna et al., 1977; Morin et al., 2005):

13

$$\Delta y = \frac{F_{max}}{m}\left(\frac{t_c}{\pi}\right)^2 - \frac{g}{8}{t_c}^2$$

A maximal change in "leg" length (ΔL) of the model at midstance can then be derived by incorporating Equation 13 into Equation 10. This relation includes the resting leg length (L_0) and the touchdown angle (α_{TD}):

14

$$\Delta L = L_0 + \frac{F_{max}}{m}\left(\frac{t_c}{\pi}\right)^2 - \frac{g}{8}{t_c}^2 - L_0 \sin\alpha_{TD}$$

The spring constant, or stiffness (k), of the system is defined as the ratio of F_{max} to ΔL per Equation 9 (McMahon & Cheng, 1990). Using this relation and Equation 14, we can express F_{max} as a quantity defined by k, α_{TD} L_0, and t_c:

15

$$F_{max} = k\frac{L_0 - \frac{g}{8}{t_c}^2 - L_0 \sin\alpha_{TD}}{1 - \frac{k}{m}\left(\frac{t_c}{\pi}\right)^2}$$

Finally, to constrain the function to be non-zero from $0 \leq t \leq t_c$, and zero-valued where $t > t_c$, we can add a logistic multiplier to continuously behave as a Heaviside function:

16 $$f(t) = 1 - \frac{1}{1+e^{-10^{10}(t-t_c)}}$$

Here, $f(t) = 1$ for $t < t_c$ and $f(t) = 0$ for $t \gtrsim t_c$. Combining Equations 12, 15, and 16, we create a parameterized sinusoidal time-varying function of the SLIP model's vertical GRF (PS vGRF) that is defined by the four parameters: k, L_0, α_{TD}, and t_c:

17 $$F_y(t) = \left(k\frac{L_0 - \frac{g}{8}{t_c}^2 - L_0 \sin \alpha_{TD}}{1-\frac{k}{m}\left(\frac{t_c}{\pi}\right)^2}\right) \sin\left(t\frac{t_c}{\pi}\right)\left(1 - \frac{1}{1+e^{-10^{10}(t-t_c)}}\right)$$

This defines each vGRF for the SLIP model as a parameter vector θ, where:

18 $$\Theta = \begin{bmatrix} k \\ \alpha_{TD} \\ L_0 \\ t_c \end{bmatrix}$$

Therefore, a runner's experimentally observed vGRF curve can be modeled as:

19 $$y = F_y(x, \Theta) + \varepsilon$$

where y is a n-by-1 vector of n discrete time points, x is a n-by-1 matrix of the n discrete time points, and ε is a n-by-1 vector of the residual error. Nonlinear regression (NLR) can thereby be used to estimate the SLIP parameters θ that minimizes ε for the observed vGRF. Standard estimation approaches, such as least squares or maximum likelihood, can be used for their determination.

2.3.2 Validation with SLIP Simulations

To validate the accuracy of the proposed functional form of the SLIP model vGRF, the PS vGRF time series (Equation 17) was compared to the vGRF time series of simulated SLIP models. Stable SLIP simulations were generated using the equations of motion of the sagittal plane SLIP system (Blickhan, 1989; Seyfarth et al., 2002). Models were simulated across seven running speeds from 3 to 6 m/s in 0.5 m/s increments. Models were simulated with masses of 50, 60, 70, and 80 kg. Leg lengths of 0.9 and 0.95 m were both used for 50 and 60 kg models, and leg lengths of 1.00 and 1.05 m were used for the 70 and 80 kg models, representative of human runners. Simulations were carried out in MatLab (2016b, MathWorks, Natick, MA, USA) using the ode45 solver to achieve a parameter set that yielded stability over 25 steps for speeds of 4.0-6.0 m/s and 10 steps for speeds of 3.0 and 3.5 m/s (Seyfarth et al., 2002). Single-step vGRF time series were then generated for each model. A time series of vGRF data points was generated using the functional form of the SLIP GRF (PS vGRF, Equation 17) with the simulated SLIP parameters as direct inputs, and this time series was compared against the actual SLIP model's vGRF by calculating the root mean-squared error (RMSE). Next, the four parameters for each SLIP simulation were estimated from the simulation's vGRF using NLR. The change in each parameter from the known and simulation values was recorded, and the subsequent vGRF time series with the NLR-estimated parameters was generated for each model to compare its RMSE from the SLIP simulation.

2.3.3 Experimental Data Collection

To apply the NLR technique to human runners and examine it against traditional measurements, vGRF recordings were used from a public dataset of running biomechanics (Fukuchi, Fukuchi, & Duarte, 2017). A detailed description of the methods are available from Fukuchi and colleagues (Fukuchi et al., 2017), but for the purpose of this study, select files were used from a subset of seven subjects running on an instrumented treadmill at 4.50 m/s. The vGRF was recorded continuously for 30 seconds at 300 Hz (FIT, Bertec, Columbus, Ohio). All vGRF time series recordings were extracted from the database and processed in MatLab using custom algorithms to isolate single step cycles with detection thresholds set at 50 N. The subject's height, weight, and foot strike pattern were matched to their coded metadata file. Additionally, each subject's standing leg length was measured as the average height of the left and right legs' anatomical markers corresponding to the greater trochanter as recorded during a standing static calibration relative to the ground. Because the purpose of this investigation was to be demonstrative in nature, analyses and summary statistics for each subject are presented individually.

2.3.4 Conventional Estimation of Spring-Mass Parameters

For each runner, L_0 was recorded as the aforementioned height of the greater trochanter (L_{00}) relative to the ground. It was also estimated using the conventional 0.53 ratio of the standing height (L_{01}) (Winter, 2005). The α_{TD} for each step was estimated per Equation 8 (α_{TD1}). The gold-standard stiffness estimation (k_0) was calculated using the method described by McMahon and Cheng (McMahon & Cheng, 1990). The conventional sinusoidal vGRFs and stiffness estimates (Method 1, k_1) were generated using the sinusoidal method proposed by Morin and colleagues (Morin et al., 2005).

2.3.5 Nonlinear Regression Estimation of Spring-Mass Parameters

For each step cycle collected, NLR was used to estimate the θ from the GRF recordings that minimized ε. First, a constrained model was used, where only k was estimated, and L_0, α_{TD}, and t_c were constrained to traditional measurements (Method 2). Second, an unconstrained NLR was performed to estimate all four parameters for each step simultaneously, treating each step as an independent observation (Method 3). Finally, a mixed-effects NLR model was estimated for each subject, treating the subject's steps as a random effect (ME NLR; Method 4). The results of these estimations were compared to the conventional measurements and stiffness estimations. The Nonlinear Regression toolbox in MatLab (2016b, MathWorks, Natick, MA, USA) was used for the NLR analysis. Custom initial parameter values for the NLR models were assigned to each subject as a parameter set that minimized the sum of squared errors against all steps together via nonlinear least-squares optimization seeded with values of corresponding to the mean value of the subject's conventional parameters: k_0, α_{TD1}, L_{00}, and t_c. Bounds were set at a lower limit of 5 kN/m, 63°, 80 cm, and 0.12 s and 30 kN/m, 74.5°, 120 cm, and 0.40 s, for the four parameters, respectively. For the full mixed-effects NLR parameter estimation, the stochastic approximation expectation maximization algorithm was used to estimate a random-effects model for each subject, treating an individual's steps as random-effects (Feodor Nielsen, 2000). Each subject's model was seeded with an initial random-effects covariance matrix with the diagonal equal to two times the observed variance in the conventional parameters across steps, with the variance in L_{00} as estimated by the variance in α_{TD0} relative to the mean t_c.

2.4 Results

2.4.1 Simulation and Validation

For each of the mass-length combinations, 5 simulations with distinct parameters were generated at each of the 7 speeds, providing 280 unique SLIP models. The parameter set for each model was used to directly generate a vGRF time series, and NLR was used to estimate parameters from each SLIP model and generate a NLR-adjusted GRF time series. The PS vGRF function (Equation 17) provided an accurate estimation of an actual SLIP vGRFs at moderate and faster speeds on its own, and use of NLR provided small adjustments of parameters that yielded more accurate estimation of actual SLIP vGRFs across all speeds. The RMSE of each method is summarized in Table 2 along with the magnitude and percent change of the NLR-adjusted parameters. The PS vGRF of Equation 17 is an excellent estimation of the spring-mass vGRF at moderate and faster speeds (4.0 m/s and faster). NLR-adjustment of the model parameters improves the fit of Equation 17 to be excellent across all speeds, and the adjustment of these parameters are small in magnitude (0.01-0.41%). Figure 5 provides sample vGRFs of three SLIP models at three speeds with the direct-input and NLR-adjusted PS vGRF functional estimations of the vGRF overlaid. The figure shows vertical ground reaction forces of a 60, 70, and 80 kg SLIP model with leg lengths of 0.95 m, 1.00 m, and 1.05 m, respectively, at 3.5, 4.5, and 5.5 m/s (green). The parameterized sinusoidal estimation of the vGRF (PS vGRF) is shown with direct input of the four SLIP parameters (magenta dash) and with the NLR-adjusted parameters (blue dash). Note the poor fit of the direct functional estimation at the lower speed and the good fit of the NLR-parameter-adjusted estimation.

	Sinusoid approx. error		**NLR parameter adjustment (absolute)**				**NLR parameter adjustment (percent)**			
v (m/s)	**RMSE (N)**	**RMSE NLR (N)**	**Δk (N/m)**	**Δa (°)**	**ΔL0 (m)**	**Δt_c (s)**	**Δk**	**Δa**	**ΔL0**	**Δt_c**
3.0	242.9	15.8	36.02	-0.037	0.00401	0.00071	0.23%	-0.05%	0.41%	0.34%
3.5	112.8	11.1	22.61	-0.029	0.00294	0.00039	0.13%	-0.04%	0.30%	0.21%
4.0	34.0	8.2	17.33	-0.020	0.00190	0.00025	0.10%	-0.03%	0.19%	0.14%
4.5	18.6	6.3	12.93	-0.015	0.00132	0.00018	0.08%	-0.02%	0.13%	0.11%
5.0	13.3	5.5	11.07	-0.013	0.00106	0.00014	0.07%	-0.02%	0.11%	0.09%
5.5	10.4	4.7	8.18	-0.009	0.00074	0.00009	0.05%	-0.01%	0.08%	0.06%
6.0	7.2	3.5	7.71	-0.007	0.00060	0.00005	0.04%	-0.01%	0.06%	0.04%

Table 2: Simulation summary across speeds

Figure 5: Sample GRFs of simulated SLIP models and functional estimates of the vGRF.

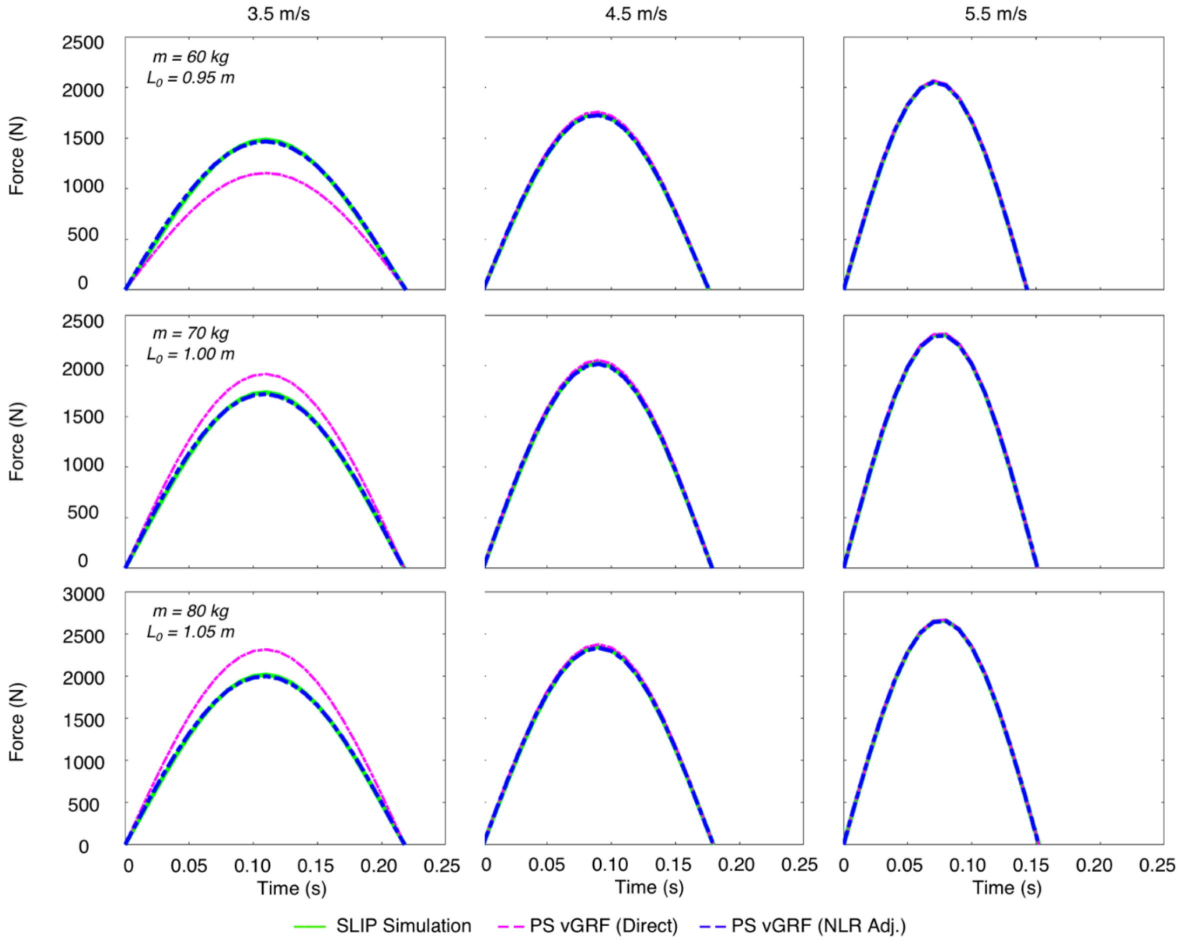

2.4.2 *NLR Estimation of Spring-Mass Parameters in Runners*

Subject characteristics and measured SLIP parameters are provided in Table 3. The two methods using measured and assumed parameters (L_0, α_{TD}, and t_c) to estimate stiffness, the conventional sinusoidal approximation (Method 1) and the single-parameter constrained NLR model (Method 2), yielded the poorest fits to the observed data in the vGRFs generated from the parameters (RMSE: 230.2 N and 221.2 N, respectively). The full NLR method estimating all four parameters and treating each step as an independent observation (Method 3) improved the fit

(RMSE: 170.6 N), and the full NLR method treating each step as a random effect yielded the best fit (RMSE: 155.3 N). Correspondingly, the vertical impulses (VI) followed the same pattern, with the traditional approximation overestimating the VI (223.6 N-s) compared to the observations (214.8 N-s), and the ME NLR models more closely matching it (209.0 N-s). The summary of parameter estimates and model fit for each method and each subject are summarized in Table 4.

The stiffness estimates from the full mixed-effects NLR model yielded values consistent with traditional kinetic approximations (-0.2±0.6 kN/m). The estimated leg lengths of the model tended to be longer than the measured leg length and the height-based approximation by 4.2±2.3 cm and 4.1±2.3 cm, respectively. The touchdown angles were slightly steeper than the conventional estimates by 1.2±0.7°. The effective contact times of this model were 12±4 ms shorter than observed. The stiffness estimates from the full independent-step NLR model were consistent with the other methods (-0.2±0.6 kN/m against the conventional method) . The effective leg lengths estimated via this approach were similar to the measured lengths (-0.7±0.4 cm), and the touchdown angles were similar to conventional approximations as well (0.4±0.1°). The effective contact times of this model were 12±4 ms shorter than observed, similar to the mixed-effect models. The subject-specific differences among parameters are summarized in Table 5. A sample sequence of steps with Method 1, 3, and 4's vGRFs fit to the observed vGRF is shown in Figure 6.

Within 5 of the 7 subjects, the mixed-effect NLR model indicated that step-to-step adjustments in leg length and touchdown angle were highly covaried (0.99), and in several subjects, adjustments in stiffness were moderately covaried with effective leg length (0.03-0.84). Changes in contact time tended to be uncorrelated with adjustments in any other parameters. Correlation matrices for the four parameters for each subject are compiled in Table 6. All steps for two single subjects with their individual models from the random-effects parameter estimates are shown in Figure 7. Note that the vGRF of the overall subject parameters (black line) are shown with individual step parameters from the random effects (colored lines) and individual observed forces (scatter points). Each color corresponds to eight consecutive steps.

	Subject								
Parameter	**A**	**B**	**C**	**D**	**E**	**F**	**G**	**Mean**	**Std. Dev.**
m (kg)	65.4	68.2	70.9	77.2	78.3	63.2	64.8	69.7	6.1
h (m)	1.770	1.745	1.750	1.819	1.778	1.732	1.690	1.755	0.04
FS	R	R	R	R	NR	NR	NR	-	-
L_{01} (m)	0.964	0.938	0.906	0.964	0.945	0.901	0.889	0.929	0.03
L_{02} (m)	0.938	0.925	0.928	0.964	0.942	0.918	0.896	0.930	0.02
F_{max} (N)	1935	1701	1867	2353	2055	1603	1712	1889	256
t_c (s)	0.194	0.195	0.188	0.195	0.195	0.173	0.186	0.189	0.008
α_{TD} (°)	63.1	62.1	62.2	63.0	62.4	64.4	62.0	62.7	0.8

Table 3: Measured parameters for each subject. Contact time (t_c) and touchdown angle (α_{TD}) are presented as averages over the 80 steps. L_{00} indicates leg length as the height of the greater trochanter, and L_{01} indicates leg length as estimated from height. FS indicates foot strike type: rearfoot (R) or non-rearfoot (NR)

Figure 6: Sample steps from a subject with GRFs modeled using the SLIP parameters from each method

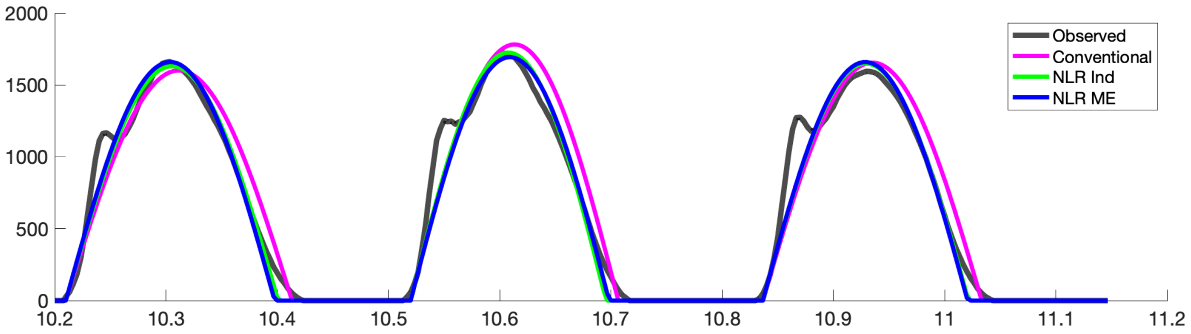

Figure 7 Eighty steps from a rearfoot striking subject (A, subject A) and a non-rearfoot striking subject (B, subject E) with modeled GRFs as estimated from the NLR mixed effects model

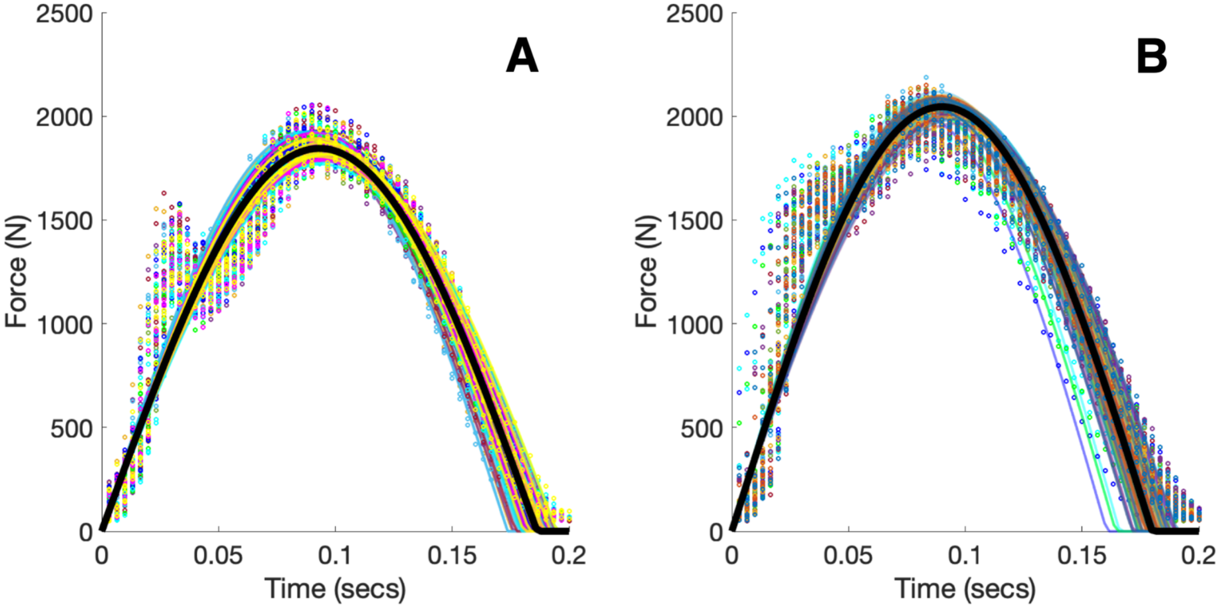

	Parameter	Subject A	 B	 C	 D	 E	 F	 G	 **Mean**	 **SD**
Traditional	k_0 (N/m)	12241	11572	13089	15001	13638	13547	11886	**12996**	1195
	k_1 (N/m)	11218	10718	11688	13287	12731	12721	11146	**11930**	980
Method 1	α_{TD1} (°)	63.1	62.1	62.2	63.0	62.4	64.4	62.0	**62.7**	0.8
Conventional	L_{00} (m)	0.964	0.938	0.906	0.964	0.945	0.901	0.889	**0.929**	0.031
Sinusoid	t_c (s)	0.194	0.195	0.188	0.195	0.195	0.173	0.186	**0.189**	0.008
	BIC	62736	64856	60668	69021	67002	58574	59573	**63204**	3921
	RMSE (N)	180.3	218.3	179.2	344.9	275.8	243.1	169.5	**230.2**	63.7
	VI (N-s)	230.9	208.1	205.0	280.9	254.4	182.8	203.3	**223.6**	34.0
Method 2	k_2 (N/m)	11067	10526	11630	13132	12480	12390	10967	**11742**	953
NLR	α_{TD1} (°)	63.1	62.1	62.2	63.0	62.4	64.4	62.0	**62.7**	0.8
Constrained	L_{00} (m)	0.964	0.938	0.906	0.964	0.945	0.901	0.889	**0.929**	0.031
(1 parameter)	t_{c1} (s)	0.194	0.195	0.188	0.195	0.195	0.173	0.186	**0.189**	0.008
	BIC	62238	64496	60588	68872	66600	58089	58869	**62822**	4021
	RMSE (N)	170.9	210.0	177.7	339.5	264.2	229.4	156.6	**221.2**	64.1
	VI (N-s)	222.2	199.0	202.6	271.4	241.7	171.0	195.4	**214.8**	33.3
Method 3	k_3 (N/m)	11887	11382	12708	14734	13487	13336	11719	**12750**	1191
NLR	α_{TD3} (°)	63.7	62.5	62.9	63.4	62.6	64.7	62.3	**63.1**	0.8
Unconstrained	L_{03} (m)	0.951	0.931	0.896	0.958	0.942	0.897	0.885	**0.923**	0.030
(4 parameters)	t_{c3} (s)	0.186	0.182	0.176	0.176	0.180	0.161	0.176	**0.177**	0.008
Independent steps	BIC	61648	63621	65814	64590	64590	57586	56468	**62045**	3669
	RMSE (N)	141.4	168.7	215.7	187.9	187.9	187.8	104.9	**170.6**	36.8
	VI (N-s)	218.5	193.8	197.6	261.7	234.5	166.3	191.1	**209.0**	31.7
Method 4	k_4 (N/m)	11622	11981	13171	14606	13912	12433	12111	**12834**	1103
NLR	α_{TD4} (°)	63.8	63.9	63.9	63.8	64.1	64.6	63.7	**64.0**	0.3
Unconstrained	L_{04} (m)	0.991	0.960	0.921	1.008	1.005	0.982	0.931	**0.971**	0.035
(4 parameters)	t_{c4} (s)	0.186	0.182	0.176	0.176	0.180	0.161	0.176	**0.177**	0.008
Random effect steps	BIC	59629	61434	55960	63835	62539	55588	54524	**59073**	3721
	RMSE (N)	136.9	164.4	112.1	208.9	182.3	181.2	101.4	**155.3**	39.7
	VI (N-s)	218.4	193.7	197.5	261.6	234.4	166.2	191.0	**209.0**	31.7
Observed	VI (N-s)	220.4	200.8	198.7	272.4	242.2	173.9	195.4	**214.8**	33.2

Table 4: Summary of subject-specific SLIP parameters estimated by conventional and NLR methods (80 steps)

		Subject								
		A	**B**	**C**	**D**	**E**	**F**	**G**	**Mean**	**SD**
Stiffness	k_1-k_0	-1023	-854	-1401	-1713	-908	-826	-739	**-1066**	358
(ΔN**)**	k_2-k_0	-1174	-1046	-1459	-1868	-1158	-1157	-919	**-1254**	316
	k_3-k_0	-354	-191	-381	-267	-151	-211	-167	**-246**	91
	k_4-k_0	-619	409	82	-395	274	-1114	225	**-163**	562
	k_4-k_3	-265	599	463	-128	425	-903	392	**83**	542
Touchdown	α_{TD3}- α_{TD1}	0.6	0.4	0.6	0.4	0.2	0.3	0.4	**0.4**	0.1
angle (Δ°)	α_{TD4}- α_{TD1}	0.7	1.8	1.7	0.8	1.7	0.2	1.7	**1.2**	0.7
	α_{TD4}- α_{TD3}	0.1	1.4	1.1	0.5	1.5	-0.1	1.3	**0.8**	0.7
Leg Length	L_{01}-L_{00}	-0.026	-0.013	0.022	0.000	-0.002	0.017	0.006	**0.001**	0.017
(Δm)	L_{03}-L_{00}	-0.013	-0.008	-0.010	-0.006	-0.003	-0.004	-0.004	**-0.007**	0.004
	L_{04}-L_{00}	0.027	0.022	0.015	0.044	0.061	0.082	0.041	**0.042**	0.023
	L_{04}-L_{01}	0.053	0.035	-0.007	0.043	0.063	0.064	0.035	**0.041**	0.024
	L_{04}-L_{03}	0.040	0.030	0.025	0.050	0.064	0.085	0.046	**0.048**	0.021
Contact	t_{c3}-t_{c1}	-0.008	-0.012	-0.011	-0.019	-0.015	-0.012	-0.010	**-0.012**	0.004
time	t_{c4}-t_{c1}	-0.008	-0.013	-0.011	-0.019	-0.015	-0.012	-0.010	**-0.012**	0.004
(Δs)	t_{c4}-t_{c3}	0.000	0.000	0.000	0.000	0.000	0.000	0.000	**0.000**	0.000

Table 5: Changes in parameters between models across subjects.

Subject		**k**	**α_{TD}**	**L_0**	**t_c**
A	k	1	-	-	-
	α_{TD}	0.154	1	-	-
	L_0	-0.844	0.401	1	-
	t_c	0.000	-0.002	-0.002	1
		k	α_{TD}	L_0	t_c
B	k	1	-	-	-
	α_{TD}	-0.070	1	-	-
	L_0	-0.233	0.987	1	-
	t_c	-0.004	0.000	0.000	1
		k	α_{TD}	L_0	t_c
C	k	1	-	-	-
	α_{TD}	0.464	1	-	-
	L_0	-0.548	0.487	1	-
	t_c	0.000	-0.002	-0.002	1
		k	α_{TD}	L_0	t_c
D	k	1	-	-	-
	α_{TD}	0.459	1	-	-
	L_0	0.431	0.999	1	-
	t_c	-0.003	0.000	0.000	1
		k	α_{TD}	L_0	t_c
E	k	1	-	-	-
	α_{TD}	0.139	1	-	-
	L_0	-0.003	0.990	1	-
	t_c	-0.004	0.000	0.000	1
		k	α_{TD}	L_0	t_c
F	k	1	-	-	-
	α_{TD}	0.518	1	-	-
	L_0	0.465	0.998	1	-
	t_c	-0.003	0.000	0.000	1
		k	α_{TD}	L_0	t_c
G	k	1	-	-	-
	α_{TD}	-0.588	1	-	-
	L_0	-0.652	0.997	1	-
	t_c	-0.001	0.000	0.000	1

Table 6: Correlation matrices of SLIP parameters across 80 steps for each subject as estimated by the mixed-effects NLR method

2.5 Discussion

2.5.1 Summary

We presented a novel method to use nonlinear regression approaches to estimate the spring-mass parameters of a runner using only the observed vertical ground reaction force time series as the input. First, we derived and validated a parameterized, time-dependent functional form of the spring-loaded inverted pendulum's vGRF using the sinusoidal approximation. Then, we applied this to a group of runners and demonstrated the similarities and differences to a conventional estimation of spring-mass behavior. The NLR technique provided stiffness estimations that were consistent with traditional methods, but it more accurately modeled the runner's vGRF and more closely approximated the observed vertical impulse of the runner. This was due to further adjustments in leg length, touchdown angle, and contact time—values typically constrained in conventional estimates of stiffness.

2.5.2 Validity of the Parameterized Sinusoidal vGRF Function

The first contribution of this work was the derivation and validation of the parameterized sinusoidal vGRF function (PS vGRF) given in Equation 17. The vGRF of a runner has commonly been modeled as a sinusoid (Cross, 1999) and adapted for spring-mass analyses (Blum et al., 2009; Morin et al., 2005; Robilliard & Wilson, 2005), yet the function has never been systematically validated against the SLIP model whose behavior it is approximating. Robilliard and Wilson compared their sinusoidal approximation of the vGRF to a numerical SLIP simulation, but they only examined a single model across several angles, and the model itself was assigned parameters simulating a horse (Robilliard & Wilson, 2005). To our knowledge, no systematic validation of the sinusoid as a SLIP approximation has been carried out across speeds and geometries nor in models representing human runners.

The PS vGRF approximation alone proved to be a valid representation of the SLIP vGRF at moderate and faster speeds (4.0 m/s and faster), and with minor adjustments of the parameters via NLR, at slower speeds. Direct input of the model parameters yielded poor approximations of the SLIP vGRF at these lower speeds. This is likely due to several features of the system. First, the SLIP model is inherently unstable at these lower speeds, with parameter configurations that are increasingly more constrained and even infeasible (Seyfarth et al., 2002; Seyfarth et al., 2003). Second, and likely most notably, the derivation of the PS vGRF's amplitude relies on the double-integration of the underlying sinusoid to approximate the vertical oscillation (Equation 13). So, if its similarity to the SLIP model decreases at lower speeds by a fractional amount, that error will propagate according to a power-law through the integrations and yield much greater discrepancies in the positional approximation and the corresponding sinusoidal amplitude approximation here.

By using NLR to estimate the spring-mass parameters from the "observed" SLIP numerical simulation rather than directly inputting the simulation's parameters into the PS vGRF, however, we obtained parameters that were very close (all $< 0.5\%$ different) to the simulation's actual values with fits that were excellent across all speeds. This is likely due to the aforementioned error propagation from the double integration, with the small parameter adjustments "correcting" any underlying deviations or rounding errors. Given that the magnitudes of the adjustments were negligible and within the common reporting sensitivity of the values, the simulation comparisons suggested that the sinusoidal approximation alone is valid at moderate and faster speeds, and that NLR estimation of SLIP parameters with the PS vGRF is a valid technique to estimate spring-mass parameters across all speeds.

2.5.3 NLR-Estimated Spring-Mass Parameters Yield More Accurate vGRFs

While conventional analyses are informed by discrete kinetic data points or spatiotemporal values (e.g., maximal force and/or contact time) and are constrained by geometric approximations of the runner's anthropometry (e.g., leg length and/or touchdown angle), this method allows the spring-mass parameter approximation to be informed by full vGRF time series and allows for uncertainly in the otherwise assumed parameters. This results in vGRFs that more closely model those produced by the runner, with the average RMSE of the ME NLR method here being 155 N versus the 230 N RMSE in the traditional sinusoidal method. The Bayesian information criterion of the NLR models, a measure of fit that penalizes the addition of parameters and overfitting, paralleled the RMSE patterns, as it decreased with each model as compared to the conventional sinusoid and was lowest in the ME NLR models (average BIC of 59073 vs. 63204 for the ME NLR vs. convention). This further results in vertical impulse values that more closely match the observation: the observed and ME NLR-estimated average VI here was 214.8 N-s and 209.0 N-s, respectively, while the traditional estimate was 223.6 N-s. The conventional methods that constrain the spring-mass estimates, especially to the explicitly observed t_c, thus yield a parameter set that overestimates the runner's total vertical force-time relation.

Both Morin et al. and Blum et al. observed this limitation of the sinusoidal approximation in their respective explorations, observing VI biases of 5.3% and 10.5%, respectively (Blum et al., 2009; Morin et al., 2005). Morin et al. used a duty factor relation to further estimate the peak vGRF (rather than explicitly constraining it), which resulted in 6.9% lower peak force, and thus the lower bias (Morin et al., 2005). Blum et al. mitigated the discrepancy by applying a correction factor to the sinusoid's amplitude, defined as the ratio of the observed and modeled VI and found it to be similar to the duty-factor correction (Blum et al., 2009). However, both of these methods simply attenuate the peak force and not the underlying temporal dynamics of the spring-mass behavior. They are thus biased by any small but significant deviations from the modeled behavior, such as the distinct non-linear elasticity in the final moments of propulsion, where the magnitude of the vGRF forces are small, but the foot is still in contact with the ground (Cavagna, 2006; Cavagna et al., 2008a). This is conceptually similar to using the "effective" t_c, —the time for which the runner exceeds body weight during stance, which has been shown to be more sensitive in discriminating spring-mass parameters between runners of varying abilities (da Rosa et al., 2019).

2.5.4 NLR-Estimated Spring-Mass Parameters Differ From Conventional Measurements

The ME NLR modeling provided stiffness values consistent with those of the traditional estimate but revealed differing geometries and temporal relations among the parameters. The hypothesis for longer "effective" leg lengths than those approximated by traditional leg-length or height-based measurements was supported. The average difference within the subjects between the traditional leg-length assumption and the ME NLR-estimated length was 4.2 cm. This suggested that the effective center-of-mass of the runners was located more distal to the ground than typically assumed. The static center of mass on a human standing is certainly higher than that of the leg height, with Clauser et al. measuring it as 0.58 of the standing height (Clauser et al., 1969). Interestingly, Blum et al. used a correction factor of 1.10 of the measured greater trochanter height (determined from subjects lying on a force plate), which would have corresponded to an effective length 9.4 cm higher than the biological leg (Blum et al., 2009). Our approximations similarly predicted longer legs, and the estimation fell roughly halfway between the measured leg length and the static center of mass. The NLR method thus ostensibly allows for subject-specific estimation of the correct effective center of mass location without the segmental assumptions, balance plates, or kinematic markers otherwise required (Lafond, Duarte, & Prince, 2004; Winter, 2005).

In addition to the longer effective legs, the NLR estimation suggested that the runners tended to run with touchdown angles that were 1.2° steeper than the conventional estimate. Given the sensitivity of spring-mass systems to this angle, inaccurate approximation of this value would mischaracterize the system and could characterize an otherwise infeasible combination of spring-mass parameters (Seyfarth et al., 2002). The traditional method of approximating the touchdown angle (Equation. 8) necessarily underestimates a SLIP system's actual touchdown angle (see Appendix A), but it is also dependent on the assumed leg length and contact time, further confounding its accuracy. Finally, as described above, the "effective" spring-mass contact times of the runners were lower than the observed values by an average of 12 ms. This was likely due to the aforementioned nonlinearity in the moments prior to toe-off. Here, the magnitude of the vGRF was small relative to the rest of the time series, but the foot nevertheless remained in contact with the ground and thus extended the contact time. Clark et al. used a cosine bell-curve to capture that nonlinear elasticity fully, but the shape was not informed by the spring-mass parameters per se (Clark et al., 2017). Also, the selected event thresholds and filtering parameters of raw vGRF data influence the precise estimations of heel contact and toe off, and thus can significantly alter contact time estimations (Tirosh & Sparrow, 2003). The NLR method presented here resolved that sensitivity by using the entire vGRF curve to estimate the contact time of a spring-mass system that best described the systemic dynamics of the runner, rather than assigning a fixed value to that system.

2.5.5 NLR Modeling Facilitates Efficient Model-Experiment Comparisons of Spring-Mass Systems in Running

Another advantage of the approach is that it facilitates comparison of a runner with a spring-mass system. Because of the complexity of the system's dynamics, there is no closed-form analytical solution that describes its mechanics. Previous attempts to compare runners to the system have been limited, restricted to iterating simulation of SLIP behavior (Geyer et al., 2005; Lipfert et al., 2012). That approach is computationally intensive, preventing more complex or comprehensive analyses of many steps within a runner or a cohort. Here, we demonstrated that the PS vGRF function provided a robust approximation of the SLIP vGRF. Therefore, comparison of experimental observation to best-fit curves can provide a metric of how closely a runner behaves to the spring-mass system. For example, subject C had dynamics that more closely resembled a simple SLIP model than subject B (RMSE: 112 N vs. 164 N)

2.5.6 Mixed-Effects NLR Modeling Reveals Correlation Patterns in Step-To-Step Spring-Mass Parameter Adjustments

In applying the NLR technique to estimate the spring-mass parameters, it was observed that mixed-effects modeling improved the fit of the model beyond independently modeling each step. This benefit of the ME models likely stemmed from several characteristics of the modeling: first, the random effect term on each parameter came from a conditional distribution that maximized the observed likelihood function of the parameters, rather than an independent, discrete value (Bates & Watts, 1988; Feodor Nielsen, 2000). This provided a solution that was more robust to the complex interactions of the parameters and less sensitive to the starting estimates. Second, this gave the model fewer overall parameters and more degrees of freedom, as evidenced by the reduction in the BIC across models, with the ME NLR model having the lowest BIC and fewest defining parameters. Third, the sensitivity of the independent models to the starting estimates may be compounded by any errors in the solution process across the 80 steps. Here, to minimize solver bias, we used each step's conventional parameters as starting estimates for its model (each step's k_0, α_{TD1} L_{00}, and t_{c1}), but that cannot rule out any bias or local optima from the gradient-based solution. The SAEM algorithm used in the mixed-effects estimation used global optimization tools, and thus it may have been more robust to this issue.

The ME NLR model provided further utility in revealing a variance-covariance structure among parameters. This allows for hypothesis testing among the parameters when fixed effect terms are introduced. Moreover, it revealed the covariance of the parameters in the model estimates. Here, it was observed that leg length and touchdown angle were highly covaried in some of the runners, suggesting that these terms may have been better modeled together as a single geometric term (see Appendix A for suggested methodology) or with one as a fixed parameter. It was further observed that the both stiffness and contact time had little covariance with the other parameters in most of the subjects, suggesting that these parameters maintained independence within the system.

The ability to characterize step-to-step parameter adjustments and their underlying variance structure presents new opportunities to study the variability patterns within an individual's gait. Current methods of characterizing gait variability assess temporal relations of single parameters (e.g., stride length (Jordan, Challis, & Newell, 2006) or center-of-mass excursion (Schutte et al., 2015)) or compare the phasic relations of specific joint segments (e.g., thigh-shank and shank-foot (Hafer et al., 2016)). Here, we used the NLR method to assess systemic behavior with the spring-mass template across the entirety of a vGRF sequence. That provided both a means to quantify the variability in the parameters and a tractable physical realization of those adjustments. Those within-subject system-level adjustments were brought into relief with the NLR analysis, and its statistical framework provided a means to further explore their dynamics with the application of more advanced mixed-effect models.

2.5.7 Limitations

While the NLR method for spring-mass analyses provided the aforementioned advantages, it had several limitations in scope and application. First, it carried assumptions of traditional spring-mass analyses in that it was restricted to level-ground, stable-speed running. Second, when considering all four parameters, the PS vGRF did not necessarily have a unique solution with respect to spring length and touchdown angle. This can be resolved by analyzing multiple steps with a mixed-effects approach (Method 4) or by using a three-parameter PS vGRF with the length-angle determination presented in Appendix A (Equation 21). However, that still only provides a measure of variance for the single "geometric" parameter (Equation 20) and not the length and angle independently. If analyzing single steps, one can also use the three-parameter PS vGRF and adopt one of the traditional approximation methods for the leg length or angle described above while still using NLR to determine best-fit stiffness and effective contact time values. Third, when analyzing independent steps, the method can be sensitive to starting parameters. We standardized this by using the conventional measure for each step as the starting estimate and the runner's average of those for all steps in the mixed-effects model. This sensitivity is further resolved as more steps are included in the analyses, incentivizing the researcher to analyze multiple steps per subject. Finally, the method was more computationally intensive than the traditional approaches. The appeal of the traditional sinusoidal method lies in its simplicity and its field-based inputs (i.e., contact time and flight time). While NLR provides a parameter set with a more accurate vGRF representation, it requires a force platform or an instrumented treadmill and correspondingly more demanding computational resources.

2.6 Conclusion

We presented a method to functionally generate a vGRF time series that is characterized by four spring-mass input variables and models the vGRF of a SLIP system. The PS vGRF accurately simulated the vGRF of simulated SLIP models, which provided the first systematic validation of the sinusoidal vGRF as a model of the SLIP vGRF and supported its application as such. We further presented a means to use this function with nonlinear regression to estimate a runner's stiffness, as well as his or her effective leg length, touchdown angle, and contact time. This liberates stiffness estimates from assumed geometric and temporal constraints, facilitating more efficient and better-fitting spring-mass approximations. When used across many steps with a mixed model, the NLR technique yielded stiffness estimations that were consistent with traditional estimates. The effective leg length approximations were longer than the traditional leg length measurements, and the effective contact times were shorter than the observed values. Together, these NLR-estimated spring-mass characteristics yielded vGRFs that more closely simulated the observed vGRFs. In addition to its fidelity as an analytical technique, this method has broad application in modeling more complex research questions with both fixed and random effects, such as including multiple runners in a multilevel ME NLR regression to allow testing of various runner covariates and cohort parameter differences.

2.7 Addendum: A Singular Length-Angle Approximation

The parameterized sinusoidal vertical ground reaction force presented in Equation 17 is not unique for a given leg length and touchdown angle combination for an isolated step. The two terms have an identity A such that:

20 $$A = L_0 - L_0 \, sin \, \alpha_{TD}$$

To enable use of NLR to estimate spring-mass parameters for isolated steps, this term can be incorporated into Equation 17 as a three-parameter model:

21 $$F_y(t) = \left(k \frac{A - \frac{g}{8} t_c}{1 - \frac{k}{m}\left(\frac{t_c}{\pi}\right)^2} \right) sin\left(t \frac{t_c}{\pi}\right) \left(1 - \frac{1}{1 + e^{-10^{10}(t - t_c)}}\right)$$

Using NLR, this method can provide an estimate for A. With that estimation, we can then use properties of the spring-loaded inverted pendulum's dynamics with a horizontal velocity approximation to isolate L_0 or α_{TD} and solve for their values with A.

Specifically, we can consider the energy of the system at its apex in flight, where y_0 is the vertical position at landing and takeoff, y_f is the peak vertical excursion during flight, and v_{xi} is the horizontal velocity during flight and at the initial point of stance:

22 $$E = \frac{1}{2} m {v_{xi}}^2 + mg(y_0 + y_f)$$

We can also consider the energy of the system at midstance, where the center-of-mass is at its lowest point, where Δy is the vertical oscillation during stance defined by Equation 13, ΔL is the change in leg length during stance as defined by Equation 14, and v_{xf} if the horizontal velocity at midstance:

23 $$E = \frac{1}{2} m {v_{xf}}^2 + mg(y_0 - \Delta y) + \frac{1}{2} k \Delta L^2$$

Without use of additional measurement equipment (i.e., markers or accelerometers), the exact values of the horizontal velocity throughout the gait cycle are unknown. The common approximation of the relation of the leg length to the touchdown angle as described in Equation 8 is inappropriate, as it will underestimate their values, given that the average velocity during stance will be necessarily less than the average velocity of the full gait cycle. If we approximate the change in horizontal velocity during stance as a linear decrease from v_{xi} to v_{xf}, the velocity values can be related with the duty factor, ß:

24 $$v \approx \frac{v_{xi}+v_{xf}}{2}\beta + v_{xi}(1-\beta)$$

25 $$\frac{v_{xi}+v_{xf}}{2} \approx \frac{2L_0 \cos \alpha_{TD}}{t_c}$$

In considering a case where the runner's average horizontal velocity is known (e.g., treadmill setting or timing gate measurement), v_{xi} and v_{xf} can thus be approximated and expressed as:

26 $$v_{xi} \approx \frac{v-\frac{2L_0 \cos \alpha_{TD}}{t_c}\beta}{(1-\beta)}$$

27 $$v_{xf} \approx \frac{4L_0 \cos \alpha_{TD}}{t_c} - \frac{v-\frac{2L_0 \cos \alpha_{TD}}{t_c}\beta}{(1-\beta)}$$

These two expressions can be incorporated into the system energy expressions (Equations 22 and 23), such that:

28 $$v_{xi}{}^2 - v_{xf}{}^2 = -2g\left(y_f + \Delta y\right) + \frac{k}{m}\Delta L^2$$

To express the above relation with known quantities, we can use the following identities:

29 $$\beta = \frac{\pi m g}{2F_{max}}$$

30 $$\beta = \frac{t_c}{t_c + t_f}$$

31 $$t_f = t_c\left(\frac{2F_{max}}{\pi m g} - 1\right)$$

32 $$F_{max} = k\frac{A - \frac{g}{8}{t_c}^2}{1 - \frac{k}{m}\left(\frac{t_c}{\pi}\right)^2}$$

33 $$y_f = \frac{1}{2}v_{y0}\frac{t_f}{2}$$

34 $$v_{y0} = g\frac{t_f}{2}$$

35 $$y_f = \frac{g}{8}{t_f}^2$$

36 $$y_f = \frac{g}{8}{t_c}^2\left(\frac{2F_{max}}{\pi m g} - 1\right)^2$$

Combining these terms, Equation 28 can be re-written as:

37 $$\left(\frac{v - \frac{2L_0 \cos \alpha_{TD}}{t_c}\beta}{(1-\beta)}\right)^2 - \left(\frac{v - \frac{2L_0 \cos \alpha_{TD}}{t_c}\beta}{(1-\beta)} - \frac{4L_0 \cos \alpha_{TD}}{t_c}\right)^2$$

$$= -2g\left(\frac{g}{8}{t_c}^2\left(\frac{2F_{max}}{\pi m g} - 1\right)^2 + \frac{F_{max}}{m}\left(\frac{t_c}{\pi}\right)^2 - \frac{g}{8}t_c\right) - \frac{k}{m}\left(A - \frac{F_{max}}{m}\left(\frac{t_c}{\pi}\right)^2 - \frac{g}{8}t_c\right)^2$$

With A known, Equations 20 and 37 can therefore be solved for unique identities of L_0 and α_{TD}. Equation 37 can be expressed with known quantities: g, m, v, k, A, and t_c, and solved numerically for L_0. With L_0, Equation 20 can be used to then solve for α_{TD}.

As a caution, it should be noted that Equations 22 – 25 rely on data derived from accelerations and are themselves approximations of velocities. Therefore, any errors or deviations from absolute dynamics are propagated when integrating to displacement values for the system. So, the approximations for v_{xi} and v_{xf} derived from solving Equation 37 tend to perform well across speeds and parameters sets, but the exact solutions for L_0 and α_{TD} may fall outside of reasonable values in some conditions, e.g., at slower speeds (< 3.5 m/s), where the spring-mass dynamics are less stable. In these instances, it may be prudent simply to fix either α_{TD} or L_0 with a conventional assumption (e.g., Equation 8 or a height approximation) and then to fit a three parameter model when analyzing independent single steps.

Chapter 3 Application of Spring-Mass NLR and Similarity Analyses Methods: A Cohort Comparison of Elite Kenyan and Recreational Runners

This work will be submitted for publication as or similar to:

Geoffrey T. Burns, Nicholas Tam, Jordan Santos-Concejero, Ross Tucker, and Ronald F. Zernicke (2020). “Kenyan distance runners behave similarly to simple elastic systems”.

3.1 Abstract

The complexity and individualization of running mechanics have made assessments of running gait challenging. Here, we explored the mechanical patterns of two distinct populations of runners against the spring-mass template to characterize systemic behavioral differences. Using both established and novel metrics, we compared the kinetics of elite Kenyan distance runners to those of non-elite recreational runners in both shod and barefoot conditions in overground running, and we characterized the spring-mass behavior of both groups. Across all measures and within foot strike types, the Kenyans behaved more similarly to the spring-mass system, with more symmetric bounces (95.4% vs. 92.7%), less discrepancy (i.e. greater coordination) between horizontal and vertical kinetic changes (10.0 ms vs 16.3 ms), and better fit to a spring-mass vertical ground reaction force (RMSE of 122.9 N vs 160.6 N). The barefoot condition elicited greater kinetic coordination but decreased model fit in the recreational runners, with the effects being less pronounced in the Kenyan runners. The Kenyan runners produced similar absolute maximal vertical forces, which corresponded to higher weight-specific forces (2.74 vs. 2.46 BW), and exhibited shorter ground contacts (213 vs. 244 ms). Together, this resulted in similar absolute leg

stiffnesses among groups, but higher relative stiffnesses within the Kenyan runners (16.5 vs. 13.0 BW/L_0). The barefoot condition resulted in slightly lower maximal forces in both cohorts (-0.05 BW), shorter contacts in the recreational runners (-7 ms), but greater overall leg stiffnesses in both cohorts (+0.7 kN/m and 1.0 BW/L_0). Nonlinear regression estimation of the effective spring-mass parameters corroborated the findings, with higher estimates of leg stiffness compared to conventional estimates (12.2 vs. 10.2 kN/m) that were similarly unchanged within groups. The effective contact times were shorter than the observed values (-17 ms), but their effect patterns followed observation, with shorter contacts among the Kenyan runners and within the barefoot condition. Overall, these results suggested that elite Kenyan distance runners exhibited greater likeness to the linearly elastic, energy-conserving spring-mass system, and that they produced dynamics that were similar in absolute magnitude to non-elite recreational counterparts despite being of smaller mass and stature. This provided another potential source of explanation for their unmatched dominance in distance running, and it also presented methods for systemic quantification of gait behavior in runners of all demographics.

3.2 Introduction

The description and quantification of "good" running form has challenged biomechanists, physiologists, coaches, and athletes alike for many decades. In his seminal training text, Fred Wilt posited that every runner must necessarily have a unique form, due to individual differences in physical make-up, likening it to a fingerprint (Wilt, 1959). Subsequent biomechanical investigations into the determinants of running performance have corroborated this individualization (Nummela et al., 2007; Williams & Cavanagh, 1987), and it was later echoed in the description from Nigg and colleagues of a runner's "preferred movement path" (Nigg et al., 2015). Several reviews have synthesized the numerous investigations of the biomechanical aspects of running economy (a critical determinant of performance), and they have consistently identified several contributing factors such as shorter contact times, lower vertical oscillation, and greater leg stiffnesses (Anderson, 1996; Moore, 2016; Saunders et al., 2004). However, component-level kinematic determinants of performance and proper "form" have remained largely elusive (Moore, 2016). This can be explained by the notion that gait is in itself a continuous, dynamic coupling of the myriad limb and joint segments (Hamill et al., 1999), and when further considering the subsequent determinants of those motions (metabolic, neurologic, and biologic), the systemic complexity approaches that of the "fingerprint" described by Wilt.

An alternative approach to characterize one's gait is to assess it systemically, and the simplest system that captures the fundamental dynamics of running is that of the spring-loaded inverted pendulum, or simply, the spring-mass model (Blickhan, 1989; McMahon & Cheng, 1990). This two-dimensional model treats the runner a simple point-mass on a linearly elastic "leg" spring that attacks and leaves the ground with a given touchdown angle. The model assumes ideal elasticity, and its dynamics are thus symmetric and energy-conserving through stance and flight. Its forward and vertical kinetic energy change in phase, with a transition from braking to propulsion occurring at mid-stance, which is the same moment the vertical position is at a minimum and the mass is transitioning from loading to unloading. This system has been proposed as the template that underlies running dynamics across species (Full, Farley, & Winters, 2000; Full & Koditschek, 1999). See Figure 8 and Figure 9 below.

Figure 8: The two-dimensional spring-mass system of a given mass, m, and speed, v, with a spring stiffness, k, a touchdown angle, α_{TD}, spring "leg" length, L_0, and a contact time, t_c. Its maximal spring compression ΔL and maximal center-of-mass displacement Δy occur at midstance.

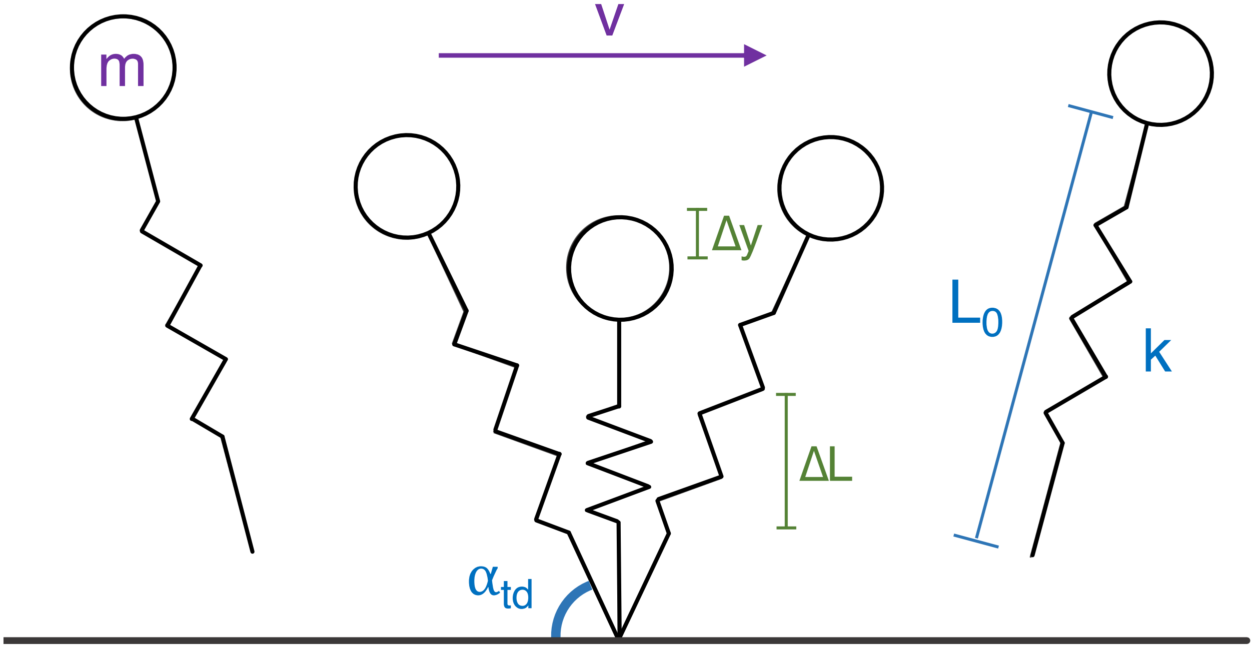

Figure 9: The realization of the spring-mass model in a human runner

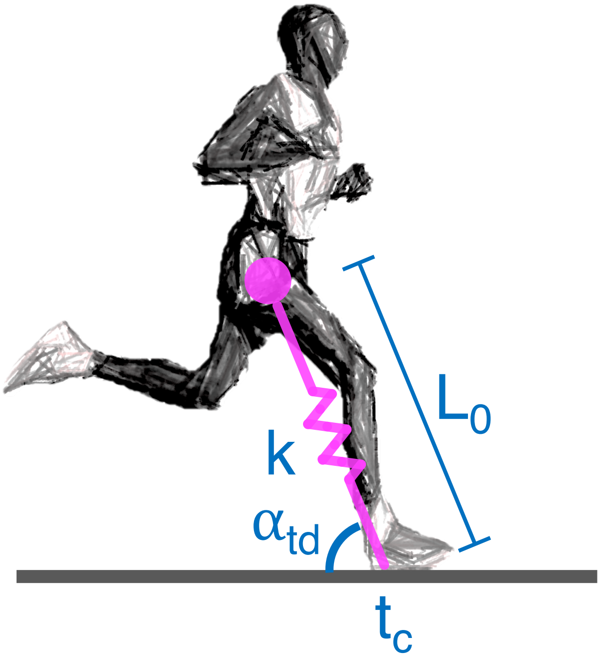

The aforementioned factors that have explained running economy (contact time, vertical oscillation, and leg stiffness) are indeed systemic characteristics related to these spring-mass dynamics, so a comparison of runners to this template may be insightful in assessing gait behavior. However, given the complexity of the underlying dynamics, no analytical solution to its equations of motion exists (Schwind & Koditschek, 2000), and the means by which we can directly compare runners to this system is limited. A simple method for assessing similarity to the elastic spring-mass system was proposed by Cavagna and Legramandi, where they described the "similarity to a symmetric bounce" of a runner. This metric was calculated as the average of the ratios of the maximal upward and downward velocity of the center-of-mass (COM) and the deceleration and acceleration times of the COM, both of which are 1.0 in an ideal spring-mass system (Cavagna & Legramandi, 2015). They previously used these metrics to demonstrate that humans behave most similarly to this simple elastic system in their teenage years, with the similarity declining with age (Cavagna et al., 2008a; Legramandi et al., 2013). Furthermore, Cavagna observed the deceleration-acceleration time asymmetry to decrease as running speeds increased, with runners approaching more elastic behavior at higher speeds (Cavagna, 2006). This asymmetry metric was further explored in a group of high- and low-performing runners, where it was observed that the two groups did not differ on their timing asymmetries, but rather diverged across other systemic spring-mass characteristics, such effective contact time, aerial time, and vertical stiffness (da Rosa et al., 2019). These applications suggest that systemic spring-mass similarity may be discriminatory and indicative of underlying musculotendinous phenomena (Cavagna et al., 2008a; Cavagna, Legramandi, & Peyre-Tartaruga, 2008b), but the concept of "elastic similarity" has yet to expanded upon or applied across other heterogenous groups.

An appealing group in which to explore whether similarity or deviations from simple elastic systems (i.e., spring-mass behavior) differs between distinct populations or performance capacities is that of the Kenyan distance runners. Their dominance in the sport has been unmatched (Tucker, Onywera, & Santos-Concejero, 2015). Biomechanical investigations of this population have identified shorter ground contact times (Kong & de Heer, 2008; Santos-Concejero et al., 2017) and longer Achilles tendon moment-arms (Kunimasa et al., 2014) as unique characteristics, but spring-mass behavior has not been explored. Additionally, Sano and colleagues observed that in hopping, elite Kenyan distance runners had smaller stretching and shortening (SS) amplitudes in the medial gastrocnemius muscles but achieved higher maximal hopping heights with greater SS ratios. This suggested that their medial-gastrocnemius muscle-tendon unit functioned more efficiently to store and release elastic energy (Sano et al., 2013a). They later observed that Kenyan distance runners had lower tibialis anterior and medial gastrocnemius activity patterns in the in pre-activation and braking phases of the gait cycle as compared to competitive Japanese runners, further suggesting more efficient elastic mechanisms (Sano et al., 2015). These findings together suggest that high-level Kenyan runners may behave more like efficient, elastic systems and that any systemic similarities and characteristics may provide further insight into gait characteristics related to performance capacity.

We undertook this investigation to explore the concept of “elastic similarity” and spring-mass behavior in a group of Kenyan distance runners. We hypothesized that the Kenyan runners with high performance capacities would exhibit greater similarity to the ideally elastic spring-mass system as compared to a cohort of recreational runners. Furthermore, we hypothesized that differences would be apparent in both shod and barefoot conditions in both populations, but that the changes would be less distinct in the Kenyans, where familiarization with barefoot activity is common in childhood and adolescence (Aibast et al., 2017; Lieberman et al., 2015). Further, we hypothesized that group differences would persist after controlling for foot strike pattern, for which we would anticipate rear foot striking to decrease similarity (Bobbert, Schamhardt, & Nigg, 1991). Furthermore, we sought to explore three new metrics of spring-mass similarity: the timing difference between the transition from braking to propulsion in the horizontal plane and the transition from to loading and unloading in the vertical plane, the time-normalized ratios of these events, and the overall similarity of a best-fit spring-mass vertical ground reaction force to that of the runner's observed force as estimated by nonlinear regression (NLR). The first two metrics are an indication of the degree to which a runner's change in forward and vertical kinetic energy is coordinated and in phase, and the last is an assessment of the overall shape of the vGRF curve against the spring-mass template. We hypothesized that these metrics would be more sensitive to any discrepancies between groups.

We also used these observations to explore systemic spring-mass behavior in the two populations with both traditional measures of stiffness and effective measures of spring-mass behavior as estimated by mixed-effects NLR from the vGRF recordings. We hypothesized that at a fixed speed, contact times would be lower in the Kenyan runners and that stiffness measures would correspondingly be higher. It was further hypothesized that these differences would follow in both groups between shod and barefoot conditions and between rearfoot and non-rearfoot striking patterns.

3.3 Methods

3.3.1 Experimental Data Collection

Our study compared the ground reaction force characteristics of high-level competitive Kenyan distance runners to a cohort of trained recreational runners in both shod and barefoot conditions. The investigation collated kinetic data collected from two previous investigations following similar experimental protocols. From the first, 15 professional Kenyan runners that were recruited from a management agency were included. From the second, 26 locally recruited male recreational runners were included (10km best: <50 minutes; >4 hours of training per week). At the time of the studies, all participants were free of lower limb injury and refrained from hard training in the two days prior to the session. All participants provided written informed consent, and the studies were approved by the University of Cape Town's ethics review board (HREC ref: 151/2013 and 504/2011).

Participants ran in shod and barefoot conditions in randomized order at 12 km/hr on a 40-meter synthetic indoor track. Speeds were verified with photoelectric timing cells. The shod condition was performed in the subject's habitual training shoe. Ground reaction forces were recorded from two 900×600 mm embedded force platforms (AMTI, Watertown, MA, USA) and sampled at 1000 Hz. Five successful trials were captured for each subject in each condition, where a successful trial was defined as the participant running within ±5% of the target speed, striking the force plate with his right foot, and giving no indication of platform targeting. Additionally, the Kenyan cohort completed 3 successful trials in each condition at 20 km/hr.

3.3.2 Data Processing

The GRF recordings were filtered using a low-pass, fourth order Butterworth filter with a cutoff frequency of 60 Hz and a landing/take-off threshold of 50 N. Subjects were classified as rearfoot striking (RF) or non-rearfoot striking (NRF) based on the presence of an impact peak in the vGRF in the shod condition. Leg and vertical stiffnesses were calculated in accordance with the method of McMahon and Cheng (Farley et al., 1993; McMahon & Cheng, 1990), and leg spring length (L_0) was estimated as 0.53 of the participant's standing height (Morin et al., 2005; Winter, 1979). Elastic similarity was quantified using the method of Cavagna and Legramandi, where they calculated the “similarity to an elastic bounce” (SB) as the average of the ratios of the maximal downward and upward velocity of the COM and the deceleration to acceleration times of the COM during stance (Cavagna & Legramandi, 2015; Legramandi et al., 2013). It was further quantified with two additional metrics: first, as the difference between the time at which the horizontal GRF crossed 0 N, indicating a transition from braking to propulsion in the horizontal plane, and the time at which the vertical GRF reached its peak, indicating a transition from loading to unloading in the vertical plane. In a perfectly elastic bounce, this horizontal and vertical timing difference (HV TD) would be zero. Second, as the ratio of the horizontal braking and propulsion times to the vertical loading and unloading times. This ratio of the braking to propulsion ratio and the loading to unloading ratio (BP:LU) is conceptually similar to the HV TD in that it attains unity (1.0) in an elastic system, but it further normalizes any asymmetry to the asymmetry in the loading and unloading phases of stance and to the total contact time of the stance. See Figure 10 and the energetic profile of a spring-mass system in Figure 2.

Figure 10: Ground reaction forces of a two-dimensional spring mass system with its vertical (blue) and horizontal (magenta) components. At midstance, the body transitions from loading to unloading and from braking to propulsion

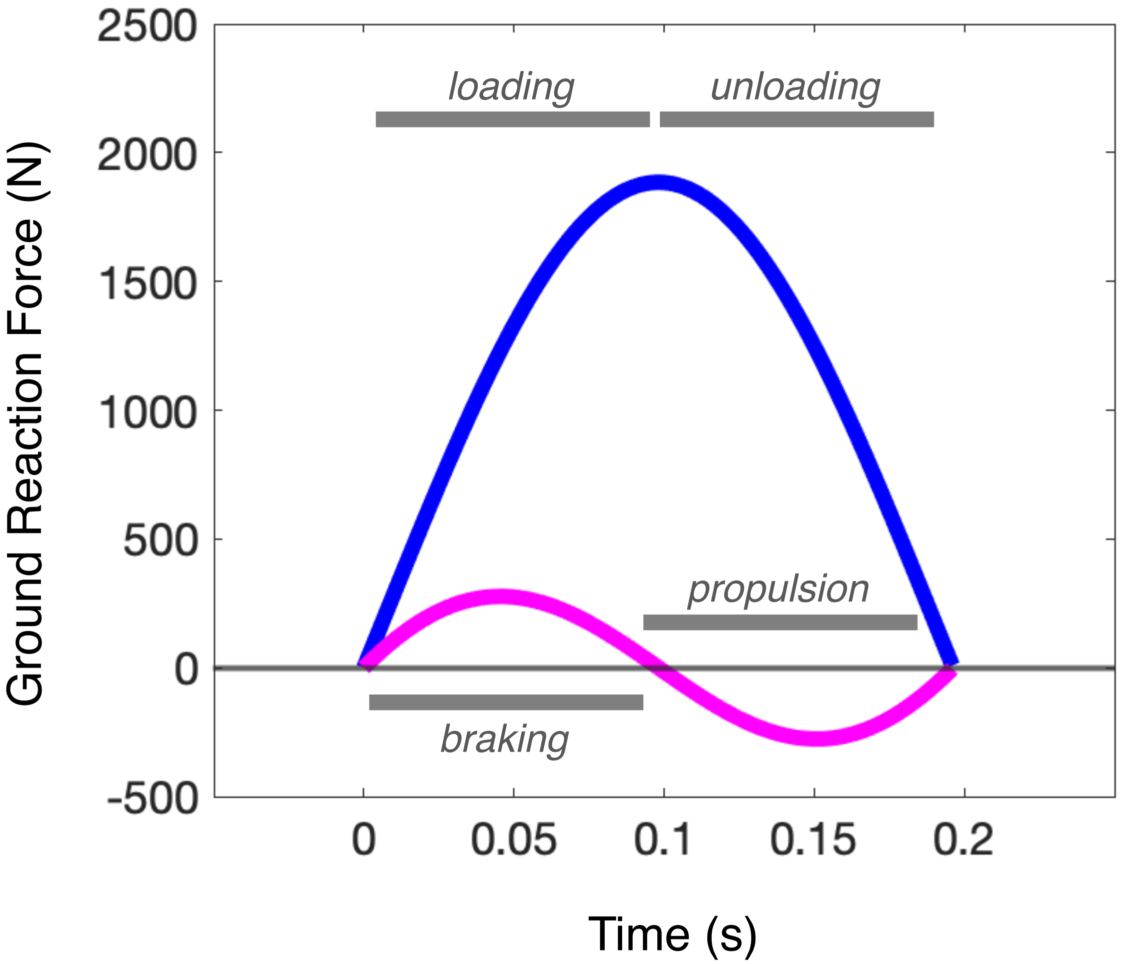

3.3.3 Nonlinear Regression Analysis

To explore the effective spring-mass behavior across groups and conditions, we used the mixed-effects Nonlinear Regression (NLR) estimation technique described in Chapter 2. The functional form of the spring-mass vGRF (PS vGRF) is described again in Equation 38, and it models the observed vGRF with the four effective spring-mass parameters: stiffness (k*), touchdown angle (α_{TD}*), leg length (L_0*), and contact time (t_c*).

38 $$F_y(t) = \left(k\frac{L_0-\frac{g}{8}t_c-L_0\sin\alpha_{TD}}{1-\frac{k}{m}\left(\frac{t_c}{\pi}\right)^2}\right)sin\left(t\frac{t_c}{\pi}\right)\left(1-\frac{1}{1+e^{-10^{10}(t-t_c)}}\right)$$

For a given group i of n_i vGRF observations, the vertical force is modeled with a fixed parameter set φ and a group-specific random effect set *b*.

$$y_i = F_y(\varphi_i, x_i), \varphi_i = \begin{pmatrix} k_i \\ \alpha_{TD\,i} \\ L_{0\,i} \\ t_{c\,i} \end{pmatrix} + b_i, b_i = \begin{pmatrix} b_{ik} \\ b_{i\alpha} \\ b_{iL} \\ b_{it} \end{pmatrix}, and\ x = \begin{pmatrix} t_{i1} \\ \vdots \\ b_{in} \end{pmatrix} \tag{39}$$

We assigned fixed effects to each parameter for the cohort (Recreational vs. Kenyan), shoe condition (Shod vs. Barefoot), foot strike type (RF vs. NRF), and speed (12 km/hr vs. 20 km/hr) so that for each observation, there were 20 fixed parameters, corresponding to the intercept values of k*, α_{TD}*, L_0*, and t_c*, and parameters for the effects of cohort, shoe, foot strike, and speed, respectively. Design matrices were assigned to each group with an identity matrix for each intercept parameter set, and dummy-coded with either zero or identity matrices for each respective fixed effect set. Each observed step was grouped, and random effects were assigned to the four intercept parameters. An example model parameter set φ for step i from a Kenyan subject (1) in the shod condition (0) with a NRF strike (1) at 12 km/hr (0) would be:

$$\varphi_i = A_i\beta_i + B_i b_i \tag{40}$$

$$\beta = \begin{pmatrix} \beta_1 \\ \vdots \\ \beta_{20} \end{pmatrix}, A_i = \begin{bmatrix} \overbrace{1\,0\,0\,0}^{Int.} & \overbrace{1\,0\,0\,0}^{Ken.} & \overbrace{0\,0\,0\,0}^{Shod} & \overbrace{1\,0\,0\,0}^{NRF} & \overbrace{0\,0\,0\,0}^{12\,kh} \\ 0\,1\,0\,0 & 0\,1\,0\,0 & 0\,0\,0\,0 & 0\,1\,0\,0 & 0\,0\,0\,0 \\ 0\,0\,1\,0 & 0\,0\,1\,0 & 0\,0\,0\,0 & 0\,0\,1\,0 & 0\,0\,0\,0 \\ 0\,0\,0\,1 & 0\,0\,0\,1 & 0\,0\,0\,0 & 0\,0\,0\,1 & 0\,0\,0\,0 \end{bmatrix}, b = \begin{pmatrix} b_{i1} \\ \vdots \\ b_{i4} \end{pmatrix}, and\ B_i = \begin{bmatrix} 1\,0\,0\,0 \\ 0\,1\,0\,0 \\ 0\,0\,1\,0 \\ 0\,0\,0\,1 \end{bmatrix} \tag{41}$$

To facilitate model convergence, vGRF data was downsampled to 500 Hz. All fitting was performed using the Nonlinear Regression toolbox in MatLab (2019a, MathWorks, Natick, MA, USA). The mixed-effects modeling was carried out using the stochastic approximation expectation maximization algorithm (Feodor Nielsen, 2000). We seeded the model with initial parameter values that minimized the sum of squared errors against all steps together via nonlinear least-squares optimization seeded with values corresponding to the mean value of all subject's conventional parameters: k_0, α_{TD}, L_0, and t_c. Bounds were set at a lower limit of 5 kN/m, 63°, 80 cm, and 0.10 ms and an upper limit of 0.12 s and 30 kN/m, 74.5°, 120 cm, and 0.40 s for the four parameters, respectively. The model was seeded with an initial random-effects covariance matrix with the diagonal equal to two times the observed variance in the conventional parameters across steps, with the variance in L_0 as estimated by the variance in α_{TD} relative to the mean t_c.

Finally, as an additional measure of elastic similarity, the NLR method was used to assess the degree to which subjects conformed to a best-fit spring-mass vGRF as assessed by the model's root-mean-squared error (RMSE) against their observed vGRF (SM Fit). We used the method described above to fit a model to each subject-condition combination without fixed effects and with random effects on each step.

3.3.4 Data Analysis

The analyses of traditional spring-mass measures and the elastic similarity measures (SB, HVTD, BP:LU, and SM fit) were conducted using mixed-effect model linear regression, treating cohort, shoe condition, foot strike, and speed as fixed effects with interactions on cohort and shoe condition. Each subject was assigned a random effect intercept.

42 $$y = \beta_{cohort} \times \beta_{shoe} + \beta_{FS} + \beta_{speed} + Error(1|Subject)$$

For the linear mixed-effect models, the fixed effects were assessed for significance via Satterthwaite's method. For the NLR models, estimates for the standard errors of each fixed effect term were approximated via the maximum likelihood and tested for significance using a Wald Test. Statistical test criterion in all models used a Type I error control of $\alpha < 0.05$. MatLab (2019a, MathWorks, Natick, MA, USA) was used for all data processing and NLR modeling, and R (v3.6.2, R Foundation for Statistical Computing, Vienna, Austria) was used for all additional statistical analyses.

3.4 Results

41 subjects were included in the study, and 500 steps were analyzed. Aggregate subject characteristics from each cohort are provided in Table 2. A sample demonstration of the NLR-fitting process is provided in Figure 11. Two hundred iterations were used at each of the three steps for the SAEM algorithm. This provided stable estimates of the random-effects covariance matrices (see bottom panel) as well as general asymptotic estimates for the fixed effect parameters.

Characteristic	**Recreational**	**Kenyan**
Subjects (n)	26	15
Foot strike (RF/NRF)	20/6	8/7
Age (yr)	28.5 ± 5.3	23.7 ± 4.0
Mass (kg)	72.3 ± 10.8	54.9 ± 5.8
Height (m)	175.9 ± 8.6	170.5 ± 6.1
10km Best (min:sec)	43:33.1 ± 04:58.9	28:42.9 ± 00:21.7

Table 7 Cohort characteristics

3.4.1 Elastic Similarity

Across all measures, the Kenyan runners behaved more similarly to the elastic system. Their SB metric was 95.4% vs. 92.7% in the recreational runners (effect SEM: 1.3%). With respect to the GRF timing difference, their discrepancy was lower (i.e. horizontal and vertical force progression more coordinated), with an HV TD of 10.0 ms vs. 16.3 ms (effect SEM: 2.6 ms), and a normalized timing difference ratio (BP:LU) of 1.21 vs. 1.32 (effect SEM: 0.05). Four representative subjects are shown in Figure 16. Their overall spring-mass model “fit” as assessed by NLR was better, with average model errors of 122.9 N vs. 160.7 N (effect SEM: 14.3 N). Four representative subjects are shown in Figure 13.

With respect to the effect of shoes, SB did not change within subjects. However, the HV TD and BP:LU were affected, with a significant interaction effect. For the recreational runners, the HV TD and BP:LU decreased in the barefoot condition (-1.8 ms, SEM: 0.6 ms and -0.03, SEM: 0.01), whereas they increased slightly in the Kenyan runners (+1.7 ms, interaction SEM: 1.2 ms and +0.02, interaction SEM: 1.2). The SM fit decreased in the barefoot condition for the recreational runners, with a 14.1 N increase in fit error, but it improved in the Kenyan runners by 13.5 N (interaction SEM: 13.0).

Foot strike type followed similar patterns, where RF striking runners demonstrated greater HV TD than NRF striking runners (+6.0 ms, effect SEM: 2.6 ms) and greater BP:LU ratios (+0.11, effect SEM: 0.02). Similarly, the NRF striking runners demonstrated better overall fit to the SM model, with an error reduction of 41.7 N (effect SEM: 13.9). Foot strike type did not significantly influence SB.

At the faster speed, the Kenyan runners had a decrease in their SB (-5.9%; effect SEM: 0.8%). Their HV TD approached zero (1.1 ms; effect SEM: 0.9 ms), and the BP:LU approached unity (1.01, effect SEM: 0.02). All model results are compiled in Table 8.

3.4.2 Spring-Mass Behavior

The Kenyan runners ran with lower absolute peak vertical forces (1482 vs. 1759 N, effect SEM: 98 N), but higher body-weight specific forces (2.74 vs. 2.46 BW, effect SEM: 0.10 BW). Their ground contact times were shorter (213 vs 244 ms, effect SEM: 5 ms) and their estimated touchdown angles steeper (67.1° vs. 64.2°, effect SEM: 0.6°). This resulted in equivocal absolute leg stiffnesses and higher relative leg stiffnesses (16.5 vs. 13.0 BW/L_0, effect SEM: 0.6 BW/L_0). This distinction was further observed in the vertical stiffnesses, where the absolute measure was lower (18.8 vs. 22.7 kN/m, effect SEM: 1.3 kN/m) with equivocal relative vertical stiffnesses. The effective stiffness as estimated by NLR was not different between the groups, and neither was the effective touchdown angle or effective leg length. The effective contact time was similarly shorter in the Kenyan runners (200 ms vs. 227 ms, effect SEM: 2 ms).

The barefoot condition elicited lower absolute and relative peak vertical forces in all runners (-30 N and -0.05 BW, effect SEM: 6.2 N and 0.01, respectively). Contact times were shorter in both groups, and there was a significant interaction effect, where the Kenyan group was less affected by the condition (-1 ms and -7 ms, interaction SEM: 2 ms). Similarly, estimated touchdown angles were steeper, with the Kenyan group less affected (+0.5° and +1.0°, interaction SEM: 0.02°). These temporal changes resulted in higher absolute and relative leg and vertical stiffnesses across both groups, where k_{leg} increased by 0.7 kN/m (effect SEM: 0.1 kN/m), k_{rel} by 1.0 BW/L_0 (effect SEM: 0.1 BW/L_0), k_{vert} by 2.0 kN/m (effect SEM: 0.4 kN/m), and $k_{vert\text{-}rel}$ by 3.0 BW/L_0 (effect SEM: 0.6 BW/L_0). In the NLR modeling, the barefoot effect was not significant for stiffness, touchdown angle, or leg length, but the effective contact time was similarly estimated as being 5 ms shorter (effect SEM: 1 ms).

Non-rearfoot striking runners had similar absolute but higher relative peak vertical forces (+0.27 BW, effect SEM: 0.10 BW). Foot strike type had no effect on contact time, touchdown angle, or any of the stiffness measures. The NLR method modeled slightly shorter effective contact times in the NRF striking runners (–3 ms, effect SEM: 1 ms).

At 20 km/hr, the Kenyans ran with significantly higher absolute and relative peak vertical forces (+99 N and +0.19 BW, effect SEM: 9.3 N and 0.02, respectively). Their contact times were shorter (-52 ms, effect SEM: 1 ms) and their touchdown angles shallower (-6.5°, effect SEM: 0.02°). Their leg stiffnesses, both absolute and relative, were unchanged at the faster speed. Their vertical stiffnesses increased (13.4 kN/m and 22.3 BW/L_0, effect SEM: 0.6 kN/m and 0.8 3.0 BW/L_0, respectively). The effect of speed was only significant on the effective contact time parameter in the NLR analysis (-44 ms, effect SEM: 2 ms), with effective stiffness, touchdown angle, and leg lengths remaining unaffected.

Figure 11: Iterative SAEM model-fitting for the NLR-based parameter estimation process. Note that the units for the four parameters are N/m, radians, meters, and seconds, respectively.

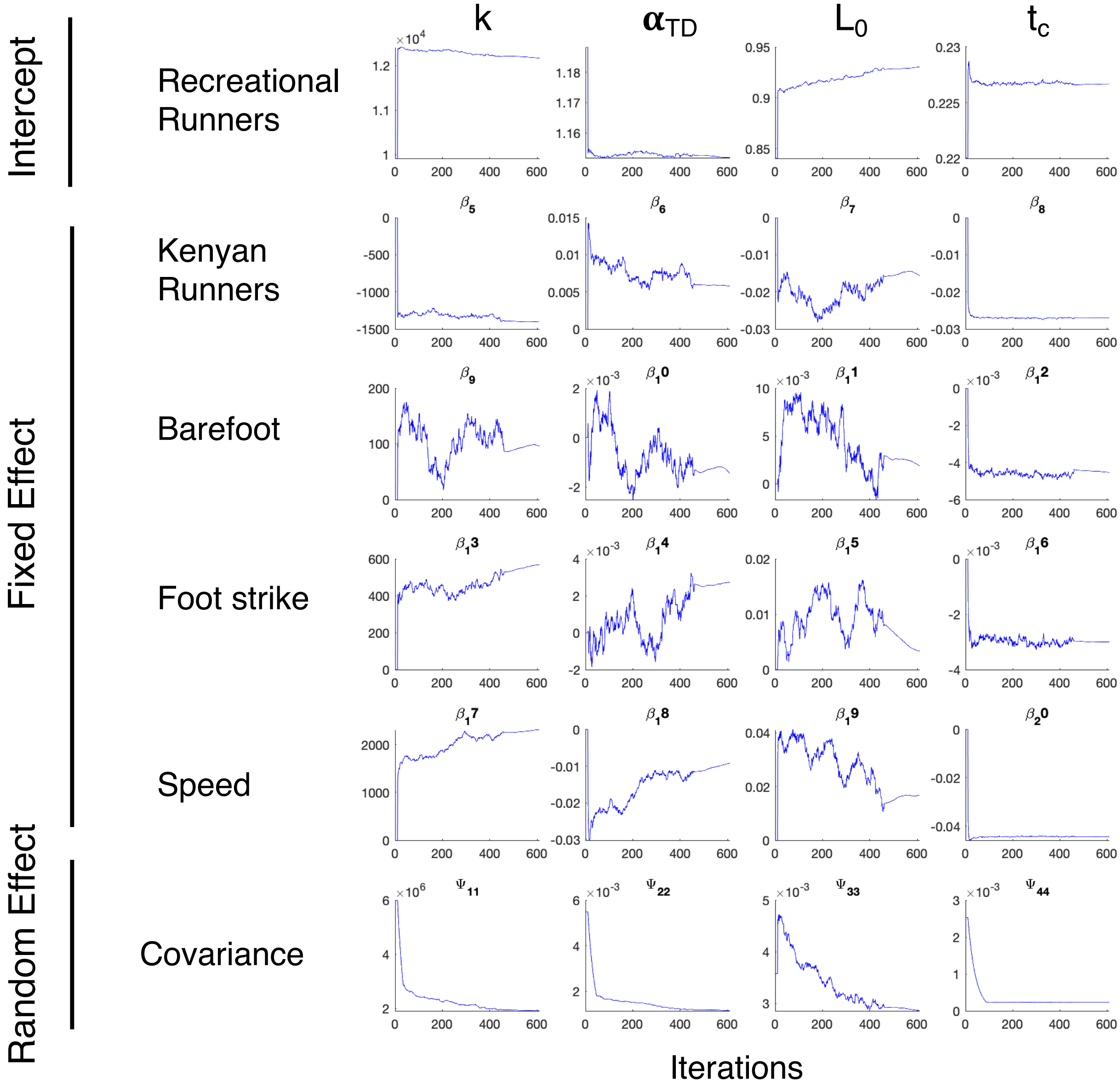

Figure 12: GRF timing differences in two rearfoot striking subjects in each shoe condition at 12 km/hr. Blue solid lines are the observed vGRF, and blue dashed lines indicate the time it reaches its peak. Red solid lines are the observed hGRF, and the red solid lines indicate the time that the hGRF transitions from braking to propulsion.

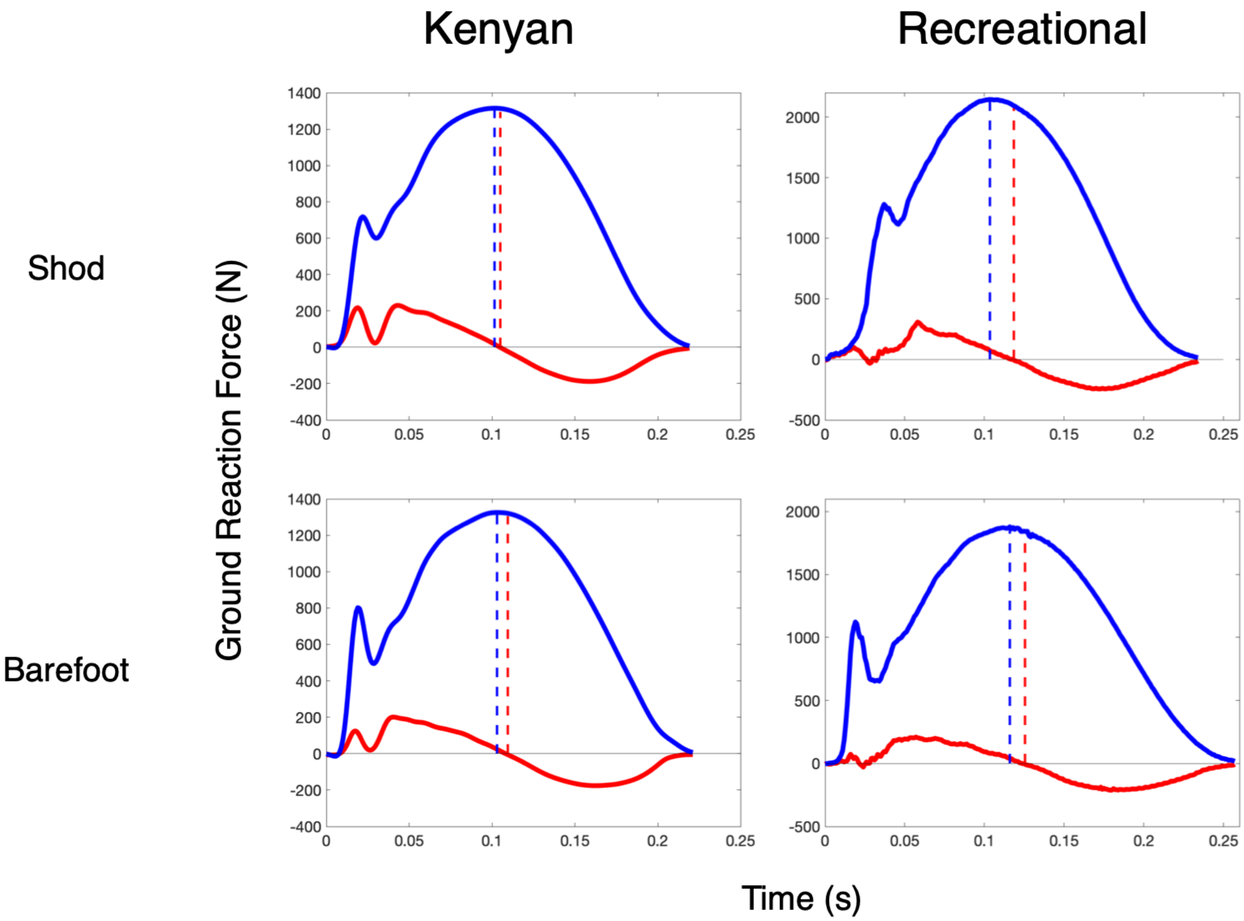

Figure 13: Spring-mass fits for four subjects from each cohort and foot strike type in the shod condition at 12 km/hr. The solid line (blue for Kenyan runners, red for Recreational runners) is the observed vGRF, and the dashed line is the best-fit spring mass vGRF estimated via NLR.

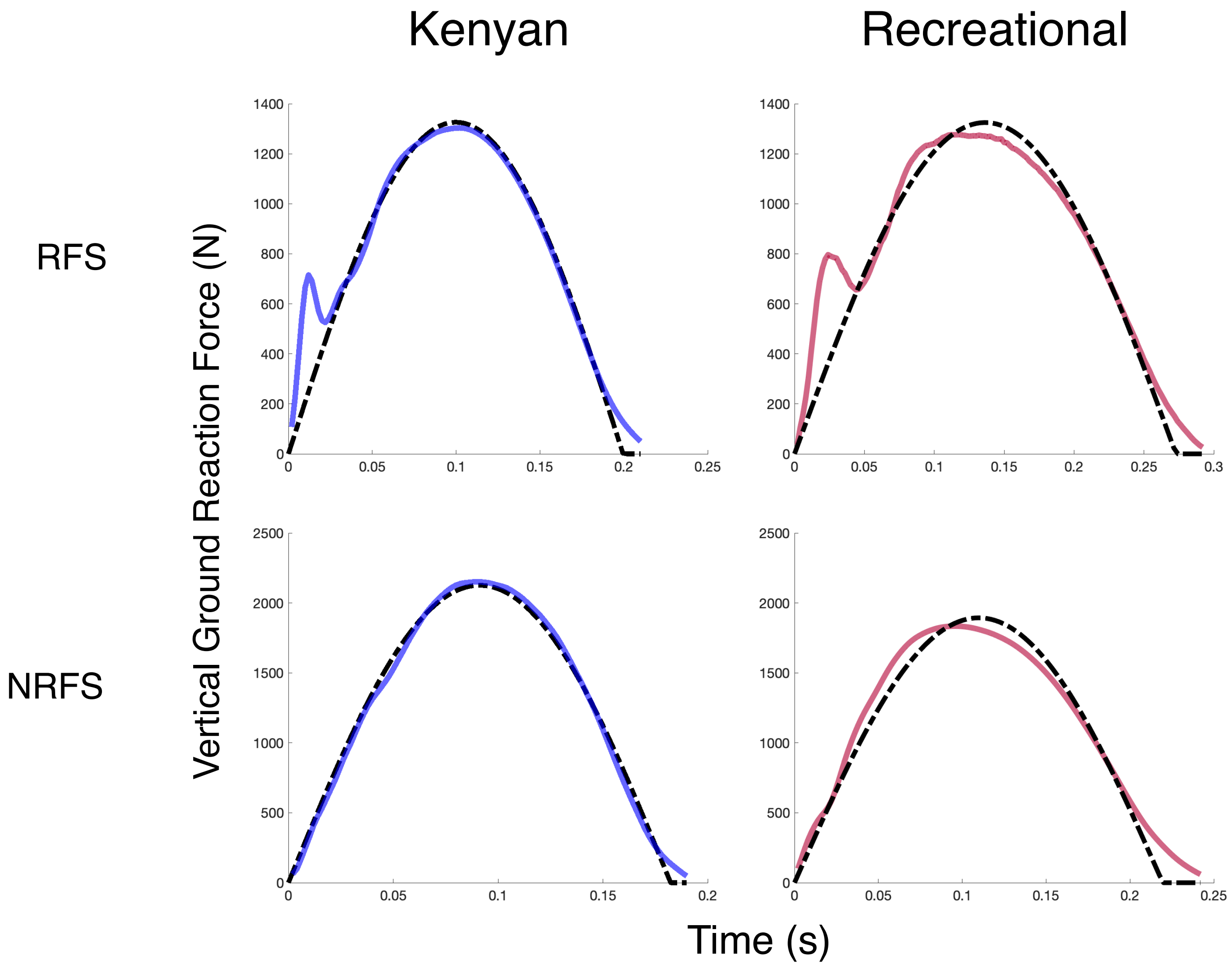

A	SB (%)	sem	p	sig.
Recreational	92.7	0.8	-	
Kenyan	+2.7	1.3	0.048	✻
Barefoot	+0.3	0.5	0.557	
Cohort x BF	+0.5	1.1	0.636	
NRF strike	-2.0	1.3	0.145	
20 km/hr (Ken.)	-5.8	0.8	<0.001	✻✻✻

B	HV TD (ms)	sem	p-value	sig.
Recreational	16.3	1.6	-	
Kenyan	-6.3	2.6	0.018	✻
Barefoot	-1.8	0.6	0.003	✻✻
Cohort x BF	+3.5	1.2	0.003	✻✻
NRF strike	-6.0	2.6	0.026	✻
20 km/hr (Ken.)	-8.9	0.9	<0.001	✻✻✻

C	BP:LU	sem	p-value	sig.
Recreational	1.32	0.03	-	
Kenyan	-0.11	0.05	0.047	✻
Barefoot	-0.03	0.01	0.048	✻
Cohort x BF	+0.05	0.03	0.041	✻
NRF strike	-0.11	0.05	0.037	✻
20 km/hr (Ken.)	-0.20	0.02	<0.001	✻✻✻

D	SM Fit (RMSE)	sem	p-value	sig.
Recreational	160.6	8.6	-	
Kenyan	-37.7	14.3	0.012	✻
Barefoot	14.1	6.5	0.034	✻
Cohort x BF	-41.7	13.9	0.005	✻✻
NRF strike	19.3	8.9	0.033	✻
20 km/hr (Ken.)	-27.6	13.0	0.038	✻

Table 8 Elastic similarity across measures: (a) similarity to a symmetric bounce (SB), (b) the time difference between the horizontal force transition and the vertical force peak (HV TD), (c) this braking to propulsion timing difference normalized to the vertical loading to unloading time (BP:LU), and (d) the fit of the subject's vGRF to that of a best-fit spring-mass system (SM Fit). Estimates for each effect (cohort, shoe condition, cohort x shoe interaction, foot strike type, and speed) and their standard error (sem) are provided. Statistical significance of each effect is indicated as: ✻ p <0.05, ✻✻ p<0.01, and ✻✻✻ p<0.001

A	**F_{max} (N)**	**sem**	**p**	**sig.**	**B**	**F_{max} (BW)**	**sem**	**p**	**sig.**
Recreational	1759.2	59.9	-			2.46	0.06	-	
Kenyan	-277.2	97.6	0.007	✻✻		0.28	0.10	0.005	✻✻
Barefoot	-30.0	6.2	<0.001	✻✻✻		-0.05	0.01	0.000	✻✻✻
Cohort x BF	-13.7	12.4	0.271			-0.04	0.02	0.096	
NRF strike	133.7	99.1	0.185			0.27	0.10	0.009	✻✻
20 km/hr (Ken.)	99.1	9.3	<0.001	✻✻✻		0.19	0.02	0.000	✻✻✻

C	**t_c (ms)**	**sem**	**p**	**sig.**	**D**	**α_{TD} (°)**	**sem**	**p**	**sig.**
Recreational	244	3	-			64.2	0.4	-	
Kenyan	-31	5	<0.001	✻✻✻		2.9	0.6	0.000	✻✻✻
Barefoot	-7	1	<0.001	✻✻✻		1.0	0.1	0.000	✻✻✻
Cohort x BF	6	2	<0.001	✻✻✻		-0.5	0.2	0.024	✻
NRF strike	-4	5	0.494			0.4	0.6	0.494	
20 km/hr (Ken.)	-52	1	<0.001	✻✻✻		-6.5	0.2	0.000	✻✻✻

E	**k_{leg} (kN/m)**	**sem**	**p**	**sig.**	**F**	**k_{rel} (BW/L_0)**	**sem**	**p**	**sig.**
Recreational	10.2	0.3	-			13.5	0.4	-	
Kenyan	-0.5	0.5	0.394			3.0	0.6	<0.001	✻✻✻
Barefoot	0.7	0.1	<0.001	✻✻✻		1.0	0.1	<0.001	✻✻✻
Cohort x BF	-0.2	0.2	0.167			-0.1	0.3	0.623	
NRF strike	0.4	0.5	0.440			0.6	0.6	0.314	
20 km/hr (Ken.)	-0.2	0.1	0.179			-0.3	0.2	0.117	

G	**k_{vert} (kN/m)**	**sem**	**p**	**sig.**	**H**	**$k_{vert\ rel}$ (BW/L_0)**	**sem**	**p**	**sig.**
Recreational	22.7	0.8	-			30.1	0.9	-	
Kenyan	-3.8	1.4	0.008	✻✻		1.7	1.5	0.272	
Barefoot	2.0	0.4	<0.001	✻✻✻		3.0	0.6	<0.001	✻✻✻
Cohort x BF	0.8	0.8	0.300			1.7	1.1	0.116	
NRF strike	-1.0	1.4	0.488			-1.8	1.5	0.260	
20 km/hr (Ken.)	13.4	0.6	<0.001	✻✻✻		22.3	0.8	<0.001	✻✻✻

Table 9 Absolute and relative spring-mass measures: (a) absolute and (b) relative maximal vertical force (F_{max}), (c) observed contact time (t_c), (d) estimated touchdown angle (α_{TD}), (e) absolute leg stiffness (k_{leg}), (f) relative leg stiffness (k_{rel}), (g) absolute vertical stiffness (k_{vert}), and (h) relative vertical stiffness ($k_{vert\ rel}$). Estimates for each effect (cohort, shoe condition, cohort x shoe interaction, foot strike type, and speed) and their standard error (sem) are provided. Statistical significance of each effect is indicated as: ✻ $p < 0.05$, ✻✻ $p < 0.01$, and ✻✻✻ $p < 0.001$

	k^* (kN/m)	sem	p	sig.
Recreational	12.2	0.6	-	
Kenyan	-1.4	1.2	0.245	
Barefoot	0.1	0.8	0.902	
NRF strike	0.6	0.9	0.527	
20 km/hr (Ken.)	2.3	2.6	0.366	

	α_{TD}^* (°)	sem	p-value	sig.
Recreational	66.0	4.0	-	
Kenyan	0.3	6.3	0.958	
Barefoot	-0.1	4.9	0.987	
NRF strike	0.2	5.5	0.978	
20 km/hr (Ken.)	-0.5	9.1	0.954	

	L_0^*	sem	p-value	sig.
Recreational	0.93	0.29	-	
Kenyan	-0.02	0.44	0.972	
Barefoot	0.00	0.36	0.996	
NRF strike	0.00	0.40	0.993	
20 km/hr (Ken.)	0.02	0.64	0.979	

	t_c^* (ms)	sem	p-value	sig.
Recreational	227	1	-	
Kenyan	-27	2	<0.001	✻✻✻
Barefoot	-5	1	0.001	✻✻
NRF strike	-3	1	0.045	✻
20 km/hr (Ken.)	-44	2	<0.001	✻✻✻

Table 10 Effective spring-mass measures as approximated by nonlinear regression and the corresponding fixed effect estimation for each parameter for effective stiffness (k^*), effective touchdown angle (α_{TD}^*), effective leg length (L_0^*), and effective contact time (t_c^*). Estimates for each effect (cohort, shoe condition, foot strike type, and speed) and their estimated standard error (sem) are provided. Statistical significance of each effect is indicated as: ✻ $p < 0.05$, ✻✻ $p < 0.01$, and ✻✻✻ $p < 0.001$

3.5 Discussion

3.5.1 Summary

We compared the elastic spring-mass behavior of high-performing Kenyan distance runners to a cohort of recreational runners in shod and barefoot conditions, assessing similarity to the spring-mass system via the "symmetric bounce" similarity metric and three new additional measures of similarity. Furthermore, we characterized their systemic spring mass characteristics with traditional measures and nonlinear regression analyses. Overall, the Kenyan distance runners demonstrated greater similarity to the simple, elastic spring-mass system than recreational runners, and this similarity persisted after controlling for foot strike type. They exhibited shorter contact times in both conditions, with similar absolute peak vertical forces but greater mass-specific forces. Thus, their absolute systemic leg stiffnesses were generally similar, but their relative stiffnesses were higher. Together, this would suggest that they achieved similar systemic behavior for a given speed with lower body masses and smaller statures, and their resulting behavior more closely mimicked energy-conserving, ideally elastic systems.

3.5.2 Elastic Similarity

3.5.2.1 Similarity of Kenyan vs. Recreational Runners

These results support our initial hypothesis that Kenyan distance runners would behave more like the simple spring-mass system. This difference was apparent across all metrics, but it was most pronounced in the HV TD and SM Fit measures. Their braking-to-propulsion transition occurred 6.3 ms closer to their vertical peak, which indicates greater coordination between their horizontal and vertical kinetic energy fluctuations. Here, the recreational cohort was continuing to do negative mechanical work in the horizontal plane (i.e., braking) after they had finished doing negative work in the vertical plane and had begun doing positive work (i.e., unloading). This kinetic discrepancy represented 6.7% of their total ground contact time as compared to the only 4.8% of the Kenyans' (see Figure 16). Moore and colleagues observed a similar phenomenon in recreational runners, where a greater alignment of the leg axis and the resultant ground reaction force vector corresponded to improved economy (Moore et al., 2016). Here, we observed better coordination of the GRF components in a group capable of superior running performances. Furthermore, their SB was also 2.7% more similar to an elastic system. This was the same magnitude of difference between teenagers and adults as observed by Cavagna and colleagues (Cavagna & Legramandi, 2015). Finally, in comparing their overall vGRF curves to spring-mass vGRFs, the Kenyans had a model error that was 24% lower than the recreational runners. These findings together suggest that the Kenyan runners coordinate their overall mechanical behavior to decelerate and accelerate their center-of-masses in a smoother, more coordinated fashion.

The differences between the groups were still apparent after controlling for foot strike type. We anticipated that runners with a RF strike pattern would generally exhibit lower absolute similarity, especially in the SM Fit measure, due to the presence of the impact peak and greater initial vertical loading rates (Cavanagh & Lafortune, 1980; Lieberman et al., 2010). This hypothesis was supported, as across both groups, the NRF striking runners had a 29% lower model error in comparing their vGRF to that of a spring-mass system and a braking-to-propulsion transition that was 6 ms closer the loading-to-unloading transition. While a greater proportion of the Kenyan runners exhibited a NRF strike pattern (47% vs. 27%), the effects were independently significant, where RF striking Kenyan runners were more similar the spring-mass system than their RF-striking recreational counterparts (e.g., Figure 13). This would suggest that independent of foot strike type, the Kenyan runners move through the stance phase with better energetic coordination and spring-mass similarity.

These kinetic observations parallel the musculotendinous observations of Sano and colleagues who found more efficient elastic mechanics in elite Kenyan runners (Kunimasa et al., 2014; Sano et al., 2013a; Sano et al., 2015). They observed that the Kenyan runners had longer Achilles tendon structures, and that in hopping, they exhibited lower overall SS amplitudes and fascicle length changes of their medial gastrocnemius (MG) muscle with greater SS ratios during pre-activation and contact. Together, this resulted in greater maximal hopping heights, which the investigators suggested was indicative of greater efficiency in elastic energy utilization (Sano et al., 2013b). The same patterns were later observed in running, where a group of elite Kenyan runners had lower SS amplitudes in the MG but greater tendon contribution to the overall muscle-tendon unit's shortening as compared to a group of similarly elite Japanese distance runners. Furthermore, they again exhibited lower pre-activation-to-braking muscle activity, facilitating greater isometric work of the MG during contact (Sano et al., 2015). Together, this indicated that their lower limbs were more efficiently transferring and recycling the kinetic energy from the flight phase to elastic strain energy in the stance phase. The lower activations in the MG and tibialis anterior in the braking phase may help explain our observations of better alignment of the horizontal braking phase to the start of vertical unloading. The lower muscle activity may prevent unnecessary extension of the braking phase or facilitate more controlled coordination of the forward and vertical center-of-mass decelerations. Finally, they also observed lower foot-lever-ratios in the elite Kenyan runners compared to their Japanese counterparts, a measure of the Achilles moment-arm to the length of the forefoot (Kunimasa et al., 2014). This may support the proposition of Maykranz and Seyfarth that a compliant ankle and the foot's lever action contribute to takeoff-landing asymmetries and deviance from a symmetric bounce in running (Maykranz & Seyfarth, 2014). With these two observation, one could hypothesize that longer foot levers may also cause greater deviation from elastic mechanics in the final moment of stance, perhaps further explaining some of the spring-mass similarity exhibited by the Kenyans here.

3.5.2.2 Effect of Footwear

In both cohorts, the barefoot condition elicited mixed results with respect to the runners' similarity to the spring-mass systems. The effects of running barefoot on the HV TD and BP:LU metrics indicated a small but significant improvement in the coordination of the vertical and horizontal force components in the recreational runners, reducing the braking and loading discrepancy by 1.8 ms, or 1% of their gait cycle. However, the cohort interaction was significant and opposite, indicating that the Kenyan runners had a slight decrement in that timing difference, increasing it by 1.7 ms, or 1% of their gait cycle. The time-normalized BP:LU ratio followed these patterns in both cohorts. This was unexpected, as we anticipated that the transition timings would be unaffected by the footwear condition, as Divert and colleagues previously observed braking times to be unchanged in barefoot conditions (Divert et al., 2005). However, the greater initial loading rates common with habitually shod runners in a barefoot conditions may explain the recreational runners' shorter relative braking times (Tam et al., 2016), and the greater prevalence of habitual barefoot activity in childhood and adolescence in Western Kenya may have influenced the variable response in the Kenyan cohort (Aibast et al., 2017; Lieberman et al., 2015). The SB was unaffected by the footwear condition. Legramandi and colleagues observed the SB to decrease in runners as impact accelerations increased (as is common with barefoot running), but here, the changes may have been small enough, and perhaps offset by compensatory changes in upward velocity during toe-off, so as not to substantially affect the overall symmetry measure (Legramandi et al., 2013). Finally, the SM Fit decreased in the recreational runners by 9%, but improved in the Kenyan runners by 11%. The reason for this deviation may be similar to that observed in the HV

TD patterns, where greater vertical impact transients associated with barefoot running in the habitually shod recreational cohort may have driven the decreasing model similarity, whereas barefoot familiarity in the Kenyans may have enhanced fit (Lieberman et al., 2010; Tam et al., 2016).

3.5.2.3 Effect of Speed

Similarity to the spring-mass system increased at 20 km/hr in the measures of energetic coordination (HV TD and BP:LU) and fit within the Kenyan runners, and decreased in the symmetry metric (SB). The former findings supported our initial hypotheses, but latter finding was partially unexpected, as Cavagna observed that the work duration symmetry in the stance phase increased with speed, with braking and pushing times approaching unity above 14 km/hr (Cavagna, 2006). However, he also observed the ratio of the COM's maximal downward velocity to its upward velocity to decrease at faster speeds, contributing to an "asymmetric rebound" that increased at faster speeds. This increasing asymmetry in the maximal downward and upward vertical velocities likely offset and outweighed the increasing symmetry in work durations here, resulting in an overall decrease in the SB metric. The HV TD and BP:LU metrics approached perfect coordination at the faster speed here, with a braking and loading difference of only 1.1 ms and the ratios of 1.01 for the horizontal and vertical acceleration changes. Moreover, the SM Fit metric was significantly improved at the faster speed, with the model fitting error decreasing by a further 22%. Cavagna hypothesized that the speed-dependent increase in work duration energetic symmetry was due to greater isometric work of the lower limb muscles at higher speeds, with greater tendinous contributions. Thus, a greater proportion of the mechanical work would be performed by the storage and release of elastic strain energy. Together, these observations support the idea that runners may behave more similarly to simple spring-mass systems at faster speeds.

3.5.2.4 Differences Between Metrics

This investigation assessed a runner's similarity to the spring-mass system with several metrics that each characterized distinct components of the elastic system's dynamics. The first metric, SB, is a measure of energetic symmetry within the stance phase (Cavagna & Legramandi, 2015). It is an average of the two common asymmetries identified by Cavagna, which are the timing of the braking and pushing (center-of-mass deceleration and acceleration, respectively) and maximal upward velocity in the latter phase of stance and the maximal downward velocity in the initial phase (Cavagna, 2009). These two values are equal in an ideal spring-mass system, as energy is conserved throughout the stance phase with perfectly elastic dynamics. We presented three additional new metrics here that move beyond the symmetry of the step to quantify the energetic coordination and kinetic similarity to the simple system throughout stance. The first, the HV TD, is a measure of alignment of forward and vertical energy fluctuations, as these change perfectly in phase in a spring-mass system (Figure 2 and Figure 10). A symmetric bounce does not necessarily demand perfect coordination in the vertical and horizontal force progressions (the timing, relative phase shifts, and magnitudes of each component could theoretically offset each other for equal braking and pushing), nor does a lack of difference in the HV TD imply a symmetric bounce. The BP:LU ratio normalizes these energetic timings in each phase of stance to each other so that discrepancy between the braking and loading times is relative to its counterpart in the latter half of stance. We observed this metric to follow the same patterns of the HV TD, indicating that the trends we observed in the absolute timing differences we not due to contact time differences. The final metric, the SM Fit, assesses the overall similarity of the runner's vGRF shape to that of an ideal spring-mass model fit to his or her behavior via NLR (see Chapter 2). This characterizes the constancy of the loading and unloading progression, which is smooth and symmetric in a spring-mass system as the linear spring is dynamically compressed and released. A perfect SM Fit would indicate symmetry in the vGRF component, but it does not necessarily imply a perfect SB metric, as the horizontal braking and propulsion could be asymmetric. It is conceptually similar to a force-displacement curve, which would be a perfectly linear line in an ideal system, but it is less biased by large deviations in the early and later phases of stance, as the force magnitudes are low. A force-displacement assessment is heavily influenced by these aspects, as the force magnitudes are low and the displacements comparatively large (Cavagna & Legramandi, 2015; Maykranz & Seyfarth, 2014). The SM Fit is influenced by common characteristics of vGRF curves, such as impact transients and take-off asymmetries, but it distinguishes the "smoothness" of the force progression despite these characteristics, capturing the overall systemic rise and fall of the curve. As anticipated, we saw NRF striking runners exhibit better SM Fits, but the measure was able to characterize better a better fit among the RF striking Kenyan runners. This supports the notion that within foot strike types, runners can behave more or less like spring-mass systems. Together, this collection of measures characterizes the energetic symmetry, coordination, and consistency of a runner during stance against a spring-mass template.

3.5.3 Spring-Mass Behavior

3.5.3.1 Absolute vs. Relative Characteristics

Both cohorts of runners produced vGRFs with similar peak magnitudes, but the maximal mass-specific forces of the Kenyan runners were higher by 0.3 BW. Furthermore, they generated these forces more rapidly, as their ground contact was 31 ms, or 13%, shorter. This parallels observations that elite Kenyan runners generally exhibit short contact times (Kong & de Heer, 2008), but it's unclear if this is a characteristic of their performance capacity or their anthropological background, as Sano and colleagues observed equivocal contact times between elite Kenyan and elite Japanese runners (Sano et al., 2015). These shorter contacts corresponded to steeper touchdown angles. Together, this resulted in equivocal leg stiffnesses but lower vertical stiffnesses among the Kenyan cohort. However, when scaled to body weight and leg length, the Kenyan runners had higher relative leg stiffnesses but equivocal relative vertical stiffnesses. This indicates that for the same speed, the Kenyan runners effectively maintained the same overall spring-mass behavior with shorter contact times and greater vertical compliance despite lower body mass and shorter stature. That is, they produced the same systemic behavior with smaller bodies. Interpreted relatively, their systemic stiffnesses were therefore higher and vertical compliance the same due to the higher weight-specific forces and shorter ground contact. Leg stiffness is generally thought to scale with body mass across the animal kingdom (Farley et al., 1993), whereas relative stiffness is thought to remain constant (Blickhan & Full, 1993). With respect to performance, greater leg stiffness has been associated with better running economy in a homogenous population (Dalleau et al., 1998), and vertical stiffness was observed to be higher in better runners (da Rosa et al., 2019). The higher performance capacity of the Kenyan runners here could therefore be due in part to their ability to produce the same systemic spring-mass behavior via higher relative forces and relative leg stiffnesses with smaller frames.

3.5.3.2 Effect of Footwear

The barefoot condition altered spring-mass behavior in both groups of runners. Across groups, the subjects produced absolute and relative forces that were lower by 2%. This is consistent with some previous observations (Divert et al., 2005), though others have found peak forces to be unaffected in the barefoot condition (Divert et al., 2008; Tam et al., 2016). Contact times in the recreational cohort were 3% lower but nearly equivocal in the Kenyan runners. This small decrease in the recreational group is consistent with previous observations in habitually shod runners

(Burkett, Kohrt, & Buchbinder, 1985; Divert et al., 2005). Similarly, touchdown angles were 1% steeper in the recreational runners with less of an effect in the Kenyan runners. These observations parallel the findings in the elastic similarity measures, where the Kenyans were less affected by the barefoot condition than their recreational counterparts. Again, this is likely due to greater familiarity and experience throughout development with barefoot activity (Aibast et al., 2017; Lieberman et al., 2015). Runners in both groups had consistently higher leg and vertical stiffnesses in the barefoot conditions. While this is at odds with the common notion that runners adjust leg stiffness to maintain a constant vertical stiffness on varying surfaces (Ferris et al., 1998), it mirrors previous observations that leg and vertical stiffnesses increase together specifically in response to barefoot running. This suggests that the systemic spring-mass adjustments runners make to new surface conditions is distinct between shod and barefoot conditions.

3.5.3.3 Effect of Speed

At the faster speed, the Kenyan runners ran with 7% greater peak vertical forces, 24% shorter contact times, and 9% shallower touchdown angles. These are predictable patterns in response to faster running speeds (Nilsson & Thorstensson, 1989; Weyand et al., 2000). Their leg stiffnesses were unchanged at the faster speeds, which is a phenomena observed across species (Farley et al., 1993). Their vertical stiffness increased at the faster speed, which is again, consistent with convention (McMahon & Cheng, 1990).

3.5.3.4 Nonlinear Regression Estimates

The NLR modeling of the runners provided a similar, albeit more conservative, characterization of the systemic behavior of the runners. The effective stiffness of the runners was unchanged between cohorts, shoe conditions, foot strike types, or speeds. This was similar to the patterns observed in the traditional absolute stiffness observations, where only the barefoot condition elicited a small but significant (7%) increase in leg stiffness. As the traditional measure is dependent on the observed contact time for its estimation, this difference could have been driven by the small decrease in the observed t_c. The effective stiffness estimate was higher than the traditional leg stiffness value (12.2 kN/m vs. 10.2 kN/m), which again, may be due to the dependencies of traditional measures on fixed assumptions relating to $t_{c,}$, leg length, and touchdown angle approximations (see Chapter 2). When assessed as a relative effective stiffness between groups, this would follow the same pattern as observed in the traditional estimates, where the Kenyans had higher relative stiffnesses. Here, using the effective leg length estimates from the NLR model, the relative group values would correspond to 21.0 BW/L_0 in the Kenyan runners vs. 16.0 BW/L_0 in the recreational runners.

The effective touchdown angles and leg lengths as estimated by NLR were unchanged across cohorts and conditions. This differed from the traditional measures, where the touchdown angle was different among groups, footwear condition, and speed. However, again, the traditional approximation for touchdown angle is simply a relation between contact time and leg length for a given speed, so the changes in the traditional measure are simply a reflection of the contact time effects. Here, the model suggest uncertainty as to whether that angle is changing between cohorts and conditions.

The effective leg length was similarly unchanged between groups and conditions. Upon initial consideration, this was at odds with the traditional measure, as the height-approximated leg lengths of the Kenyan cohort was lower than the Recreational runners due to their smaller stature (90.4 cm vs. 93.2 cm, 95% confidence interval for the difference: 0.4 – 5.3 cm). However, the conventional approximation of 53% of the standing height (Winter, 2005) may not be universal here. Larsen and colleagues observed adolescents in Western Kenya to have proportional leg lengths of 55.4% of standing height, which was also consistent with their unpublished observations in elite Kenyan runners of the area (Larsen et al., 2004). This was greater than the 52.8% observed in elite Caucasian runners, which is consistent with the conventional estimate of 53% (Svedenhag & Sjodin, 1994). Furthermore, Mooses and colleagues observed that within elite Kenyan runners, proportional leg length was associated with better racing performances (Mooses et al., 2015). This further supports the comparative models of Pontzer, who proposed that mass-specific longer limbs are associated with a lower cost of transport across species (Pontzer, 2007). Here, our effective leg length estimate was 93.1 cm for both cohorts, which would correspond to proportional effective lengths of 52.9% in the recreational runners and 54.6% in the Kenyan runners. This could serve as a further explanation for some of the difference in performance capacities between groups, and it suggests opportunity for future investigation into the relation of effective limb lengths and performance.

The effective contact times estimated by NLR followed the same patterns as the observed contact times, where the Kenyan cohort, barefoot condition, and faster speed all elicited shorter ground contacts. As expected, the effective contact times were consistently shorter than the observed values. Because the NLR model uses the entirety of the vGRF curve to inform the spring-mass fit, it is less biased by the distinct non-linear elasticity in the final moments prior to toe-off that extend traditional measures of contact time (see Figure 13). This contributes to the observed asymmetry between braking and propulsive phases (Cavagna, 2006), and is thought to be due to compliant ankle mechanics (Cavagna et al., 2008a; Maykranz & Seyfarth, 2014). This suggests that the NLR estimate of effective contact time represents a systemic spring-mass contact measure, and that here, that measure follows the same trends as the observed values.

3.5.4 Limitations

Several important considerations should be made when interpreting the findings observed here. The first corresponds to the heterogeneity of the two groups. Because the cohorts were elite Kenyan runners and non-elite recreational South African runners, it is impossible to ascribe the differences observed here to the performance capacity or demographic. The purpose of the study was to characterize elastic behavior and spring-mass similarity in two very distinct populations of runners so as to explore the sensitivity of the new metrics presented, but it came at the cost of confounding the effect attribution. Moreover, the performance homogeneity was high among groups, as was the heterogeneity between groups, preventing this measure from being used as a covariate to more distinctly model the effects. Future investigations within elite populations or across a greater continuum of performance capacity could reveal further insight into the mechanisms and relations of spring-mass behavior and performance observed here.

The post hoc nature of the investigation must also be taken in to consideration. As the study was conducted on kinetic data previously collected, we were limited by both sample size and design. The effects were generally distinct enough for detection across the measures of interest, but it's unclear whether some of the unaffected factors, such as the some of the NLR-estimated fixed effects, were truly indicative of no effect or the result of Type II error. We attempted to mitigate this by assessing repeated steps within subjects, but future investigations into these behaviors would benefit from using these findings to anticipate effect and sample sizes. Similarly, because the investigation was performed retrospectively, we did not have data on the recreational runners at the faster speeds. Given the interactions observed between cohorts and footwear conditions, it would be interesting to explore whether the recreational runners change their spring-mass similarity and behavior in the same fashion as the Kenyan runners. Furthermore, the investigations did not measure the anthropometric leg lengths of the runners initially, forcing us to use the height-estimations here. The previous observations of proportional differences in Kenyan runners versus Caucasian runners discussed above would suggest that this conventional assumption may not be accurate in this population (Larsen et al., 2004). The NLR modeling is independent of this parameter, and it further suggested some discrepancy in proportional leg length between the populations. Given its potential implications for performance (Mooses & Hackney, 2017) and its bearing on traditional spring-mass measures (Morin et al., 2005), future investigations in this population would benefit from collecting this anthropometric measure, and further exploration into its relation to economy and performance is warranted.

Finally, the NLR modeling revealed that estimates for the effective touchdown angle and leg length were highly covaried within each of the fixed effect categories (see Figure 14). While this could be expected given the non-singularity of those two measures in independent steps, the random-effect component was unable to resolve this here. We therefore need to interpret the above discussions of leg length estimates with caution. To mitigate this, one could fix one of the parameters, either leg length or touchdown angle or fit a fit a three-parameter model combining the two terms (as discussed in Chapter 2). However, this would come at the cost of capturing essential fluctuations in each parameter that may occur within individuals or across effects. Future work in refining the model architecture, the fixed and random effect structures, and the estimation procedures may build on this to improve the parameter sensitivity.

Figure 14: Correlation-covariance matrix for the NLR model's fixed effects. Note that within each fixed effect grouping, effective leg length and touchdown angle tend to be highly covaried. Effective stiffness and contact time are consistently independent of the other parameters.

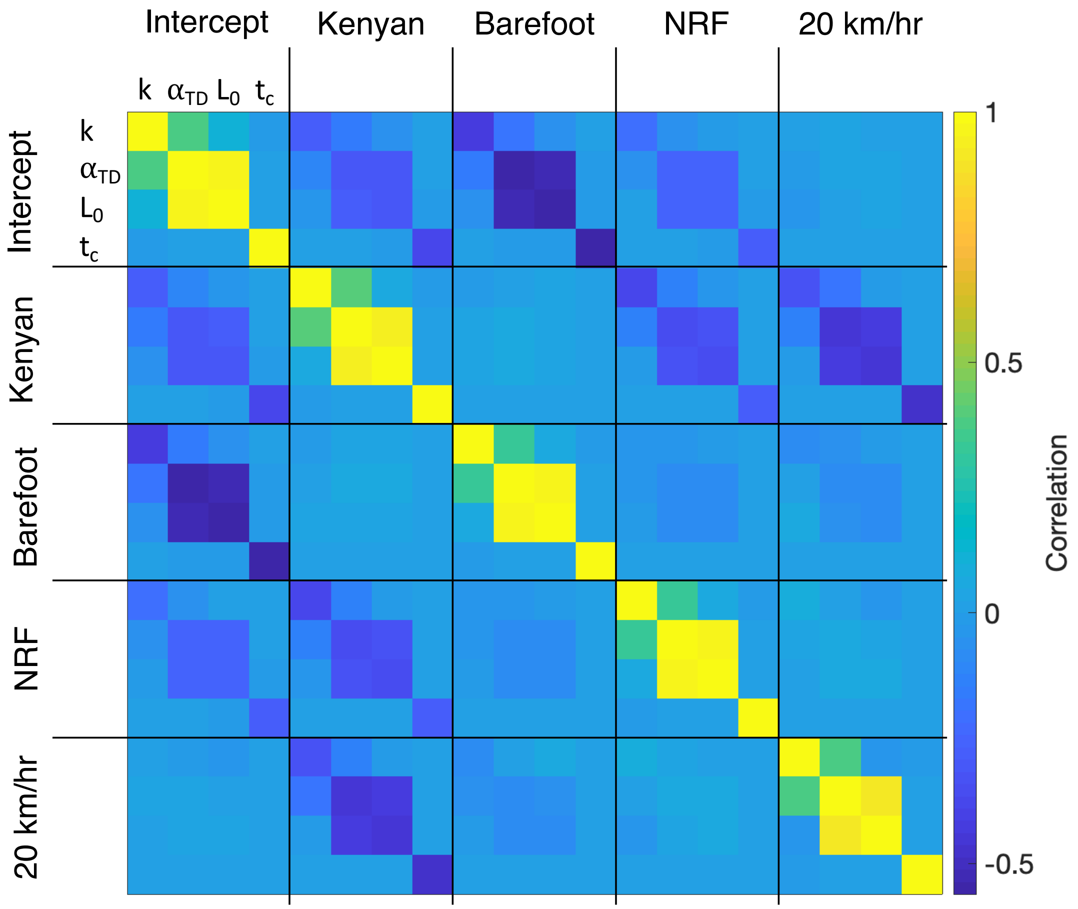

3.6 Conclusion

We examined the systemic spring-mass similarity and behavior in elite Kenyan and recreational distance runners. We used traditional measures for each characteristic, and we further presented and applied several novel metrics and methods. Overall, the Kenyan runners exhibited kinetic patterns that more closely resembled simple linearly elastic spring-mass dynamics. They demonstrated greater similarity to a symmetric bounce, and they had better coordination in their horizontal and vertical force components, indicative of more in-phase energy fluctuations within stance. Their vertical ground reaction forces correspondingly more closely fit that of a spring-mass model. These effects were enhanced at faster speeds within the Kenyan runners, and in runners exhibiting non-rearfoot striking patterns within both groups. Barefoot running elicited mixed results across measures and within groups, improving force coordination but decreasing vGRF similarity in the recreational runners with less of an effect in the Kenyan runners. In examining spring-mass behavior, the Kenyan runners had similar absolute force magnitudes, which corresponded to higher mass-specific forces, and their ground contacts were consistently shorter. This resulted in similar absolute leg stiffnesses and higher relative stiffnesses. This was confirmed with nonlinear regression estimation of the parameters. The barefoot condition elicited small changes across both cohorts in many of the parameters, with lower forces, shorter contacts, and stiffer legs, but these changes were not detected by the nonlinear regression modeling. Overall, this suggested that the elite Kenyan runners produced spring-mass behavior that was similar to the non-elite recreational runners despite being of smaller mass and stature. These characteristics and observations may provide further insight into their unmatched performance capacities in distance running, and they may also suggest new opportunities for systemic quantification of running patterns among broader populations.

Chapter 4 Application of Spring-Mass NLR and Similarity Analyses Methods: A Within-subject Analysis of Post-race Fatigue

This work will be submitted for publication as or similar to:

Geoffrey T. Burns, Nicholas Tam, Nelleke G. Langerak, Ronald F. Zernicke, and Robert P. Lamberts (2020). “Effect of Fatigue on the Spring-Mass Behavior of Runners after a 56-kilometer Road Ultra-marathon.”

4.1 Abstract

Ultramarathons are a unique model to study the effects of global fatigue in athletes, as they induce extreme mechanical and physiological stress via prolonged loading and competitive pressure. This investigation sought to apply the spring-mass template to the study of runners before and after a road ultramarathon in order to characterize the effects of fatigue on the systemic gait patterns of the runners. Fourteen runners completed a 56-kilometer road race, and kinetic recordings during overground running were captured 7 days before and 2 days after the event. From these recordings, traditional kinetic and spring-mass measures were calculated as well as systemic parameters via nonlinear regression. Spring-mass model fit metrics were also calculated. Following the race, the peak vertical force magnitudes and average vertical loading rates were unchanged, but the impact peaks increased (1.88 to 1.95 BW). The ground contact times were modestly shorter (-3 ms), but the stride frequencies were ultimately unchanged. This resulted in small but significant increases in leg stiffness (10.0 to 10.3 kN/m) without a change in vertical stiffness. Systemic spring-mass parameter estimation via nonlinear regression did not detect an

effect of the race on any of the model parameters. The overall fit of the spring-mass dynamics to that of the runners, however, decreased after the race (model error increased from 171.3 N to 181.4 N). This indicates that the systemic mechanical behaviors in the runners generally persisted despite the fatigue and stress induced by a road ultramarathon. Thus, the current results support previous findings that runners maintain gross mechanical behaviors when fatigued with small compensatory changes in spatiotemporal and traditional spring-mass measures. However, these findings also indicated that while runners maintained their overall mechanical behavior, the "noise" of that behavior may increase after stress, suggesting new opportunities for quantifying those deviations.

4.2 Introduction

Tests of endurance are, by definition, fatiguing, and characterizing the extent to which one is fatigued following such a test, be it acute or chronic, is critical for tailoring recovery and facilitating future performance. However, the phenomenon of fatigue is in itself physiologically complex and multimodal, so its assessment is correspondingly difficult to objectively characterize (Robson-Ansley, Gleeson, & Ansley, 2009). Common analytical tools include psychological and mood assessments such as the Profile of Mood States (POMS) questionnaire (Morgan et al., 1987) or the Daily Analyses of Life Demands for Athletes (DALDA) questionnaire (Rushall, 1990), plasma (Hecksteden et al., 2016; Julian et al., 2017) and salivary (Hough et al., 2013; O'Connor et al., 1989) biomarkers, resting physiological metrics such as heart rate variability (Schmitt et al., 2013) and heart rate recovery (Lamberts, Maskell, et al., 2011), and functional physiological tests such as the Lamberts and Lambert Submaximal Cycling Test (Lamberts, Swart, et al., 2011) and the Submaximal Ergometer Rowing Test (Otter et al., 2015).

Running biomechanics have been found to be sensitive to fatigue (Gerlach et al., 2005; Mizrahi et al., 2000; Morin, Samozino, et al., 2011; Williams, Snow, & Agruss, 1991). These changes have been shown to induce changes in musculoskeletal loading and strain patterns (Mizrahi et al., 2000), which may predispose athletes to injury risk (Edwards, 2018; Grimston & Zernicke, 1993). However, no generalized tool exists for assessing fatigued gait in runners, as consistent effects tend to be highly individualized (Williams et al., 1991) and implications often unclear (Dierks, Davis, & Hamill, 2010). For example, the impact forces and loading rates in a fatigued state have received considerable attention given their relation to injury-risk (Grimston & Zernicke, 1993; Zadpoor & Nikooyan, 2011), yet while some investigations have observed increased loading profiles in the fatigued state (Verbitsky et al., 1998), others have found decreases (Gerlach et al., 2005), and others observed no changes (Slawinski et al., 2008). Given running's ubiquity as both a popular standalone endurance activity and as a critical component of team sports, understanding the effects of fatigue on systemic mechanics may better inform coaches, athletes, and practitioners in their recovery and performance planning.

The spring-mass model of running (Figure 8 and Figure 9) is a common analytical tool used to assess systemic mechanical behavior in runners. It treats the body as point-mass on a linearly elastic spring with a constant leg stiffness (Blickhan, 1989; McMahon & Cheng, 1990), and despite its simplicity, it serves as a template that captures the fundamental dynamics of running (Full & Koditschek, 1999). It has been applied to the study of fatigue in a variety of running contexts (Dutto & Smith, 2002; Fourchet et al., 2015; Girard, Micallef, & Millet, 2011; Morin, Samozino, et al., 2011; Morin, Tomazin, et al., 2011; Slawinski et al., 2008), but the findings have been inconsistent, dependent on protocol, environment, and population. For example, the acute fatigue induced by a sprinting (Morin et al., 2012) and short exhaustive distance running (Slawinski et al., 2008) elicited no changes in spring-mass behavior, while the prolonged fatigue induced by 24 hours of running elicited increases in both leg and vertical stiffness (Morin, Samozino, et al., 2011).

Just as fatigue is in itself a broad and complex phenomenon, assessment of its effects should be assessed with consideration given to the method of inducement and context of the activity.

The ultramarathon serves as a useful model for studying the effects of global fatigue and the stress responses of the musculoskeletal system (Millet & Millet, 2012). The prolonged loading and neuromuscular challenges that runners endure during these events may be indicative of the stress induced by analogous types of running-related fatigue, such as periods of heavy training or overreaching. The spring-mass model has been used to explore mechanical changes related to fatigue within several ultramarathon contexts. After mountainous trail ultramarathon races, increases in stride frequency and vertical stiffness have been observed (Degache et al., 2013; Morin, Tomazin, et al., 2011) with similar findings of increased leg and vertical stiffnesses observed in laboratory conditions attributed to runners adopting a “safer” running pattern (Morin, Samozino, et al., 2011). However, to our knowledge, only one investigation (Giovanelli, Taboga, & Lazzer, 2017) has explored these changes in runners following an ultramarathon on a paved road course, where they observed the opposite effect: decreases in leg and vertical stiffness. As this is the environment in which the majority of runners practice the activity, further characterization of these systemic mechanical changes are necessary for the understanding of fatigue-related alternations in gait. Moreover, the effect of fatigue has not been explored in relation to systemic spring-mass similarity in runners, which has previously been observed to decline with age and presumed to be related to losses in the capacity for elastic energy storage and return (Cavagna et al., 2008b; Legramandi et al., 2013). This loss in elastic capacity has also been attributed to some of the physiological and mechanical consequences of ultramarathon running (Lazzer et al., 2015; Lazzer et al., 2014), suggesting that a spring-mass similarity analysis may also yield further insight into gait patterns related to fatigue.

We sought to characterize spring-mass changes in runners following an ultramarathon road race. We hypothesized that the fatigue induced by the race would cause the runners to exhibit decreases in the peak magnitudes of their vertical force parameters similar to those previously observed after ultramarathon events (Millet et al., 2009; Morin, Samozino, et al., 2011). We further hypothesized that this fatigue would cause runners to take shorter, more frequent steps and thus ultimately increase their vertical and leg stiffnesses. Finally, we hypothesized that the kinetic similarity of the runners to simple, elastic spring-mass systems would decrease following the race.

4.3 Methods

4.3.1 Experimental Data Collection

This study compared the spring-mass behavior and mechanical similarity within runners before and after a 56 kilometer ultramarathon road race. The investigation was part of a broader study investigating the fatiguing effects of the race, and the physiological effects have been reported elsewhere (Siegl et al., 2017). The sample size was determined so as to detect changes in heart rate and heart rate recovery that exceeded an anticipated inter-day within-subject variation average of 9 beats-per-minute with a standard deviation of 6 beats-per-minute (Lamberts et al., 2004). For a Type I error control of 95% and a Type II error control of 80%, this effect implied a sample size of 7 subjects for within-individual comparisons. Anticipating drop-outs and non-completions in the race, fifteen subjects were recruited to participate. At the time of the initial visit, all participants had been free of lower limb injury for six months. All subjects were experienced runners with weekly training volumes between 35 and 100 kilometers per week, had completed at least one marathon in the year prior to the study, and were registered entrants in the Old Mutual Two Oceans 56-kilometer Ultramarathon (Figure 15). All participants provided written informed consent, and the study was approved by the University of Cape Town's ethics review board (HREC ref: 626/2015).

The subjects reported to the laboratory for three visits. The first visit was two weeks prior to the race, where they completed a maximal treadmill running test to establish peak treadmill running speed (PTRS) (Mann et al., 2015). The second visit was exactly 7 days prior to the race, and the third visit was exactly 2 days following the race.

Following this assessment, kinetic recordings were captured during overground running. Participants ran at 70% of their peak treadmill running speed (PTRS) on a 40-meter synthetic indoor track. This speed corresponded to the approximate speed at which they would be running the race. It was verified in all trials with photoelectric timing cells. Ground reaction forces were recorded from two 900×600 mm embedded force platforms (AMTI, Watertown, MA, USA) and sampled at 2000 Hz. Six successful trials were captured for each subject with 3 captured on both dominant and non-dominant limbs. A successful trial was defined as the participant running within ±5% of the target speed, cleanly striking the force plate with the designated limb, and giving no indication of platform targeting. The participants wore their habitual training shoes in both sessions and had refrained from strenuous exercise in the 24 hours prior to each session.

Figure 15: Course profile for the Two Oceans 56-kilometer ultramarathon. The course is entirely on paved roads, and it has approximately 1000 meters of ascent and 940 meters of descent with a maximum elevation of 230 meters above sea level and a minimum elevation of 4 meters above sea level.

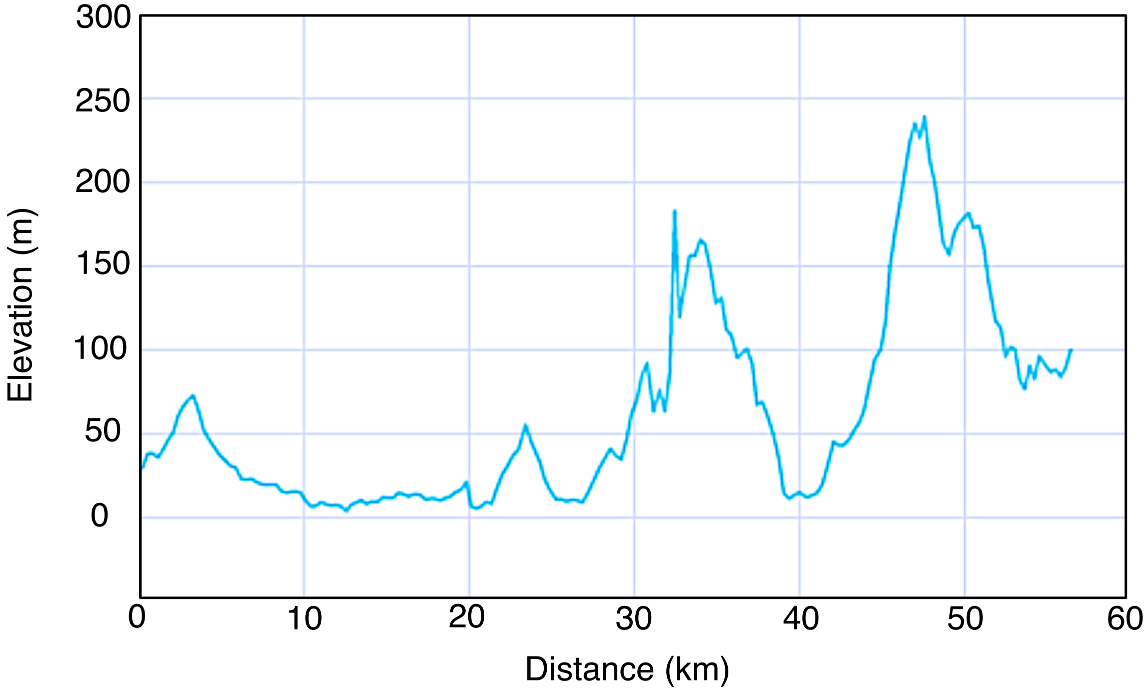

4.3.2 Data Processing

The GRF recordings were filtered using a low-pass, fourth order Butterworth filter with a cutoff frequency of 60 Hz and a contact threshold of 50 N. Vertical loading rates (VLR) were calculated as the slope of the vGRF time series between 20% and 80% of the time corresponding to the impact peak (F_{impact}) (Milner et al., 2006). If no impact peak was present, the measures were taken at the mean percentage of stance at which F_{impact} occurred in the trials in which it was present, and the VLR was calculated over the observed standard deviation below and above that percentage (Lieberman et al., 2010). Leg and vertical stiffnesses were calculated via the method of McMahon and Cheng (Farley et al., 1993; McMahon & Cheng, 1990), and leg spring length (L_0) was estimated as 0.53 of the participant's standing height (Morin et al., 2005; Winter, 1979). Elastic similarity was quantified with three metrics. First, Cavagna and Legramandi's "similarity to an symmetric bounce" (SB) was calculated, which is the average of the ratios of the deceleration to acceleration times of the COM during stance and of the maximal downward and upward velocities of the COM, both of which are 1.0 in a perfectly symmetric bounce (Cavagna & Legramandi, 2015; Legramandi et al., 2013). Second, the horizontal and vertical timing difference (HV TD) was used, which is the difference between the time at which the horizontal GRF crossed 0 N, indicating a transition from braking to propulsion in the horizontal plane, and the time at which the vertical GRF reached its peak, indicating a transition from loading to unloading in the vertical plane. In a perfectly elastic system, the HV TD would be zero (Figure 10). Third, the spring-mass fit (SM Fit) was quantified via nonlinear regression (NLR) for each subject, grouping observations for each leg and treating his or her steps as random effects. This assessed the degree to which the subject's vGRF matched that of a best-fit spring-mass system (Chapter 2 and Figure 16).

4.3.3 Nonlinear Regression Analysis

To explore the effective spring-mass behavior before and after the race and in relation to any leg asymmetries, we used the mixed-effects Nonlinear Regression (NLR) estimation technique (Chapter 2). The functional form of the spring-mass vGRF is described again in Equation 43, and it models the observed vGRF with the four effective spring-mass parameters: stiffness (k*), touchdown angle (α_{TD}*), leg length (L_0*), and contact time (t_c*):

$$F_y(t) = \left(k\frac{L_0-\frac{g}{8}t_c-L_0\sin\alpha_{TD}}{1-\frac{k}{m}\left(\frac{t_c}{\pi}\right)^2}\right)sin\left(t\frac{t_c}{\pi}\right)\left(1-\frac{1}{1+e^{-10^{10}(t-t_c)}}\right) \quad (43)$$

Therefore, for a given grouping *i* of n_i observations in the vGRF time series t_{i1} to t_{in}, the vertical force is modeled with a fixed parameter set φ and a group-specific random effect set *b*:

$$y_i = F_y(\varphi_i, x_i), \varphi_i = \begin{pmatrix} k_i \\ \alpha_{TD\,i} \\ L_{0\,i} \\ t_{c\,i} \end{pmatrix} + b_i, b_i = \begin{pmatrix} b_{ik} \\ b_{i\alpha} \\ b_{iL} \\ b_{it} \end{pmatrix}, and\ x = \begin{pmatrix} t_{i1} \\ \vdots \\ t_{in} \end{pmatrix} \quad (44)$$

We assigned fixed effects to each parameter for the session (Before vs. After) and leg (Dominant vs. Non-Dominant), so that for each observation, there were 12 fixed parameters, corresponding to the intercept values of k^*, α_{TD}^*, L_0^*, and t_c^*, and parameters for the effects of session and leg, respectively. Design matrices were assigned to each group with an identity matrix for each intercept parameter set, and dummy-coded with either zero or identity matrices for each respective fixed effect set. Each observed step was grouped within a subject-session-leg combination (three steps per grouping), and random effects were assigned to the four intercept parameters. An example model parameter set φ for step *i* from a subject after the race (1) on his or her dominant leg (0) would be:

$$\varphi_i = A_i\beta_i + B_i b_i \tag{45}$$

$$\beta = \begin{pmatrix} \beta_1 \\ \vdots \\ \beta_{12} \end{pmatrix}, A_i = \begin{bmatrix} \overbrace{1\,0\,0\,0}^{Int.} & \overbrace{1\,0\,0\,0}^{After} & \overbrace{0\,0\,0\,0}^{Dom.} \\ 0\,1\,0\,0 & 0\,1\,0\,0 & 0\,0\,0\,0 \\ 0\,0\,1\,0 & 0\,0\,1\,0 & 0\,0\,0\,0 \\ 0\,0\,0\,1 & 0\,0\,0\,1 & 0\,0\,0\,0 \end{bmatrix}, b = \begin{pmatrix} b_{i1} \\ \vdots \\ b_{i4} \end{pmatrix}, and\ B_i = \begin{bmatrix} 1&0&0&0 \\ 0&1&0&0 \\ 0&0&1&0 \\ 0&0&0&1 \end{bmatrix} \tag{46}$$

To facilitate model convergence, vGRF recordings were downsampled to 500 Hz. All fitting was performed using the Nonlinear Regression toolbox in MatLab (2019a, MathWorks, Natick, MA, USA). The mixed-effects modeling was carried out using the stochastic approximation expectation maximization algorithm (Feodor Nielsen, 2000). The model was seeded with initial parameter values that minimized the sum of squared errors against all steps in aggregate via nonlinear least-squares optimization that itself was started with initial values corresponding to the mean value of all subjects' conventional spring-mass parameters: k_{leg}, α_{TD}, L_0, and the observed t_c. Bounds were set at a lower limit of 5 kN/m, 63°, 80 cm, and 0.10 ms and an upper limit of 0.12 s and 30 kN/m, 74.5°, 120 cm, and 0.40 s for the four parameters, respectively. The model was given an initial random-effects covariance matrix with the diagonal equal to two times the observed variance in the conventional parameters across steps, with the variance in L_0 as estimated by the variance in α_{TD} relative to the mean t_c.

4.3.4 *Data Analysis*

The kinetic measures (F_{max}, F_{impact}, and VLR), spatiotemporal measures (contact time (t_c), aerial time (t_a), duty factor (DF), and stride frequency (SF)), traditional spring-mass measures (k_{leg}, k_{vert}, center-of-mass displacement (Δy), and leg compression (ΔL)) and the elastic similarity measures (SB, HV TD, and SM fit) were analyzed using mixed-effect model linear regression, treating the measure as the response variable and the session and leg as fixed effects with interactions. Each subject was assigned a random effect intercept with a limb asymmetry slope.

47 $$y = \beta_{session} \times \beta_{leg} + Error(Leg|Subject)$$

For the linear mixed-effect models, the fixed effects were assessed for significance via Satterthwaite's method. For the NLR models, estimates for the standard errors of each fixed effect term were approximated via the maximum likelihood and tested for significance using a Wald Test. Statistical test criterion in all models used a Type I error control of $\alpha < 0.05$. MatLab (2019a, MathWorks, Natick, MA, USA) was used for all data processing and NLR modeling, and R (v3.6.2, R Foundation for Statistical Computing, Vienna, Austria) was used for all additional statistical analyses.

Figure 16: An example vertical ground reaction force (vGRF) recording with a spring-mass model vGRF fit via nonlinear regression (NLR).

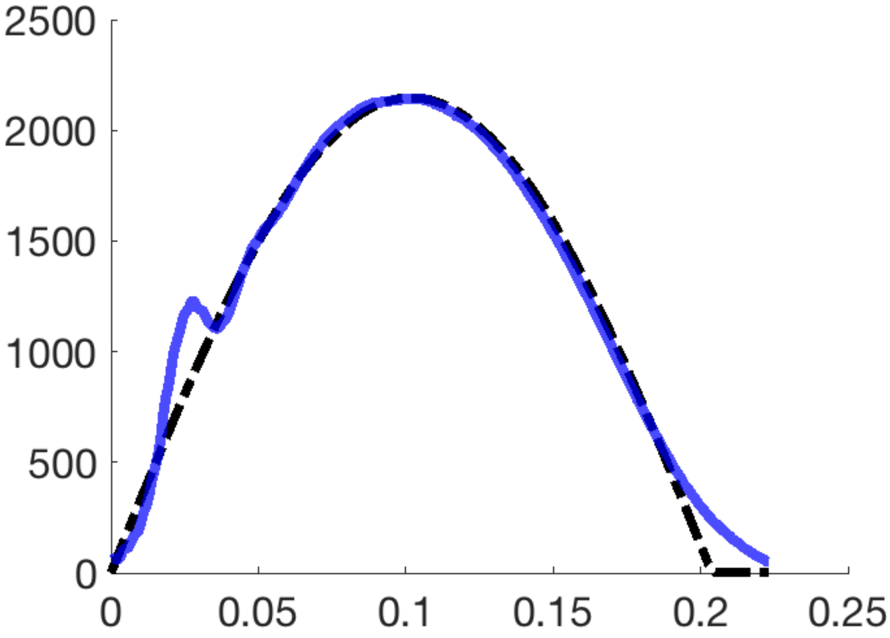

4.4 Results

Fourteen subjects completed the Two Oceans 56-km Ultramarathon (Figure 13 for route information) in an average time of 5 hours and 42 minutes (range: 3:59 – 6:52). One subject suffered an ankle injury and could not participate in the post-race testing session. The subject characteristics are provided in Table 2. In the results descriptions provided below, the observed effect of the race is reported if it was found to be significant, and the average values across the two sessions are reported if it was not. Standard error of the measurement estimates (±sem) are provided for each effect. The full results of the analyses are compiled in Tables 12 – 14.

Following the race, peak vGRF values were unchanged for the subjects (2.50 ± 0.08 BW) but the impact peak significantly increased after the race (+0.07 ± 0.02 BW, $p = 0.004$). The average vertical loading rate was unchanged (54.0 ± 3.2 BW/s). There was a small but significant decrease in ground contact time (–3 ± 1 ms, $p = 0.002$) with no significant change in flight time

(122 ± 8 ms). Overall, the duty factor and stride frequency changes were ultimately insignificant (0.33 ± 0.01 and 2.89 ± 0.04 Hz).

The leg stiffness of the runners increased after the race (+0.3 ± 0.1 kN/m, $p = 0.004$) while the vertical stiffness remained unchanged (22.7 ± 1.0 kN/m). Correspondingly, the vertical displacement of the center-of-mass during stance was unchanged (8.1 ± 0.5 cm), while the leg compression significantly decreased (–0.6 ± 0.2 cm, $p = 0.006$). Limb dominance did not significantly affect any of the measures, nor did any asymmetries in the response variables emerge as a result of the race. Table 12 provides detailed results of the kinetic, spatiotemporal, and spring-mass measures. The systemic spring-mass parameters as estimated by NLR were not influenced by the effect of the race, where the effective stiffness was modeled as $k^* = 12.6$ kN/m, the effective touchdown angle $\alpha_{TD}^* = 65.6$, $L_0^* = 96.5$ cm, and $t_c^* = 212$ ms. NLR modeling results are detailed in Table 13.

The similarity to a symmetric bounce and horizontal-vertical force timing difference remained consistent after the race (93.3 ± 1.1% and 15 ± 3 ms, respectively). However, the subjects' similarity to the spring-mass vGRF decreased after the race, with the model errors increasing by 10.1 ± 4.2 N. Table 14 provides detailed results, and Figure 17 is a visual representation.

Figure 17: Representative vGRF measurements from two subjects (A and B) before and after the race on both the dominant and non-dominant legs with spring-mass models fit via NLR. Note the slight increase in the impact peak magnitudes and slight decrease in model fit following the race.

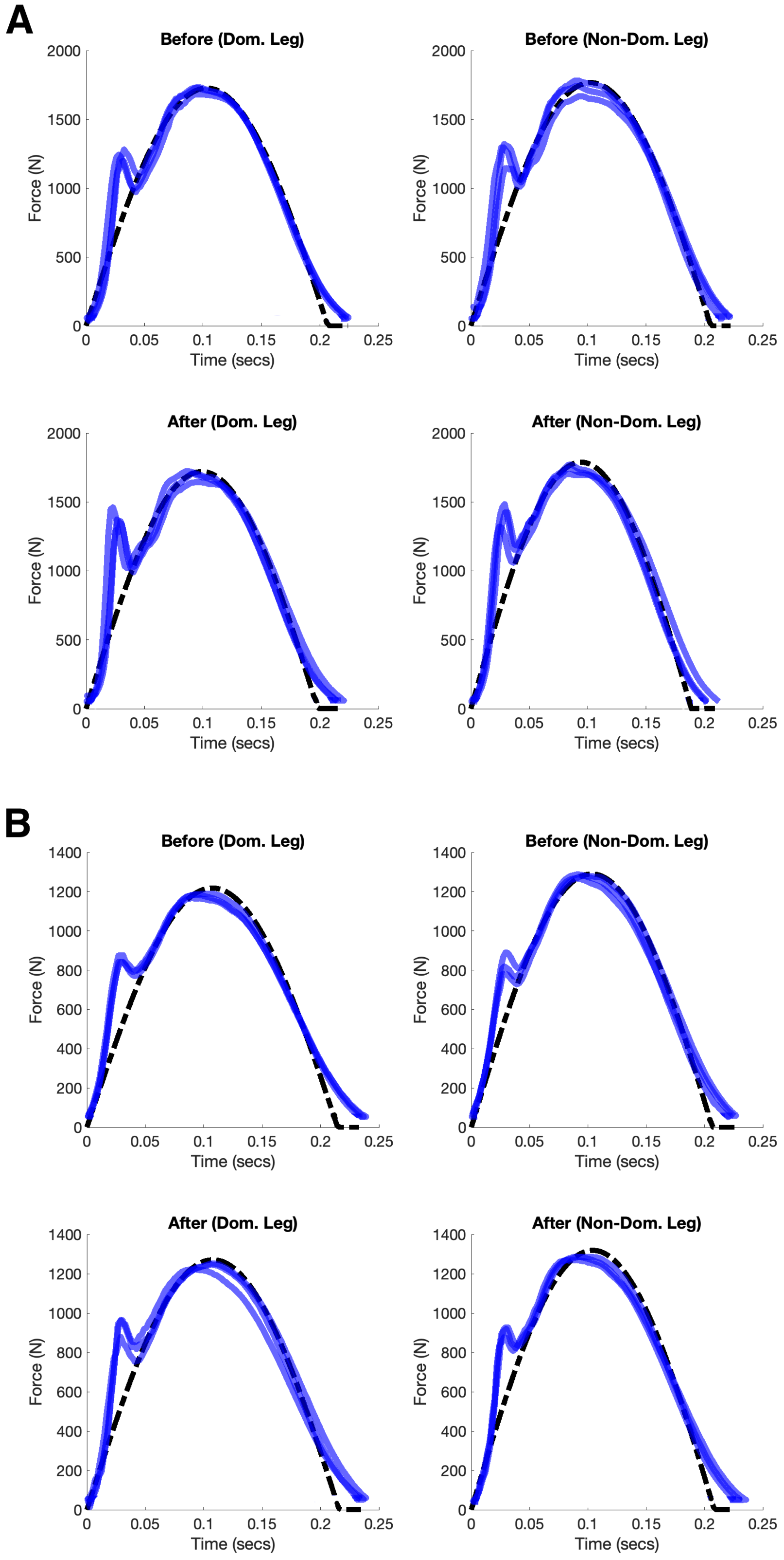

Figure 18: Correlation-covariance matrix for the NLR model's fixed effects. Note that within each fixed effect grouping, the effective leg length and touchdown angle tended to be highly covaried (correlation > 0.90). Effective stiffness and contact time were consistently independent of the other parameters within and across effects.

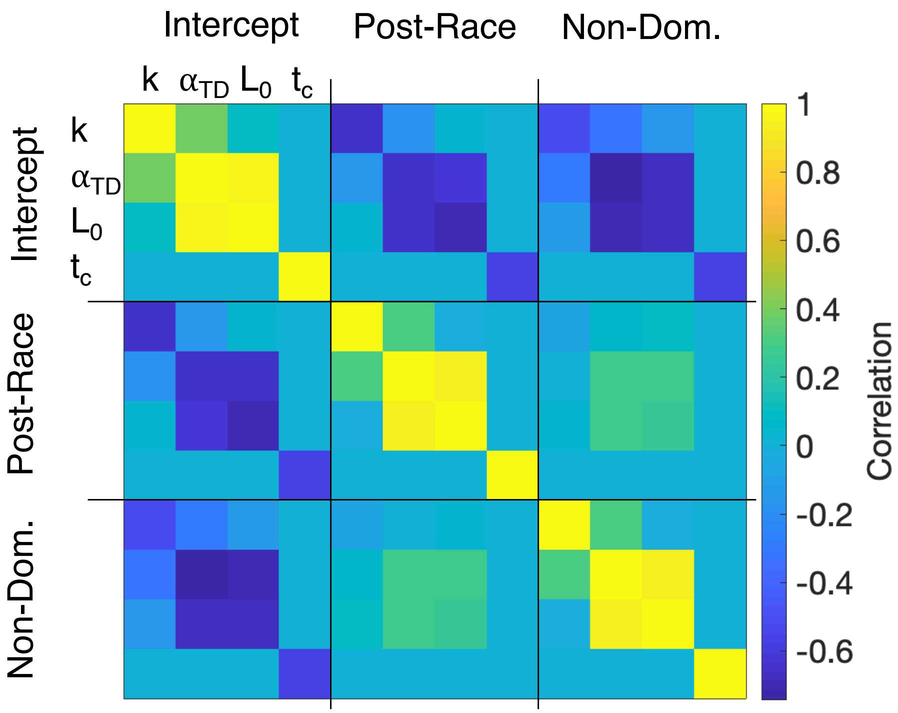

Characteristic	**Mean ± SD**	**Range**
Subjects (n)	14	(11 M − 3 F)
Age (yr)	38 ± 8	(25 − 47)
Height (m)	1.77 ± 0.09	(1.64 − 1.93)
Mass (kg) *pre-race*	72.4 ± 9.8	(54.4 − 89.3)
Mass (kg) *post-race*	72.6 ± 10.1	(53.7 − 90.4)
Average Weekly Training (km)	60 ± 21	(35 − 100)
PTRS (m/s)	5.12 ± 0.45	(4.17 − 5.83)
70% PTRS (m/s)	3.58 ± 0.32	(2.92 − 4.08)
Race Finish Time (hours:mins)	5:42 ± 0:47	(3:59 − 6:52)

Table 11 Cohort characteristics. Data are presented as means ± standard deviations and ranges, respectively. Weekly training volumes were given as the average volume during the three months preceding the race as reported by the subject in the initial visit. PTRS indicates the observed peak treadmill running speed, where 70% PTRS was the speed used for the biomechanical analyses.

		Pre-race	SEM	Post-race (Δ)	SEM	p-value	Sig.
Kinetic	F_{max} (BW)	2.51	0.08	-0.02	0.01	0.268	
	F_{impact} (BW)	1.88	0.08	0.07	0.03	0.017	✻
	VLR (BW/s)	53.14	3.16	1.67	1.19	0.160	
Spatiotemporal	t_c (ms)	231	5	-3	1	0.003	✻✻
	t_a (ms)	116	8	11	7	0.109	
	DF	0.33	0.01	-0.01	0.00	0.133	
	SF (Hz)	2.90	0.04	-0.01	0.04	0.696	
Spring-Mass	k_{leg} (kN/m)	10.0	0.5	0.3	0.1	0.004	✻✻
	k_{vert} (kN/m)	22.3	1.0	0.8	0.5	0.156	
	Δy (cm)	8.3	0.5	-0.3	0.2	0.139	
	ΔL (cm)	17.9	0.7	-0.6	0.2	0.007	✻✻

Table 12 Kinetic, spatiotemporal, and spring-mass measures with pre-race values and the average within subject change after the race. Standard errors of the measurements (sem) are provided. Variables listed: F_{max} (peak vGRF), F_{impact} (vertical impact peak), VLR (average vertical loading rate), t_c (observed contact time), t_a (observed flight time), DF (duty factor), SF (stride frequency), k_{leg} (leg stiffness), k_{vert} (vertical stiffness), Δy (vertical displacement of the center-of-mass during stance), and ΔL (leg compression during stance). Statistical significance of each effect is indicated as: ✻$p < 0.05$ and ✻✻$p < 0.01$

Parameter	Effect	Estimate	SEM	p-value	Sig.
k* (kN/m)	Pre-race	12.6	3.6	-	
	Post-Race	–0.4	3.9	0.918	
	Non-Dom. Leg	+0.3	3.8	0.930	
α_{TD}* (°)	Pre-race	65.6	18.4	-	
	Post-Race	–0.8	18.5	0.967	
	Non-Dom. Leg	+0.0	18.9	0.999	
L_0* (m)	Pre-race	0.965	1.296	-	
	Post-Race	+0.017	1.333	0.990	
	Non-Dom. Leg	–0.026	1.364	0.985	
t_c* (ms)	Pre-race	212	4	-	
	Post-Race	–3	5	0.533	
	Non-Dom. Leg	–2	5	0.657	

Table 13 Effective spring-mass measures as approximated by nonlinear regression and the corresponding fixed effect estimation for each parameter for effective stiffness (k), effective touchdown angle (α_{TD}*), effective leg length (L_0*), and effective contact time (t_c*). Estimates for each effect (post-race, non-dominant leg) and their estimated standard error (sem) are provided. Note that the intercept and effect estimates for α_{TD}* and L_0* were highly covaried (corr. >0.90). Estimates for their respective standard errors should be interpreted with caution.*

	Pre-race	SEM	Post-race (Δ)	SEM	p-value	Sig.
SB (%)	93.7	1.1	-0.9	1.0	0.382	
HV TD (ms)	17	3	-3	3	0.281	
RMSE (N)	171.3	15.0	10.1	4.2	0.025	✻

Table 14 Elastic similarity across measures: Similarity to a symmetric bounce (SB), the timing difference between the horizontal force transition and the vertical force peak (HV TD), and the model error of the subject's vGRF against that of a best-fit spring-mass system (SM fit). Estimates for the pre-race average, the post-race effect, and their standard errors (sem) are provided. Statistical significance is indicated as: ✻ p <0.05.

Parameter	Effect	Estimate	SEM	p-value	Sig.
k* (kN/m)	Pre-race	10.3	2.9	-	
	Post-Race	0.7	3.3	0.828	
	Non-Dom. Leg	0.7	2.9	0.819	
A* (cm)	Pre-race	11.9	4.8	-	
	Post-Race	-0.8	5.1	0.990	
	Non-Dom. Leg	-0.9	4.4	0.985	
t_c* (ms)	Pre-race	212	4	-	
	Post-Race	-3	5	0.483	
	Non-Dom. Leg	-2	5	0.680	

Table 15 Effective spring-mass measures as approximated by a three-parameter nonlinear regression model and the corresponding fixed effect estimation for each parameter for effective stiffness (k), effective non-vertical leg compression (A*), and effective contact time (t_c*). Estimates for each effect (post-race, non-dominant leg) and their estimated standard error (sem) are provided. See Appendix A for details.*

4.5 Discussion

4.5.1 Summary

We examined the kinetic characteristics and spring-mass behavior of runners before and after a 56-kilometer road ultramarathon. Two days after the race, the runners exhibited no change in peak vertical force as compared to their pre-race values, but their vertical impact peaks were elevated while their average vertical loading rate was unchanged. Their ground contact times decreased slightly in the post-race session, but the aerial times weren't substantially different, and ultimately, neither the duty factor nor stride frequency were significantly altered. Their leg stiffnesses were modestly increased due a slight decrease in leg compression, while their vertical displacements during stance and correspondingly their vertical stiffnesses during stance remained the same. Their systemic spring-mass characteristics as determined by nonlinear regression were unchanged after the race. While their similarity to a symmetric bounce and horizontal-vertical force timing were consistent before and after the race, their overall spring-mass vGRF similarity decreased following the race.

4.5.2 Kinetic Characteristics

The findings support rejection of our first hypothesis that the peak vertical forces following the race would decrease. This phenomenon was observed in an ultra endurance context by Morin and colleagues after 24 hours of treadmill running (Morin, Samozino, et al., 2011) as well in a single subject case study following a trans-continental run from Paris to Beijing (Millet et al., 2009). It was hypothesized that the decrease was due to both a protective response of the body to preserve the musculoskeletal structures as well as to a decreased capacity for force production (Morin, Samozino, et al., 2011). Degache and colleagues observed this phenomenon at lower speeds (10 km/hr) following a five-hour running bout, but they did not observe a change in F_{max}

when the subjects ran at higher speeds (12 and 14 km/hr) following the race (Degache et al., 2013). In a meta-analysis of vGRF parameters in response to fatigue, Zadpoor and Nikooyan concluded that there has been no clear effect of fatigue on F_{max}, and that any effect was likely due to both the context and population (Zadpoor & Nikooyan, 2012). As opposed to other kinetic studies conducted on ultramarathon runners before and after races, this investigation took measurements two days after the race, which itself likely elicited a different response than the protocols measuring kinetics immediately following the race.

However, we observed an increase in F_{impact} following the race. This was consistent with findings observed in studies with shorter-duration exhaustion protocols (≤1 hour). Dickinson and colleagues observed F_{impact} to increase from 1.86 to 2.03 BW throughout a 45-minute treadmill run, and others have observed increases in peak lower-limb impact accelerations as a consequence of fatigue (Derrick, Dereu, & McLean, 2002; Mizrahi et al., 2000; Verbitsky et al., 1998). Dickinson speculated that this was due to a decrease in the capacity of the lower limb musculature to attenuate shock or to an altered proprioception itself due either to the experience of pain or the release of endorphins to inhibit it (Dickinson, Cook, & Leinhardt, 1985). We are not aware of any investigations that examined the effect of an ultramarathon on F_{impact}. Following the 24-hour treadmill runs, Morin and colleagues observed an increase in average vertical loading rate, but it did not meet the criteria for statistical significance. Thus, they suggested it indicated a trend towards a decreased capacity for shock attenuation, but the effect was highly individualized. Siegl and colleagues reported significantly higher Visual Analog Scale (VAS) pain scores for Delayed Onset Muscle Soreness (DOMS) symptoms in this population following the race (Siegl et al., 2017), so perhaps the mechanisms proposed by Dickinson, both decreased muscular capacity and decreased proprioception (Dickinson et al., 1985), resulted in the greater impact forces following the race observed here.

4.5.3 Spring-Mass Behavior

The hypothesis that leg and vertical stiffness would increase following the race was partially supported, as leg stiffness was modestly increased in the runners post-race (+3.0%), while the vertical stiffness was unchanged. Several studies have examined these parameters within and after ultramarathon races, but the effects have been inconsistent. For example, Morin and colleagues observed both k_{leg} and k_{vert} to increase following 24 hours of treadmill running, but they did not observe a change in k_{leg} following a 166-kilometer trail ultramarathon (Morin, Samozino, et al., 2011; Morin, Tomazin, et al., 2011). Similarly, Degache and colleagues observed this increase in both parameters following five hours of hilly running, but not after 330 kilometers of mountainous running (Degache et al., 2013; Degache et al., 2016). Furthermore, Lazzer and colleagues observed significant decreases in k_{leg} and k_{vert} after an uphill ultramarathon (Lazzer et al., 2015). Many of these findings were driven by observed decreases in contact time and/or aerial time, which resulted in higher stride frequencies. We observed this decrease in t_c, but it was small in magnitude (-1.3%), and the corresponding changes in SF were not significant. Given that F_{max} was unchanged, it was likely this small temporal adjustment accounted for the small decrease in leg compression (-3%) and the corresponding adjustment in leg stiffness (-3%). Moreover, the characteristics of each of these races was different, likely resulting in distinct fatigue mechanisms, as were the means of biomechanical measurement and calculation of the spring-mass parameters.

When the parameters were analyzed systemically via nonlinear regression, we did not observe any changes in the spring-mass behavior following the race. As this method used the entirety of the vGRF curve to inform the parameter estimations, it was less sensitive to the discrete values and assumptions used to calculate conventional spring-mass parameters. For example, the traditional leg compression calculation was determined by the vertical displacement and observed contact time for a given speed (Farley et al., 1993; McMahon & Cheng, 1990). Thus, small changes in the final moments of ground contact that extend or shorten the temporal measure of the step but do not substantially influence the center-of-mass's displacement may have substantially affected estimations of leg compression and ultimately k_{leg}. We saw this phenomenon here, where k_{leg} increased due to the small but significant decrease in t_c. The estimated effective contact time, tc*, however, was unchanged (Figure 17). This value represented the time course as approximated by spring-mass dynamics, and it was correspondingly less influenced by the nonlinear elasticity that characterizes take-off asymmetries (Maykranz & Seyfarth, 2014). That suggested that despite small decreases in t_c and corresponding alterations in k_{leg} and ΔL, the overall systemic spring-mass dynamics of the runners in this investigation were largely unaffected post-race.

4.5.4 Elastic Similarity

The similarity of the runners to ideal spring-mass systems was, however, influenced by the race. The results partially supported our initial hypothesis that the measures of elastic similarity would decrease. SB and HV TD were unchanged, which indicated that their timing and coordination of kinetic energy fluctuations through stance were unaffected. However, the SM Fit decreased, with the spring-mass model fitting error increasing by 5.9% in the post-race session. This, coupled with the unchanged NLR-estimated parameters, suggested that their vGRF curves maintained the same systemic shape, but that they were less consistent, or "nosier". This increase in model error was likely due in part to the post-race increase F_{impact}, where greater peaks on the rising edge of the vGRF drove greater error when compared against the smooth rise of the spring-mass system (Figure 17).

This finding may also be interpreted against the concept of "muscle tuning" with relation to impact forces, where the body is thought to adjust its dampening properties to mitigate loads (Nigg, 1997). Fiesenbichler and colleagues examined this in relation to fatigue, and they observed an increase in the amplitudes of soft-tissue compartment vibrations in the lower limbs as runners fatigued (Friesenbichler et al., 2011). Without a change in the general frequency of the vibrations, their conclusions were that increased amplitudes were a consequence of a reduction in the "muscle tuning" mechanism. Here, we observed the maintenance of the general shape and peak of the vGRF in fatigued runners, but there was greater variability throughout its time series. This may have been a manifestation of a loss of dampening capacity, or a decreased functionality of the body's control mechanism. Winter postulated that the body seeks to maintain a consistent systemic response external loading through component- and joint-level motor adjustments via the neuromuscular system (Winter, 1984). The decrease in SM Fit, here, may be a manifestation of that hypothesis—a maintenance of the response to the external load (i.e., consistent F_{max}) with diminished control (i.e., a more variable shape).

4.5.5 Limitations

There are several considerations one should make in interpreting the findings of this investigation. The first relates to the number of trials recorded for each participant. Here, we captured three steps on each limb in each session for each subject. This corresponded to six trials in each session. Several authors have recommended capturing more trials for optimal intraday reliability. Bates and colleagues recommended capturing eight trials (Bates et al., 1983), whereas Davita and Bates later recommended as many as 25 trials to detect intraday differences less than 1 N/kg in vertical force magnitudes (Devita & Bates, 1988). However, Driss later reported that three trials were necessary to capture >90% reliability in F_{max}, F_{impact}, and VLR measures. Given the fatigued state that we anticipated for our runners in the post-race conditions, we therefore used three trials on each limb (six in total for each session), but we cannot rule out that smaller changes in force magnitudes may have been present that we were not able to detect. Furthermore, we would have liked to capture more trials so as to explore the variability patterns in the collected measures before and after the race. We observed increases in step frequency variability throughout a road ultramarathon in elite runners (Burns, Zendler, & Zernicke, 2019), and Candau and colleagues similarly observed an increased SF variability in triathletes as a consequence of fatigue (Candau et al., 1998). Given the increase in vGRF shape variability we observed here (i.e., decreased SM Fit), variability of gait measures, rather than their mean values, may lend more insight into manifestations of fatigue.

The timing of our data collection should also be considered when comparing results to previous investigations in ultramarathons. We recorded our post-race measurements two days following the race. This was done to capture the kinetic patterns when DOMS symptoms had peaked in the runners (Braun & Dutto, 2003; Cheung, Hume, & Maxwell, 2003), as opposed to capturing the acute fatigue that would be present immediately post-race. This may have explained why we failed to observe some of the patterns commonly reported in measurements taken immediately after ultramarathon races, such as increased stride frequencies (Degache et al., 2016; Giandolini et al., 2016; Morin, Samozino, et al., 2011; Morin, Tomazin, et al., 2011). It also highlighted the different mechanisms and manifestations of fatigue in gait: changes due to acute fatigue following an exhausting event versus recovery or persistence of those changes due to prolonged chronic fatigue symptoms in the days and weeks following. Future investigations into the time course of these changes and their recoveries following exhaustive and fatiguing running events would provide further insight into recovery mechanisms and their implications for athlete monitoring.

Finally, the results of the nonlinear regression spring-mass parameter estimations indicated that the touchdown angle and leg length metrics were highly covaried. This indicated that the estimates for the standard errors on those parameters were unreliable and therefore cannot be used to infer any effect (or lack thereof) from the race on those measures. This pattern was similarly observed in Chapter 2 and Chapter 3. We conducted an additional analyses modeling these two terms as one geometric term (Chapter 2 and Section 2.7). The results are provided in Section 4.7 (Table 15), and the corresponding correlation-covariance matrix is given in Figure 19. As expected, the race did not affect any of the parameter estimates. In the reduced model, effective contact time remained consistently independent of other parameter estimates, but the effective stiffness and non-vertical leg compression terms exhibited a negative correlation. This may have contributed to the larger standard error observed on the effective stiffness term as compared to the errors on the traditional measures (2.9 kN/m vs. 0.5 kN/m). Though it did not affect the SM fit values, it may have indicated a reduced sensitivity of the model to capture low-magnitude significant parameter differences. Therefore, we cannot rule out the potential for undetected small changes in effective stiffness—as observed in the traditional leg stiffness measure. However, the independence of tc* and its corresponding lack of a post-race effect coupled with the consistent F_{max} values before and after the race together supported the notion that the systemic spring-mass parameters were not substantially altered two days after the race.

4.6 Conclusion

We examined the effect of a road ultramarathon on the spring-mass behavior in runners. The runners exhibited higher vertical impact peaks after the race despite consistent peak vGRF magnitudes. The runners also exhibited small but significant decreases in contact time, which did not affect stride frequency but did lead to an increase in leg stiffness and leg compression while leaving vertical stiffness and displacement unchanged. When analyzed systemically via nonlinear regression, the system spring-mass parameters were not significantly altered in the post-race condition. The measures of similarly to a spring-mass system indicated that while the kinetic energy progressions through stance were not changed, the overall similarity of the vGRF time series to that of a spring-mass model fit to each runner decreased following the race. This suggested that the runners produced gait patterns that were systemically very similar before and after the race but that the fatigue induced greater variability in the production of those patterns. Together, these findings suggested that fit and variability measures of gait patterns may be more informative in describing or monitoring post-event fatigue in runners.

4.7 Addendum: Three-Parameter Nonlinear Regression Model Analysis

The parameterized sinusoidal vertical ground reaction force presented in Equation 43 is not unique for a single leg length and touchdown angle combination, as the two terms have an identity A such that:

48 $$A = L_0 - L_0 \, sin \, \alpha_{TD}$$

To enable use of NLR to estimate spring-mass parameters for isolated steps, this term can be incorporated into Equation 17 as a three-parameter model:

49 $$F_y(t) = \left(k \frac{A - \frac{g}{8} t_c}{1 - \frac{k}{m}\left(\frac{t_c}{\pi}\right)^2}\right) sin\left(t \frac{t_c}{\pi}\right)\left(1 - \frac{1}{1 + e^{-10^{10}(t - t_c)}}\right)$$

Using NLR, this method can provide an estimate for A, which corresponds to the non-vertical leg compression during stance ($A = \Delta L - \Delta y$). We used the methods described in Section 4.3.3 to repeat the NLR parameter estimation with a three parameter model corresponding to k*, A*, and t_c*. The results are presented in Table 15 with the correlation-covariance matrix given in Figure 19.

Figure 19: Correlation-covariance matrix for the three-parameter NLR model's fixed effects from Appendix A. Note that in this reduced model, the effective stiffness and non-vertical displacement measure (a combined term for effective touchdown angle and leg length) tend to be inversely correlated.

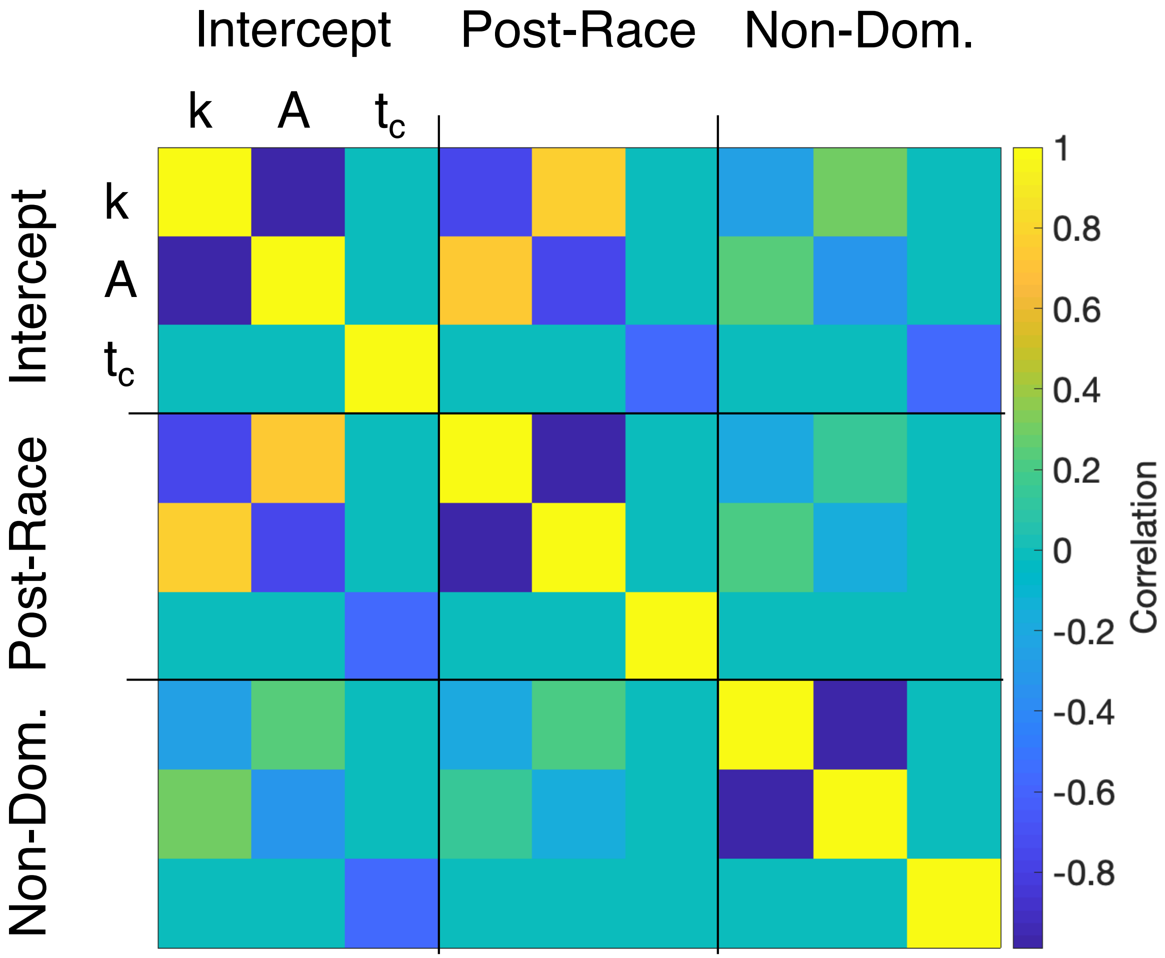

Chapter 5 Traditional Spring-Mass-Analyses with a Mixed-Effect Model Design: A Study of Elite Middle-Distance Runners

This chapter will be submitted for publication as or similar to:

Geoffrey T. Burns, Richard Gonzalez, Jessica M. Zendler, and Ronald F. Zernicke (2020). "Spring-Mass Characteristics of Elite Middle Distance Runners Across a Variety of Training and Racing Speeds"

5.1 Abstract

Elite middle distance runners present as a unique population in which to explore biomechanical phenomena in relation to running speed, as their training and racing spans a broad spectrum of paces. However, there have been no comprehensive investigations of running mechanics across speeds within this population. Here, we used the spring-mass model of running to explore global mechanical behavior across speeds in these runners. Ten elite-level 1500m runners (mean best: 3:37.3±3.6s) and ten highly trained 1500m runners (mean best: 4:07.6±3.7s) ran on a treadmill at 10 speeds where temporal measures were recorded. Spatiotemporal and spring-mass characteristics and their corresponding variation were calculated within and across speeds. All spatiotemporal measures changed with speeds in both groups, but the changes were less substantial in the elite runners. The elite runners ran with greater approximated vertical forces (+0.16 BW) across speeds. Moreover, they ran as stiffer systems, with greater leg and vertical

stiffnesses (+2.1 kN/m and +3.6 kN/m) across speeds. Neither group changed leg stiffness with increasing speeds, but both groups increased vertical stiffness (1.6 kN/m per km/hr), and the elite runners more so (further +0.4 kN/m per km/hr). The elite runners also demonstrated lower variability in their spatiotemporal behavior across speeds. Together, these findings suggested that elite middle distance runners may have distinct global mechanical patterns across running speeds, where they behave as stiffer, less variable spring-mass systems compared to highly trained, but sub-elite counterparts.

5.2 Introduction

The flight phase and the single-support stance phase that define running allow humans to realize an enormous variety of velocities, and no athletes are more fluent across this spectrum of speed than those of the middle-distance runners. In one of the earliest studies examining the oxygen cost of running across speeds, Sargent chose his lone subject to be a competitive middle-distance runner, as he was “a performer capable in both sprint and long-distance work” (Sargent, 1926). Their racing demands enormous fluctuations in speed, spanning the aerobic and anaerobic continuum (Sandford, 2018). At a global level, recent championships in the men’s 1,500m have seen average speeds ranging from 6.5 to 7.1 m/s (Sandford, Day, & Rogers, 2019), with inter-lap variability often exceeding 10% of that (Mytton et al., 2015), and intra-lap variability even more (Hanley, Stellingwerff, & Hettinga, 2019). Training for this variety itself requires greater variety. The Australian 1,500m runner Herb Elliott, 1960 Olympic champion and former world record holder in the event, included in his training regimen not only runs themselves ranging from 220-yard maximal sprints to 30-mile distance sessions, but also “fast climbing of mountainsides, running up stairs of buildings up to ten stories, trudging in snow, and… long distance swimming” (Wilt, 1959). While modern middle-distance training is slightly less eccentric, it still routinely consists of running that may span 50 to 115% of racing speeds with substantial volumes at the lower end of that spectrum (Kenneally, Casado, & Santos-Concejero, 2018; Noakes, 2003; Sandford, 2018).

While middle-distance runners therefore present as a population that have developed their gait patterns across a variety of speeds, elite runners further present as a population that has refined their gait patterns under high volumes training and competitive pressure to maximize performance capacity. They are therefore thought to have undergone a process of mechanical "self-optimization" (Williams & Cavanagh, 1986, 1987). Previous biomechanical investigations of elite distance runners have focused on middle-long and long-distance specialists (Cavanagh et al., 1977; Padulo et al., 2012; Santos-Concejero et al., 2015; Williams et al., 1987), and relatively little work has examined the biomechanical patterns in elite middle-distance runners. Leskinen and colleagues studied the in-race biomechanics of elite and national-class 1500m runners (average bests: 3:36 and 3:49, respectively) via high-speed video. While the racers ran with similar speeds and contact times in the races studied, they observed the elite cohort to run with faster hip flexion during the swing phase and greater knee stiffness during stance. They concluded that the latter may have indicated a more efficient recycling of energy through the gait cycle via elastic storage and return as opposed to the greater amount of concentric work observed in the lower-caliber runners (Leskinen et al., 2009). Trowell and colleagues studied the kinematics and kinetics of a group of national-class middle distance runners (best 1500m: 3:31 to 4:01) at a racing speed (7.2 m/s) and used multiple regression to identify mechanical characteristics that explained differences in performance. Among the group of runners, better performance was explained primarily by a smaller range of motion in the hip during the swing phase, less plantarflexion in the ankle at contact, and less thorax flexion during propulsion. Contrary to the in-race findings of Leskinen and colleagues, they observed that the better runners also exhibited greater knee flexion during stance (Trowell et al., 2019). It is unclear if the differences in the findings were related to the methodology, context, or relative homogeneity of populations (elite- and national-class athletes). Moreover, the studies were limited to single racing speeds, which revealed important insights in competition-specific patterns, but it has yet to be established how these high-level runners do or do not alter their gait across the spectrum of speeds to which they are exposed and practiced.

An alternative method to the component-level kinematic investigations described above is to assess the systemic characteristics of the runners. The spring-mass model is commonly used to describe runners (Blickhan, 1989; McMahon & Cheng, 1990). It treats the runner as a single point-mass on a linear elastic spring that strikes and leaves the ground at a constant touchdown angle, and it has been proposed as the mechanical template that underlies the running gait across species (Full & Koditschek, 1999). It has been applied to characterize systemic gait behavior within a variety of running contexts, including temporal alterations (Farley & Gonzalez, 1996); surface variations (Ferris et al., 1998); energy costs (Dalleau et al., 1998); sprinting (Morin et al., 2006), distance (Hayes & Caplan, 2014), and ultradistance (Morin, Samozino, et al., 2011) performance; and fatigue (Hunter & Smith, 2007). As such, the spring-mass model and its spatiotemporal characteristics have exhibited relations to running performance and economy, such as leg and vertical stiffness (Dalleau et al., 1998; Heise & Martin, 1998), vertical oscillation (Folland et al., 2017; Slawinski & Billat, 2004; Williams & Cavanagh, 1987), contact time (Nummela et al., 2007), stride frequency (de Ruiter et al., 2014), and stride length (Cavanagh et al., 1977). Figure 20 shows the model as interpreted in human running (adapted from Muybridge (Muybridge, 1887)).

Figure 20: The spring-mass model of running

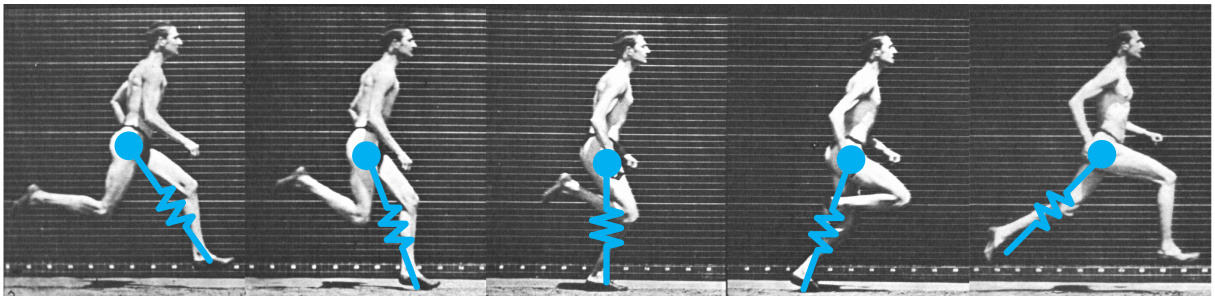

The model has been applied to elite runners in the study of sprinting (Taylor & Beneke, 2012) and triathlon (Rabita et al., 2011), but it has not been systematically examined in elite middle-distance runners. Rogers and colleagues studied leg stiffness in a group of highly-trained middle-distance runners (average 1,500m best: 4:02) at a single submaximal speed (14 km/hr) and at a maximal sprinting speed and observed that the leg stiffness in sprinting was strongly correlated to both running economy and maximal sprinting speed (Rogers et al., 2017). Similarly, Fourchet and colleagues studied the spring-mass characteristics of youth middle-distance runners during an exhaustive run, and found contact time, vertical displacement, and leg compression to increase following the run, resulting in decreased leg stiffnesses with consistent stride lengths and frequencies (Fourchet et al., 2015). These investigations suggest the importance of spring-mass characteristics in mediating middle-distance performance. Additionally, some spring-mass characteristics are speed dependent (Farley et al., 1993; McMahon & Cheng, 1990), and while several studies have assessed these changes in runners of varying abilities (Arampatzis et al., 1999; Garcia-Pinillos et al., 2019; Padulo et al., 2012), none have systemically examined speed-dependent patterns in elite middle- or long-distance runners.

Furthermore, these model characteristics are often reported as stationary values without indication of intra-individual variability patterns. Mechanical patterns within runners are not stationary (Bates et al., 1983; Cavanagh et al., 1985; Winter, 1984), and the patterns of variability may have implications for injury and performance (Hamill, Palmer, & Van Emmerik, 2012; Preatoni et al., 2013). It has been proposed that there are two broad classes of variability in biomechanical patterns: task-level outcome variability (e.g., stride length in running) and process-level component variability (e.g., joint coordination patterns). These are referred to as end-point variability and coordinative variability, respectively (Hamill et al., 2012). There are divergent thoughts on how coordinative variability relates to expertise in biomechanics, with some observing U-shaped curve for the amount of component variability (Wilson et al., 2008), some finding decreasing variability in important movements among skilled performers (Hiley, Zuevsky, & Yeadon, 2013), and some finding no difference between skill levels (Floria et al., 2018). At the task level, it has been shown that variability decreases in more experienced or skilled performers in race-walking (Preatoni et al., 2010) and running (Nakayama, Kudo, & Ohtsuki, 2010). Belli and colleagues observed variability in center-of-mass displacement and step time to increase with running speed in moderately trained runners, with the amount of variability across speeds further bearing a moderate correlation to the energy cost of running (Belli et al., 1995). Similarly, Candau and colleagues found a significant relation between lower levels of step frequency variability and better running economy and that the variability increased with fatigue (Candau et al., 1998) Furthermore, outcome variability assessed within stride lengths has been observed to decrease with training (Slawinski et al., 2001). Together, these observations indicate that variability within global mechanical behaviors may be a barometer for performance, skill, and fatigue in runners, but it has yet to be studied within elite runners or investigated in relation to the systemic spring-mass parameters across speeds.

As global mechanical parameters that are modeled by spring-mass dynamics and their respective levels of variability may have implications for running performance, the systemic characterization of the model's behavior across a variety of speeds in a group of elite runners may reveal fundamental mechanistic insights that relate to expertise and performance in the sport. The goal of this study was to explore how spring-mass mechanics changed across a variety of training and racing speeds in elite middle-distance runners and to compare those patterns to trained, but non-elite middle-distance runners. The hypothesis was that all parameters would exhibit similar speed dependencies in both groups, but that the variation in the parameters across speeds would be lower in the elite runners.

5.3 Methods

5.3.1 Experimental Data Collection

5.3.1.1 Subjects

Ten elite-level (inclusion criteria below) male middle-distance runners were recruited and enrolled in the study. They were matched by 10 trained, but not elite-level male middle-distance runners. The study was restricted to self-identified 1500m/mile specialists. Given the high heterogeneity of training and physiological profiles within middle-distance disciplines, we chose this athlete profile so as to select runners exposed to and familiar with a large spectrum of speeds in training (Sandford & Stellingwerff, 2019). Given the distinct nature of the subject population, this enrollment was subject to convenience sampling, and the target was based on similar studies of elite distance runners. A previous biomechanical study of elite distance runners found an average coefficient of variation of 8% among stride length, stride rate, swing time, flight time, and contact time (Cavanagh et al., 1977). Assuming this coefficient of variation in the observations and controlling for Type I error with $\alpha = 0.05$, 9 subjects in each cohort would allow for detection of a 10% difference in means with statistical power of 1-β = 0.80 (Van Belle, 2011). Though this investigation sought to analyze the gait patterns of the runners with the mixed-effects linear regression modeling described below, this effect size approximation of the convenience sample nonetheless provided some context for the expected power of the study.

Inclusion criteria for the elite cohort of runners required that the subjects had achieved a sanctioned race performance in a long middle-distance track event (1500m or mile) equivalent to or greater than 1075 points per IAAF scoring tables in the current or previous competitive season (1500m equivalent of 3:42.4 for males) (Spiriev & Spiriev, 2017). Inclusion criteria for the trained cohort of middle-distance runners required that they had achieved a sanctioned race performance equivalent to or greater than 465 but less than 1075 points in the current or previous competitive season (1500m equivalent of 3:42.5 to 4:38.0) (Spiriev & Spiriev, 2017). All participants were required to be free of lower limb injury at the time of testing and possess familiarity with treadmill running.

5.3.1.2 Running Protocol

All subjects ran for 20 minutes at a self-selected pace on a treadmill as a warm-up. Following this warm-up, subjects ran at four submaximal running velocities for four minutes each, separated by a brief (30-45 s) pause. The elite cohort ran at 12 km/hr, 14 km/hr, 16 km/hr, and 18 km/hr, and the trained cohort ran at 10 km/hr, 12 km/hr, 14 km/hr, and 16 km/hr. These speeds represent typical training speeds for runners of this caliber (Daniels, 2014). Following these steady-state submaximal running bouts, the runners ran a series of six 30-second trials at interval-training and racing paces incrementing from 20 to 25 km/hr in the elite cohort and 18 to 23 km/hr in the trained cohort. Each trial was separated by 90 seconds of jogging at 11-12 km/hr so that the full bout of six 30-second runs was continuous.

Each 4 minute trial was expected to capture 600-700 step cycles for each runner, and each 30 second trial was expected to capture 80-100 step cycles for each runner, totaling approximately 3000 steps per runner for analysis. This exceeded the 32-64 steps recommended as a minimum by Belli an colleagues to characterize mechanical parameter variability (Belli et al., 1995). The investigation was approved by the University of Michigan's Institutional Review Board (ref: HUM00129528), and all subjects provided written informed consent.

5.3.1.3 Spatiotemporal Measures

Contact time (t_c) and flight time (t_f) were recorded continuously throughout the running sessions at 100 Hz via a treadmill instrumented with a pressure plate (h/p/cosmos Quasar, h/p/cosmos Sports & Medical gmbh, Nussdorf-Traunstein, Germany). This system has demonstrated agreement and reliability in these measures with a photoelectric timing system (Lee et al., 2014). The platform had a sensing area of 1.36 x 0.64 cm with 10,240 sensors with detection thresholds of 1 N/cm^2. The trials were recorded using Noraxon MyoMotion software (Noraxon USA, Scottsdale, AZ, USA), and the continuous data were exported for step cycle analysis in MatLab (MathWorks, Natick, MA, USA).

5.3.1.4 Spring-Mass Characteristics

The spring-mass parameters for each step were calculated using the method of Morin et al. (Morin et al., 2005). Briefly, this modeled the vertical ground reaction force as a sinusoid with the subject's body mass, m, and used the observed t_c and t_f to approximate the maximal vGRF, F_{max}:

$$F_{max} = mg\frac{\pi}{2}\left(\frac{t_f}{t_c}+1\right) \tag{50}$$

The center-of-mass's absolute displacement during stance, Δy, was then modeled as:

$$\Delta y = \frac{F_{max}}{m}\frac{{t_c}^2}{\pi^2} - g\frac{{t_c}^2}{8} \tag{51}$$

Maximal leg compression of the spring during stance, ΔL, was approximated using the subject's measured leg length, L_0, and running speed, v, as:

52 $$\Delta L = L_0 - \sqrt{{L_0}^2 - \left(\frac{vt_c}{2}\right)^2} + \Delta y$$

From these values, leg stiffness, k_{leg}, was calculated as $F_{max}/\Delta L$, and vertical stiffness, k_{vert}, was calculated as $F_{max}/\Delta y$.

5.3.2 *Data Analysis*

Spatiotemporal measures (contact time (t_c), flight time (t_f), duty factor (DF), stride length (SL), and stride frequency (SF)) and traditional spring-mass measures (k_{leg}, k_{vert}, center-of-mass displacement (**Δ**y), leg compression (**Δ**L), and approximated maximal vertical force, F_{max}) were calculated for each step captured. Within each trial at each speed, the coefficient of variation (CV) for each measure was calculated as σ/μ. Analysis of the measures across speeds was conducted using mixed-effect model linear regression, where the measure was treated as the response variable, the cohort (elite vs. trained) as a discrete fixed effect, and the speed as a continuous fixed effect with an interaction. Each subject was assigned a random effect intercept with a random slope corresponding to an individual speed-dependency:

53 $$y = \beta_{cohort} \times \beta_{speed} + Error(Speed|Subject)$$

For the coefficient-of-variation models, the random slope was excluded, as the measures were aggregated as single observations at each speed for each subject. For the linear mixed-effect models, the fixed effects were assessed for significance via Satterthwaite's method. Statistical test criterion in all models used a Type I error control of $\alpha < 0.05$. MatLab (2019a, MathWorks, Natick, MA, USA) was used for all data processing, and R (v3.6.2, R Foundation for Statistical Computing, Vienna, Austria) was used for all statistical analyses.

5.4 Results

The subject characteristics are given in Table 2. A total of 70,812 steps were recorded. For each subject across the ten speeds, 3540 ± 157 steps were captured (mean ± s.d.), with 738 ± 60 steps for each of the four submaximal speeds, and 98 ± 30 steps for each of the six interval/racing speeds. For all fixed effects and interactions presented below, the values are described as the effect ± standard error.

Characteristic	**Elite**			**Trained**		
Subjects (n)	10			10		
Age (yr)	27.7	±	3.8	23.7	±	4.0
Mass (kg)	70.4	±	6.2	64.1	±	3.6
Height (m)	1.82	±	0.08	1.78	±	0.06
Leg Length (m)	0.956	±	0.044	0.925	±	0.049
1500m Best (min:sec)	03:37.4	±	3.6 s	04:07.6	±	3.7 s
1500m Speed (m/s)	6.90	±	0.12	6.06	±	0.09

Table 16 Elite and trained cohort characteristics.

5.4.1 Spatiotemporal Measures

The results for the spatiotemporal measures are provided in Table 17, where the intercept terms for the trained cohort are scaled to values for 14 km/hr and the fixed effect for the elite runners are presented below that term along with the speed slope and its grouping interaction. Each of the spatiotemporal measures had significant speed dependencies independent of cohort (all speed effects $p < 0.001$). The elite runners exhibited less of a speed dependency than the trained runners, with their interaction on the speed being +2±0.4 ms per km/hr ($p < 0.001$). Their flight times were 15±7 ms higher ($p = 0.040$) but the speed dependency –1±0.3 ms per km/hr lower ($p = 0.019$). This resulted in duty factors that were lower, though the fixed effect estimate did not reach the threshold for significance (p = 0.059). As such, stride frequencies and stride lengths were ultimately not significantly different between groups.

5.4.2 Spring-Mass Measures

The spring-mass characteristics (Table 18) include the intercept terms for the trained cohort scaled to values corresponding to 14 km/hr, and the fixed effect for the elite runners are presented below with the speed slope and its grouping interaction. The approximated peak vertical forces were higher in the elite runners (+0.16 ± 0.07 BW, p = 0.045), but their speed dependency was not different from the trained runners. The elite runners had higher leg stiffnesses (+2.1 ± 0.7 kN/m, p = 0.007) across speeds, but neither cohort significantly altered their stiffnesses with speed. Similarly, the elite runners exhibited higher vertical stiffnesses (+3.6 ± 1.5 kN/m, p = 0.031). While both groups increased their vertical stiffnesses across speeds (6.6 ± 0.1 kN/m per km/hr, p < 0.001), the elite runners did more so (0.40 ± 0.1 kN/m per km/hr, p = 0.006). However, their vertical displacements during stance were similar, with both groups decreasing vertical motion at faster speeds equivalently (–0.2 ± 0.02 cm per km/hr, p < 0.001). Both groups increased their leg compression at faster speeds (0.5 ± 0.03 cm per km/hr, p < 0.001), but the elite runners' compressions were less affected by speed increases (–0.2 ± 0.07 cm per km/hr, p = 0.024). The spatiotemporal and spring-mass trends are presented in Figure 21, where within each measure, the population effects (fixed) and individual effects (random) are presented on the left and right, respectively. The full set of observations for two representative subjects from each cohort are shown (Figure 22) for contact time, flight time, vertical force, leg stiffness, and vertical stiffness.

The coefficients of variation for the spatiotemporal measures are presented similarly (Table 19). Both cohorts had greater variation in contact time at faster speeds (+0.05 ± 0.02% per km/hr, p = 0.014), but there were no differences between groups. The elite runners had significantly lower variations in their flight times (–1.3 ± 0.4%, $p = 0.006$). Both groups decreased variation at faster speeds (–0.24 ± 0.02% per km/hr, $p < 0.001$), but the elite runners were less affected by speed increases (+0.19 ± 0.04% per km/hr, $p < 0.001$). Ultimately, variations in duty factors were similar between groups and unaffected by speed, but stride frequency variation was significantly lower the elite runners (–0.3 ± 0.1%, $p = 0.017$) and higher across speeds in both groups (+0.04 ± 0.01%, $p < 0.001$). Similarly, stride length variability was lower in the elite runners (–0.3 ± 0.1%, $p = 0.019$), and both groups increased stride length variability at faster speeds (+0.03 ± 0.01%, $p < 0.001$).

The coefficients of variation for the spring-mass characteristics (Table 20) indicated that the variations in peak vertical forces were equal between groups and did not change with speed. Leg stiffness and vertical stiffness variation was similarly similar between both groups, but both measures saw significant increases across speeds of 0.30 ± 0.06% per km/hr ($p < 0.001$) and 0.17 ± 0.04% per km/hr ($p < 0.001$), respectively. Leg compression variation was similarly equal between groups and also increased with speed 0.22 ± 0.04% per km/hr ($p < 0.001$). The variation in vertical displacement was lower in the elite runners across speeds (– 0.7 ± 0.3%, $p = 0.018$), and both groups exhibited modest increases with speed (+0.05 ± 0.02% per km/hr, $p = 0.008$). The group trends for the variation patterns in each measure are presented in Figure 23.

Figure 21: Spatiotemporal and spring-mass characteristics for elite and trained runners across speeds. Population (fixed, left) and individual (random, right) effects given for each measure

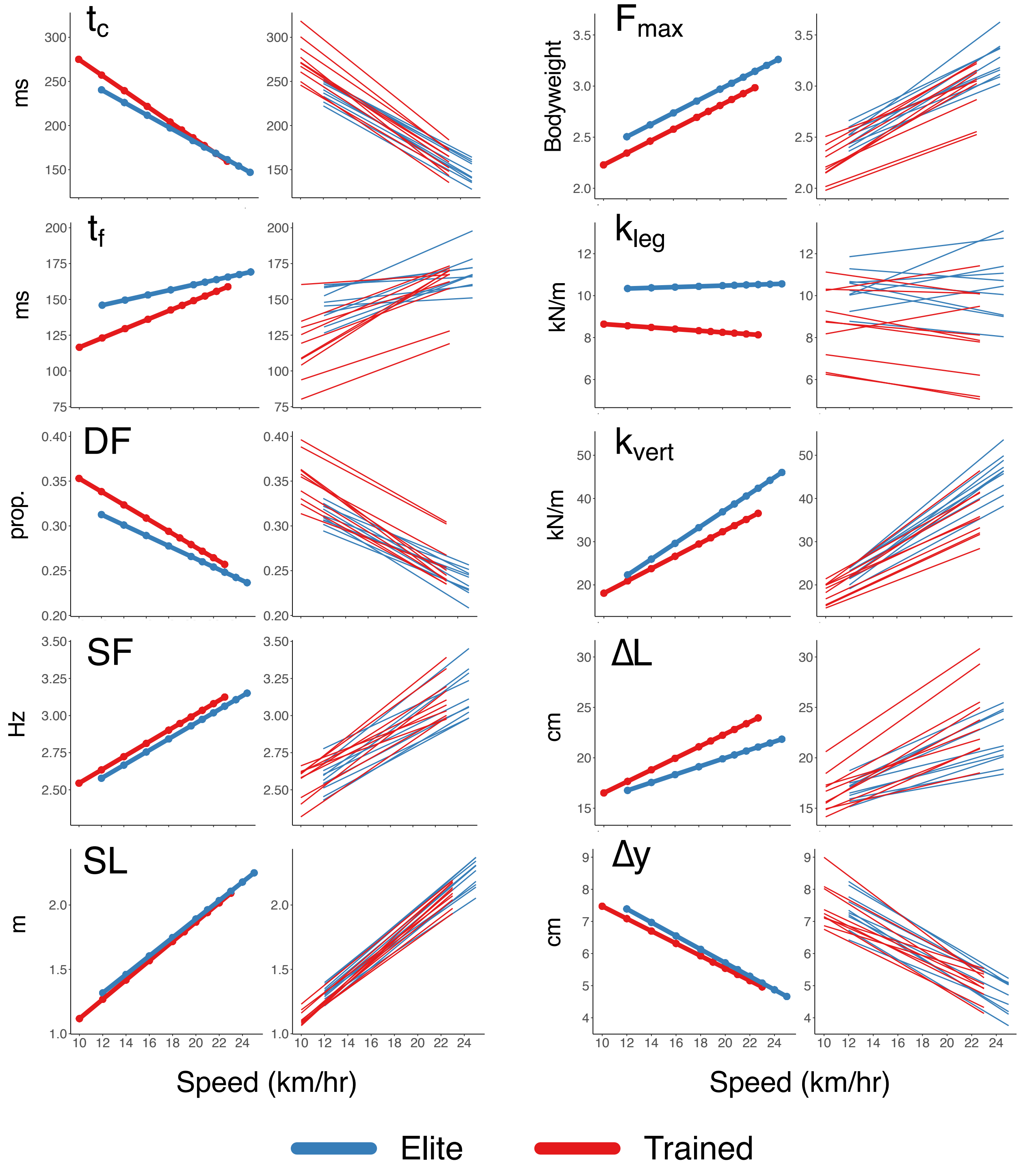

Figure 22: Select spring-mass characteristics across speeds for two representative subjects for the elite (left) and trained (right) cohorts

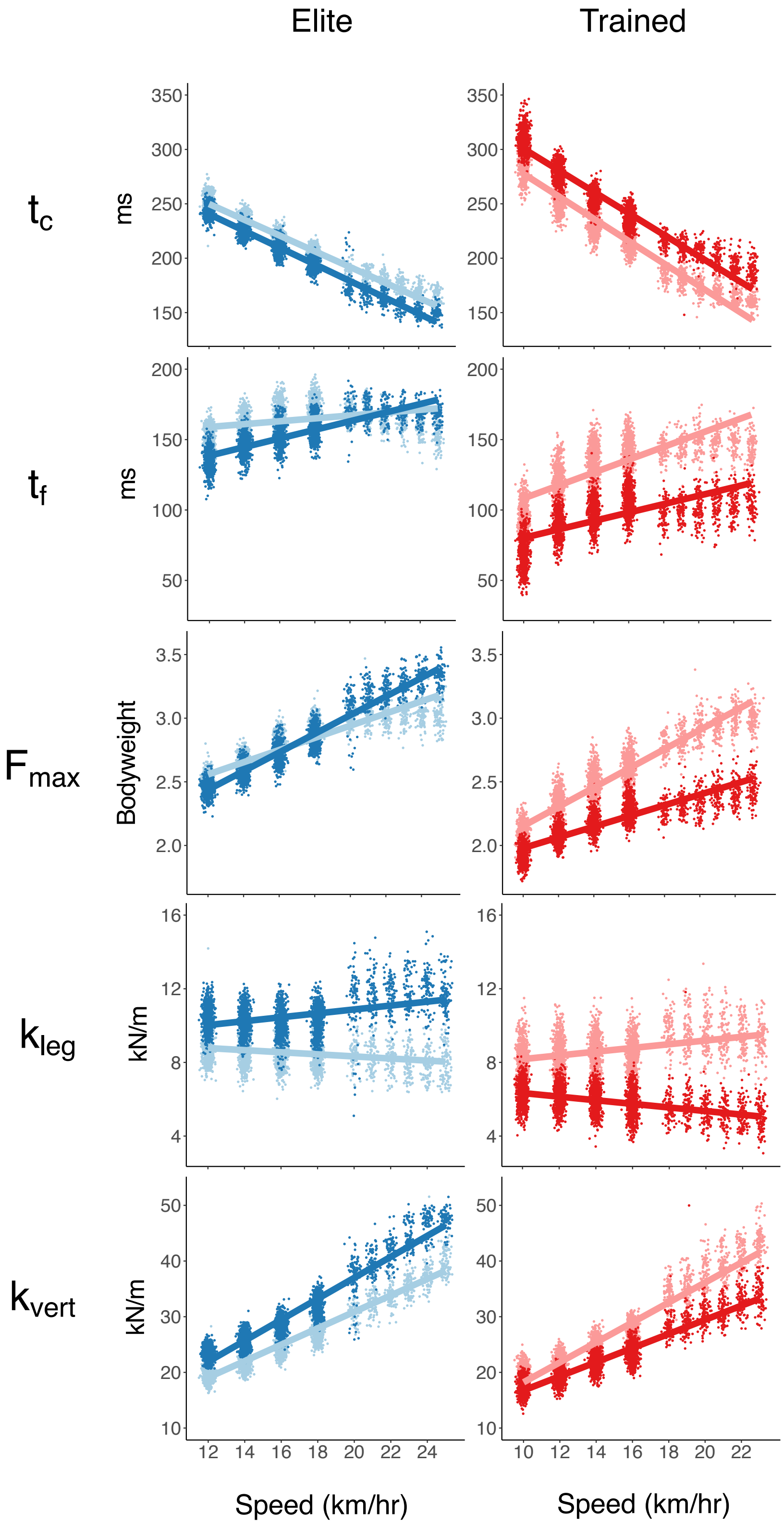

Figure 23: Coefficient of variations at each speed for the spatiotemporal and spring-mass characteristics of the elite and trained runners

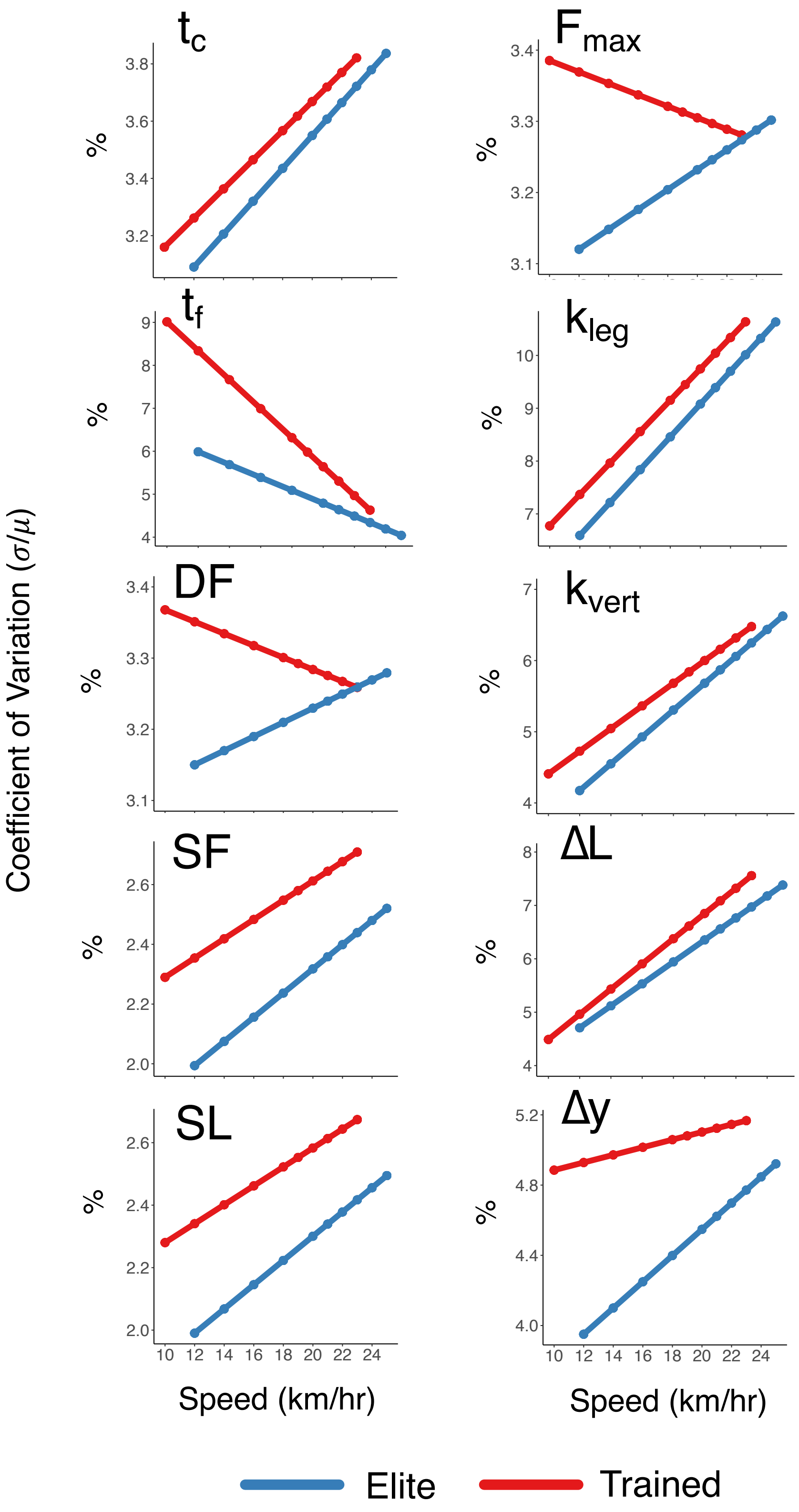

	t_c (ms)	**sem**	**p-value**	
Trained	237	3.2	-	
Elite	–7	6.5	0.262	
Speed	–8	0.2	<0.001	✻✻✻
Cohort x Speed	2	0.4	<0.001	✻✻✻
	t_f (ms)	**sem**	**p-value**	
Trained	132	3.3	-	
Elite	+15	6.7	0.040	✻
Speed	3	0.3	<0.001	✻✻✻
Cohort x Speed	–1	0.6	0.019	✻
	DF	**sem**	**p-value**	
Trained	0.32	0.004	-	
Elite	–0.02	0.008	0.059	
Speed	–0.01	0.000	<0.001	✻✻✻
Cohort x Speed	0.00	0.001	0.016	✻
	SF (Hz)	**sem**	**p-value**	
Trained	2.72	0.02	-	
Elite	–0.06	0.05	0.254	
Speed	0.04	0.00	<0.001	✻✻✻
Cohort x Speed	0.00	0.00	0.913	
	SL (m)	**sem**	**p-value**	
Trained	1.42	0.015	-	
Elite	+0.03	0.030	0.289	
Speed	0.07	0.001	<0.001	✻✻✻
Cohort x Speed	0.00	0.00	0.294	

Table 17 Spatiotemporal estimates for the groups with effects for group, speed, and the interactions. The values provided for the trained cohort correspond to the model estimate at 14 km/hr. Estimated standard errors are provided for each effect (sem). Statistical significance of each effect is indicated as: ✻ $p < 0.05$ and ✻✻✻ $p < 0.001$

	F_{max} (BW)	**sem**	**p-value**	**sig.**
Trained	2.46	0.037	-	
Elite	+0.16	0.074	0.045	✻
Speed	0.06	0.003	<0.001	✻✻✻
Cohort x Speed	0.00	0.006	0.997	
	kl_{eg} (kN/m)	**sem**	**p-value**	
Trained	8.39	0.344	-	
Elite	2.09	0.689	0.007	✻✻
Speed	–0.01	0.021	0.607	
Cohort x Speed	0.06	0.042	0.197	
	k_{vert} (kN/m)	**sem**	**p-value**	
Trained	23.07	0.769	-	
Elite	+3.60	1.538	0.031	✻
Speed	1.62	0.065	<0.001	✻✻✻
Cohort x Speed	0.40	0.130	0.006	✻✻
	ΔL (cm)	**sem**	**p-value**	
Trained	19.12	0.536	-	
Elite	–1.89	1.072	0.095	
Speed	0.48	0.037	<0.001	✻✻✻
Cohort x Speed	–0.18	0.074	0.024	✻
	Δy (cm)	**sem**	**p-value**	
Trained	6.73	0.108	-	
Elite	+0.21	0.216	0.340	
Speed	–0.20	0.010	<0.001	✻✻✻
Cohort x Speed	–0.02	0.019	0.409	

Table 18 Spring-mass characteristics for the groups with effects for group, speed, and the interactions. The values provided for the trained cohort correspond to the model estimate at 14 km/hr. Estimated standard errors are provided for each effect (sem). Statistical significance of each effect is indicated as: ✻$p < 0.05$, ✻✻$p < 0.01$, and ✻✻✻$p < 0.001$

	t_c (ms)	sem	p-value	sig.
Trained	3.35	0.12	-	
Elite	–0.13	0.24	0.573	
Speed	0.05	0.02	0.014	✻
Cohort x Speed	0.01	0.04	0.881	
	t_f (ms)	**sem**	**p-value**	
Trained	7.34	0.21	-	
Elite	–1.32	0.43	0.006	✻✻
Speed	–0.24	0.02	<0.001	✻✻✻
Cohort x Speed	0.19	0.04	<0.001	✻✻✻
	DF	**sem**	**p-value**	
Trained	3.30	0.103	-	
Elite	–0.10	0.205	0.631	
Speed	0.00	0.015	0.957	
Cohort x Speed	0.02	0.029	0.528	
	SF (Hz)	**sem**	**p-value**	
Trained	2.40	0.06	-	
Elite	–0.31	0.12	0.017	✻
Speed	0.04	0.01	<0.001	✻✻✻
Cohort x Speed	0.01	0.02	0.595	
	SL (m)	**sem**	**p-value**	
Trained	2.39	0.06	-	
Elite	–0.30	0.12	0.019	✻
Speed	0.03	0.01	<0.001	✻✻✻
Cohort x Speed	0.01	0.01	0.564	

Table 19 Coefficients of variation for spatiotemporal measures with effects for group, speed, and the interactions. The values provided for the trained cohort correspond to the model estimate at 14 km/hr. Estimated standard errors are provided for each effect (sem). Statistical significance of each effect is indicated as: ✻ $p < 0.05$, ✻✻ $p<0.01$, and ✻✻✻ $p<0.001$

	F_{max} (BW)	sem	p-value	sig.
Trained	3.31	0.10	-	
Elite	–0.13	0.21	0.542	
Speed	0.00	0.01	0.836	
Cohort x Speed	0.02	0.03	0.441	
	k_{leg} (kN/m)	**sem**	**p-value**	
Trained	7.94	0.26	-	
Elite	–0.70	0.52	0.195	
Speed	0.30	0.06	<0.001	✻✻✻
Cohort x Speed	0.01	0.12	0.909	
	k_{vert} (kN/m)	**sem**	**p-value**	
Trained	4.99	0.17	-	
Elite	–0.39	0.35	0.274	
Speed	0.17	0.04	<0.001	✻✻✻
Cohort x Speed	0.03	0.07	0.683	
	ΔL (cm)	**sem**	**p-value**	
Trained	5.49	0.21	-	
Elite	–0.42	0.41	0.322	
Speed	0.22	0.04	<0.001	✻✻✻
Cohort x Speed	–0.03	0.08	0.706	
	Δy (cm)	**sem**	**p-value**	
Trained	4.88	0.13	-	
Elite	–0.69	0.27	0.018	✻
Speed	0.05	0.02	0.008	✻✻
Cohort x Speed	0.05	0.04	0.139	

Table 20 Coefficients of variation for spring-mass characteristics with effects for group, speed, and the interactions. The values provided for the trained cohort correspond to the model estimate at 14 km/hr. Estimated standard errors are provided for each effect (sem). Statistical significance of each effect is indicated as: ✻ $p < 0.05$, ✻✻ $p < 0.01$, and ✻✻✻ $p < 0.001$

5.5 Discussion

5.5.1 Summary

Across running speeds, elite middle distance runners generally ran as stiffer mechanical systems than their highly-trained but non-elite counterparts, and they tended to adjust their mechanics differently in response to speeds changes. The spatiotemporal characteristics of both groups were strongly speed-dependent, but the flight times and corresponding duty factors were less affected in the elite runners. The maximal vertical forces were similarly speed-dependent in both groups but were consistently higher in the elite runners. Spring-mass analyses demonstrated that the elites had higher leg and vertical stiffnesses, and they augmented their vertical stiffnesses more at faster speeds. The elite runners also demonstrated less variability in some of the mechanical parameters, with their fight times, stride lengths, stride frequencies, and vertical displacements being less variable across speeds than that of the trained runners. These results suggested that elite middle-distance runners exhibited systemic mechanical patterns that distinguish them from other highly-trained middle-distance runners.

5.5.2 Spatiotemporal Patterns

As hypothesized, all of the spatiotemporal measures exhibited strong relations with speed. In both cohorts, contact time decreased substantially across speeds, and flight time increased modestly, resulting in a duty factor that progressively decreased across speeds. In the elite runners, the speed relation was significantly smaller, where their ground contacts were shorter in the submaximal speeds but similar at the faster speeds. Their flight times were 11% greater on average across speeds, and their speed-dependent increase was smaller, with their flight phases being relatively longer at lower speeds. This was consistent with both the observations of Leskinen and colleagues, who observed similar contact times and stride frequencies between national-class and elite-level 1500-m runners during a race (~23 km/hr) (Leskinen et al., 2009), and Folland and colleagues, who observed a significant negative correlation between performance and ground contact time at lower speeds (10-12 km/hr) in a large group of middle- and long-distance runners. This was also similar to the observations of Williams and Cavanagh, who observed a modest correlation between contact time at 12.8 km/hr and a 10-km time trial time (Williams & Cavanagh, 1987), as well as Nummela and colleagues, who observed a correlation between submaximal oxygen consumption and contact time that diminished with speed (Nummela et al., 2007). The contact and flight time trends resulted in stride lengths and frequencies that were still equivocal between groups, and similarly exhibited strong speed-dependent increases. This was consistent with previous observations of speed relations within these parameters (Cavanagh & Kram, 1989), as well as their independence from ability or performance (Cavanagh et al., 1977; Folland et al., 2017; Williams & Cavanagh, 1987).

5.5.3 Spring-Mass Patterns

The findings here supported the hypothesis for distinct spring-mass behavior among the elite runners. Their estimated peak vertical forces were 6% higher relative to their body weight, and this, coupled with the temporal differences, resulted in higher stiffness measures. Their leg and vertical stiffnesses were 25% and 16% higher on average across speeds, and while both groups increased vertical stiffness with speed, the elites did so more substantially (5.2 vs. 3.6 kN/m per km/hr). Leg stiffness was independent of speed in both groups, consistent with previous observations in other runners (He, Kram, & McMahon, 1991; Morin et al., 2005) and across animal species (Farley et al., 1993). Farley and her colleagues posited that runners maintain leg stiffness across speeds by decreasing their touchdown angle. With greater vertical forces, they thereby compress their effective spring more. The increased angle, greater force, and greater speed interact to maintain a consistent center-of-mass trajectory through stance across speeds, which with the greater force, then ultimately increases vertical stiffness and decreases the contact time (Farley et al., 1993). This was consistent with our observations, where leg compression increased across speeds by 0.5 cm per km/hr, while vertical displacement only decreased by 0.2 cm per km/hr.

These patterns together suggested that the elite runners may be better exploiting the elastic mechanisms underpinning spring-mass dynamics. Their stiffer effective springs, coupled with greater vertical forces and more sensitive vertical stiffnesses, suggested that they may be recycling kinetic energy more efficiently throughout the gait cycle. The patterns observed here indicated more vertical orientation of their effective elastic mechanisms, which would imply steeper touchdown angles and shorter braking and propulsive periods. As horizontal force generation is metabolically much more expensive than vertical force generation (Chang & Kram, 1999), this propensity to orient their spring-mass dynamics more vertically may explain their greater performance capacity. Furthermore, their exhibition of lower contact times and longer flight times at lower speeds may also be a reflection of more efficient use of these elastic storage and return mechanisms. A more rapid and forceful stretch of musculoskeletal tendinous structures has been demonstrated to improve the elastic efficiency of those structures (Cavagna, Dusman, & Margaria, 1968; Cavagna, Saibene, & Margaria, 1965). Moreover, the contribution of recycled elastic energy to the cost of running has been shown to increase with speeds (Cavagna & Kaneko, 1977), and this elastic, spring-like behavior has been proposed as the predominant means that mediates the energetic efficiency of running across speeds and species (Alexander, 1991a, 1991b). As such, it may be that the elite middle distance runners had more robust or refined mechanisms to exploit this advantage. Moreover, that this behavior was distinctly persistent at lower speeds may further indicate a “mastery” of these mechanisms. However, whether this is a product of their innate ability or their high volume of accumulated lifetime training could not be inferred from this investigation. It is more likely that the characteristics described above are not products of one or the other attributes exclusively, but rather that their innate characteristics facilitated their exceptional training to further refine and exploit those characteristics. That is, the interaction of nature and nurture may have given rise to their emergent, elite ability.

5.5.4 Parameter Variability

The elite runners further demonstrated lower variability in several of the measures across speeds, including flight times, stride frequency, stride length, and their vertical displacements during stance. This was consistent with previous investigations that explored pattern variability in relation to running economy. In trained runners, stride time and vertical oscillation have been associated with better economy (Belli et al., 1995; Candau et al., 1998) and experience level (Nakayama et al., 2010), similar to the stride frequency, vertical displacement, and flight time patterns observed here. Furthermore, Slawinski et al. observed stride frequency variability to decrease after a structured training program in already competitive runners (Slawinski et al., 2001). This decrease was associated with an improvement in running economy and velocity at VO_{2max} despite maximal aerobic capacity remaining unchanged, suggesting that the decreased variability was related to the improvement in efficiency. Spatiotemporal variability has also been observed to be lower among elite racewalkers (Preatoni et al., 2010). These observations coupled with our findings support the notion that variability is associated with skill and expertise. However, the "optimal" amount is still unknown, and it is likely highly individualized. The elite runners here exhibited more control over those parameters across speeds, but it is certainly plausible that further decreasing the variability would be detrimental, where the motor control required could come at an energetic or structural cost. Elite triple jumpers demonstrated a parabolic curve with relation to coordination variability and performance, suggesting that optimality was not simply a minimization exercise (Wilson et al., 2008). It would be interesting to explore these patterns longitudinally within elite runners in a fashion similar to the investigation of Slawinski and colleagues (Slawinski et al., 2001). Would these patterns change with performance level or injury status? It is also curious that distinct trends emerged within the spatiotemporal measures, yet they were mostly absent among the spring-mass parameters. This may indicate that the spring-mass dynamics are an emergent phenomena that are mediated by the others, with spatiotemporal adjustments interacting with each other in more or less variable ways to produce a consistent bounce for a given speed. This would indicate that these control strategies are better regulated in the elite runners with less step-to-step "tuning" occurring.

5.5.5 Methodological Advantages

Aside from the mechanical observations, a secondary goal of the study was to demonstrate the methodological value of a mixed-model experimental design. Here, we studied these patterns not only between groups, but across speeds and within individuals. One notable observation was the relative homogeneity of patterns within the elite runners as compared to the trained cohort that presented across parameters (Figure 21 and Figure 22). Many of the findings observed here may not have emerged if observations were made at a single speed, as the nuanced differences and interactions only emerged across speeds and with prolonged observation within individuals. It was notable that among the elite runners, most demonstrated relative linearity across speeds within most of the parameters, while some of the trained runners had nonlinear shifts at the faster speeds. This might be indicative of distinct mechanical strategies for submaximal running and sprinting, whereas the elite runners demonstrated a greater "fluency" across speeds. While this phenomenon warrants further investigation, it is suggestive that further insights that may be afforded by such an analysis.

Furthermore, as these experimental approaches gain traction and become standard-of-practice in biomechanical investigations, investigators should take great care in formulation of their analytical models. As an example, our mixed-effect models assigned not only a random intercept to each individual, but also a random slope across speeds, assuming that the speed-dependent changes would have an individualized pattern beyond that which was characteristic of the group (Figure 21 and Figure 22). Had we simply used a random intercept model for each subject, it would have appeared that leg stiffness was not only significantly different between groups, but that there was a small, significant speed dependency and interaction. Both effects maintain similar values to what is reported in Table 18 (which were similarly small in magnitude), but their estimated standard errors were drastically reduced due to the apparent increase in degrees of freedom. By adding the random slope, the statistical significance of those marginal effects disappear, but the fit of the model significantly improves because the variance is better explained by the individualized response. The model's Akaike information criterion decreases from 197299 to 189857 ($p < 0.001$) with the addition of the random slope term for speed, indicating significantly better fit. This difference between the appearance of the effects between the two models is displayed in Figure 24. For the variability analyses, we were restricted to using random intercept models, as the variation measures were aggregate values within a speed for each individual. As such, there were not repeated measures within individuals within speeds. Given the value demonstrated by random slope models for speed dependencies, it will be an interesting future line of investigation to aggregate groups of steps within a speed to further characterize these patterns with more individualized speed-dependencies modeled.

Figure 24: Leg stiffness estimates with the fixed effects model and two different random effects models

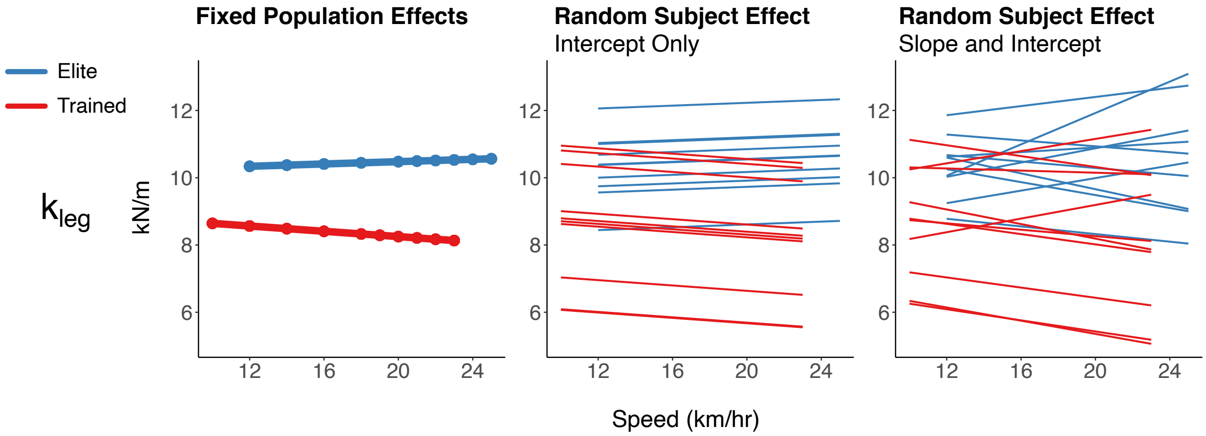

5.5.6 *Limitations*

When interpreting the findings of this investigation, consideration must be given with respect to several aspects of the design. The first is that the spring-mass parameters reported here were calculated via the speed, contact time, and flights time as proposed by Morin et al. (Morin et al., 2005). While this method has been validated against the traditional kinetic methods and has demonstrated excellent agreement with those values (Coleman et al., 2012; Serpell et al., 2012), measures of maximal vertical force and center-of-mass displacement during stance reported here were nonetheless approximations using these temporal and dynamic relations. Furthermore, the temporal characteristics were measured at 100 Hz, which was low compared to gold-standard kinetic measurements. Some investigators analyzing spring-mass or spatiotemporal dynamics have used rates as low as 80 Hz (Morin, Tomazin, et al., 2011) and even 50 Hz (Fourchet et al., 2015; Slawinski et al., 2001), and they mitigated the low sensitivity by aggregating multiple observations. The system used here has demonstrated excellent agreement and reliability with a commonly used photoelectric timing system (Lee et al., 2014), so we anticipated that the sensitivity of the measures would be similarly reduced compared to systems with higher resolution. This would have been problematic in analyzing a limited number of steps, but it was increasingly resolved as more observations were taken. As one of the strengths of the study was the large number of observations captured for each subject, we were able to detect trends between groups and across speeds with a large number of data points for each subject at each condition. However, we cannot rule out errors or detection failure on any effects or trends due to the sensitivity reduction. Finally, when interpreting the results within different contexts, it should be remembered that these observations were collected during treadmill running as opposed to overground running. This afforded the continuous collection, and the participants were required to be experienced with treadmill running. However, some of the runners may have exhibited different behavior in this different context (Nigg, De Boer, & Fisher, 1995).

5.6 Conclusion

Elite middle-distance runners exhibited distinct systemic spring-mass behavior across a wide spectrum of running speeds as compared to a group of competitive, yet sub-elite counterparts. We examined these global mechanical characteristics in an elite cohort of 1500m runners that included Olympians, National Champions, and NCAA All-Americans, and we compared the observations to those from a trained cohort that included 1500m runners who were regionally competitive NCAA and university club-level athletes. Despite the high ability and training status of both groups, the elite runners distinguished themselves across a number of spatiotemporal and spring-mass parameters, and those differences were further mediated across speeds. The elite group generally ran with longer flight phases and as stiffer systems, producing greater vertical forces and higher leg and vertical stiffnesses. Furthermore, their spatiotemporal patterns were less variable across speeds. These distinct systemic patterns and interactions across running speeds may be related to some combination of superior ability, training demands, or inherent physiological characteristics. The findings presented a profile of global mechanics in top-level middle distance runners, which may serve as a reference for future investigations or for coaches and athletes conducting performance assessments. Furthermore, it highlighted the importance of analyzing running mechanics both across and within a breadth of speeds for individuals.

Chapter 6 Collocation and Reflection

6.1 Summary

This body of work has broadened our collective understanding of the systemic mechanical behavior of runners and advanced the methodologies with which we can assess running mechanics. Using the canonical spring-mass model of running, these studies presented several new means to assess how runners run with respect to this template, and these assessments were applied to a variety of novel research questions to examine systemic performance behaviors in distinct populations and across conditions of runners. These investigations were coupled with traditional spring-mass analyses to broaden and generalize the findings. These methods and findings can be leveraged by researchers and practitioners across the sport to frame, design, contextualize, and analyze new experiments with this systemic perspective.

The overarching contribution of these aggregated studies is three-fold: (1) it provides the biomechanics field with novel, validated methods to model runners using a canonical template that captures system-level mechanical behaviors; (2) it exemplifies the efficacy and utility of these methods in gait analysis through application and extension of the model; and (3) it provides novel biomechanical insights into the spring-mass parameter differences across populations of runners and across conditions within runners.

6.1.1 Methodological Contributions

6.1.1.1 Nonlinear Regression for Spring-Mass Parameter Estimation

Within this body of work, there are several distinct methodological contributions. The first is the presentation and validation of a means to use nonlinear regression to estimate spring-mass parameters in runners using only kinetic recordings. This method used the full time series of the vertical ground reaction force to inform estimation of the four spring-mass parameters: leg stiffness, touchdown angle, leg length, and contact time. This method freed the estimates from their traditional constraints. The nonlinear regression spring-mass parameters provided stiffness estimates that were consistent with traditional methods, provided a leg length estimate that may be more representative of the center-of-mass location, and estimated an effective contact time that was more robust against the traditional biases during the final moments of propulsion.

6.1.1.2 The Parameterized Sinusoidal vGRF: A Functional Form of the Spring-Mass vGRF

The second contribution was the derivation of a functional form of a spring-mass vertical ground reaction force time-series based on SLIP dynamics and the sinusoidal approximation of Morin and colleagues (Morin et al., 2005). The parameterized sinusoidal vGRF (PS vGRF) used that sinusoidal approximation and was characterized by the four deterministic SLIP parameters (Equation 17). Despite the widespread use of this approximation for spring-mass calculations, it had never been systematically validated against the SLIP model that it approximates. The work presented here validated this sinusoidal approximation using SLIP simulations across sizes and speeds and demonstrated that NLR can further improve its ability to accurately model a SLIP system across a wide spectrum of speeds. This not only facilitated the future use of functional analytical tools with vGRF data such as nonlinear regression, but it also provided researchers with a form with which to explore parameter relations within the SLIP model. Equation 17 can inform sensitivities, trade-offs, and adjustments within SLIP dynamics without the numerical simulation that would otherwise be required.

6.1.1.3 Spring-Mass Similarity Metrics

The third contribution was the presentation of three new metrics to quantify a runner's similarity to an ideal spring-mass system. The horizontal-vertical force timing difference (HV TD) and the analogous time-normalized braking-to-propulsion and loading-to-unloading ratio (BP:LU) described the degree to which a runner was coordinating his/her horizontal and vertical forces, indicating the degree to which energetic fluctuations were occurring in phase. Observations were provided to show that elite Kenyan distance runners did this better than recreational runners for a given speed. Coupled with a recent finding that runners aligned the resultant vector of the horizontal and vertical GRF to their leg axis as their running economy improved (Moore et al., 2016), this may be a simple, yet informative analytical measure. As these two metrics require only force plate recordings, it may be an efficient means for researchers and clinicians to quantify this coordinative behavior in runners. The NLR-derived spring-mass fit (SM Fit) metric was also presented to describe the degree to which a runner's vGRF behaved like a best-fit spring-mass system. Of note, this approach quantitatively revealed the more similarly elastic characteristics of elite Kenyan runners and the reduced similarity in runners following an ultramarathon race. This metric followed the dynamics of a SLIP model, unlike linear vertical force-displacement analyses, and it again used only kinetic recordings as an input, as opposed to kinematic equipment and assumptions required for force-leg-length relations—thus, highlighting its experimental simplicity and informative capacity.

6.1.1.4 Demonstration of Mixed-Model Experimental Design for Spring-Mass Analyses

The fourth methodological contribution of the current series of studies was a demonstration of mixed-model experimental design with traditional spring-mass measures to more accurately characterize individualized mechanical running behavior. A repeated-measures random slope-intercept design was effective in capturing spring-mass dynamics more holistically within runners and better describing group characteristics. While these statistical methods themselves were not new, their application in biomechanical investigations have been limited, and as such, they have not been broadly leveraged in running investigations to assess global mechanical behavior. Furthermore, the spring-mass metrics used in the investigation were computationally simple and operationally easy to capture. The method and design, therefore, should have strong potential for extended application with field-based research and practice, which itself may inspire and facilitate further applied spring-mass modeling for researchers, coaches, clinicians, and runners.

6.1.2 Biomechanical Contributions

6.1.2.1 Systemic Assumptions

In tandem with the methodological contributions, this series of investigations revealed new insights into global dynamics and spring-mass behavior in runners. The first stemmed from the NLR modeling, where it was demonstrated that model-based estimations of system parameters deviated from traditional temporal and anthropometric assumptions. By following the trend of the vGRF time series, the NLR-modeled contact time for runners was 12 ms (6%) less than the observed time. Traditionally, observed contact times are subject to several sources of bias, such as the ankle dynamics (Maykranz & Seyfarth, 2014) or filtering methods (Tirosh & Sparrow, 2003). Thus, deviations from the global behavior in the final moments of stance have little bearing on systemic mechanical output but may bias traditional spring-mass measures that are sensitive to their values (Equations 6 – 8). Furthermore, NLR-estimated leg lengths were 4.3 cm (5%) longer than the measured values, indicating that the approximated center-of-mass during stance was more distal than traditionally assumed and closer to the static center-of-mass location (Clauser et al., 1969).

6.1.2.2 Elastic Similarity of Kenyan Runners

Chapter 3 employed three new spring-mass similarity metrics as well as a previously used metric to show that elite Kenyan distance runners behaved more like the simple SLIP model. This model is characterized by coordinated transfer of its kinetic and potential energies (Figure 2), and it is energetically conservative. This may therefore provide a new source of explanation for their ubiquitous dominance in distance running, and it supports future investigations into these metrics as barometers of mechanical efficiency. It was also observed that recreational runners improved their energetic coordination but decreased their systemic spring-mass fit when running barefoot, whereas the Kenyan runners were less affected. Again, this highlighted the discriminatory characteristics of these metrics, which may catalyze future investigation and application.

6.1.2.3 Spring-Mass Characteristics of Kenyan Runners

Chapter 3 also used traditional spring-mass measures and NLR-estimated spring-mass measures to characterize the systemic mechanical behavior of the elite Kenyan runners as compared to the lesser capable recreational cohort. The Kenyan runners exhibited similar spring-mass characteristics despite being of smaller stature, resulting in higher relative stiffnesses. This provided a global mechanical characterization for their running pattern and suggested a systemic strategy that may facilitate their performance capacities.

6.1.2.4 Fatigue-induced Changes in Spring-Mass Characteristics

Chapter 4 presented a systemic characterization of runners before and after a road ultramarathon. The runners maintained their absolute spring-mass behavior, but they became more dissimilar to the system. That is, they achieved the same mechanical outcome in a “noisier” fashion. This decrease in fit was likely due in part to an observed increase in vertical impact peaks, suggesting a potential decrement of mechanical control and response. Moreover, the findings highlighted the co-dependencies of traditional spring-mass parameters that may bias estimates. The contact times in the runners were observed to be slightly but significantly shorter after the race (2%), which manifested as slightly increased leg stiffnesses. However, the systemic NLR-based analysis did not detect a change in the effective contact times nor the leg stiffnesses. Again, this suggested that the absolute spring-mass behavior was maintained in the post-race state, but the spring-mass fit decrement and impact peak increase suggested a possible deterioration of their control strategy.

6.1.2.5 Global Spring-Mass Profiles of Elite Middle Distance Runners

Chapter 5 characterized the systemic mechanical behaviors of elite 1500m runners across 10 training and racing speeds. This was the first biomechanical investigation of elite-level middle distance runners across speeds. In it, they were compared against a cohort of highly trained, but non-elite 1500m runners. The elite runners ran as significantly stiffer mechanical systems with longer flight times across speeds and shorter contact times at slower speeds. The patterns of the elite runners were also less influenced by speed than in the non-elite group. Together, the findings suggested that they may better recycle elastic energy vertically, which may be energetically advantageous. Moreover, the patterns that they exhibited at faster speeds were more persistent at lower speeds. These findings may serve as sources of context against which future performance studies can be compared and as metrics to monitor for athletes and coaches.

6.1.2.6 Mechanical Variability Within Elite Middle Distance Runners

Chapter 5 also characterized the global mechanical variability in the elite 1500m runners across speeds. The elite runners demonstrated less variability in spatiotemporal measures than the non-elite runners but similar variation within their spring-mass behavior. This provides further mechanical evidence that expert performers exhibit less motor variability in task-specific outcome measures. It also suggested that the spring-mass behavior may be an emergent outcome that could be manipulated by traditional end-point variables, such as stride length and frequency, and may be characterized by constancy.

6.2 Future Directions

6.2.1 Nonlinear Regression Modeling Improvements

While this work presented and demonstrated several applications of the NLR method for spring-mass analyses, there remain many areas of improvement and refinement to be developed and refined with the approach. The first pertains to resolution of the tendency for covariance among the fixed effects, chiefly the leg-length and angle approximations. As discussed in Chapter 2 and Section 2.7, the relation of these two parameters within the PS vGRF is not singular. The random effect distributions partially resolve this within subjects, but it becomes problematic when parsing out the sources of variance for the fixed effects analysis. This was demonstrated in both Chapters 3 and 4, where the estimates for the length and angle had substantial standard errors and high covariances. In Chapter 4, the three-parameter model was employed, but the result yielded estimates that were then covaried with the stiffness estimate, further challenging the estimation. Future endeavors could seek to explore the application of this three-parameter model with the length-angle approximation from Section 2.7. Depending on the research question, it may be appropriate to simply drop these fixed effect terms all together, acknowledging the limitation of the equation's non-singularity around these two values and using the model to test stiffness and contact time hypotheses. However, there are still future opportunities to refine model specification and to explore additional alterations, such as scaling the parameters, employing weighted residuals, or manipulating the random-effects design matrices.

Another area of opportunity for exploration would be in a sensitivity analysis of its random-effect parameter estimations in humans. While the method demonstrated excellent ability to model SLIP simulations, it would be interesting to vary the parameters in humans in a known way and assess the sensitivity of the model to detect these changes. It is clear that it would detect contact time differences, and it demonstrated good agreement with traditional stiffness measurements. However, its accuracy and ability to detect length or angle adjustments in a runner is unknown. The model consistently fit longer legs to the subjects in Chapter 2, which supported the hypothesis of a more distal effective leg than commonly assumed, but it remains unknown how sensitive or how accurate this data-driven estimation is. In Chapter 3, a modeled leg length difference was not observed between the Kenyan and recreational runners despite a height difference. This would imply longer relative effective legs in the Kenyans. There is evidence to suggest that Kenyan distance runners tend to have longer limbs than European counterparts, and that it may be related to performance capacity (Mooses & Hackney, 2017). If accurate, this method is a promising tool to assess the effective dynamic leg length of a runner, which could subsequently be used to drive novel investigations into running performance and test hypotheses related to leg length and the cost of transport (Pontzer, 2007). As such, the ability of the model to sensitively and accurately assess that needs to be established before conclusions can be drawn from its outputs.

Finally, the model application could be improved with the use of nested random-effect designs. As currently implemented in MatLab (2019a), the nonlinear regression tools do not support nested random effects with the SAEM algorithm. In practice, this means that the number of random effects must be no less than the number of unique fixed effect grouping combinations. In Chapter 3, random effects were assigned to each individual step, and this may have contributed to the high degree of covariance among some of the parameters, as distinct lengths and angles were fit to each step. The ideal model would have had a random effect on each subject with the fixed effects nested. In Chapter 4, in attempt was made for a resolution, where the random effects were grouped to include one effect for each condition-leg combination, but it did not entirely resolve the issue. One possible resolution would be to hybridize the estimation process with the conventional mixed-model implementation. The conventional mixed-model algorithm was unable to converge with the PS vGRF, which necessitated using the more robust but less flexible SAEM algorithm. There may be an opportunity to realize a nested structure and potentially resolve some of the fixed-effect covariance issue by first using the SAEM algorithm to fit a robust starting estimate for the conventional algorithm.

6.2.2 Nonlinear Regression Modeling Opportunities

The NLR methodology itself presents an exciting framework to explore research questions related to systemic gait behavior. The approach is experimentally simple and flexible, as its only input is a vGRF time series recorded from a force plate. The mixed-model approach presented in Chapters 3 and 4 lends itself naturally to a broad spectrum of experimental designs. It can be used to further explore how each of these parameters vary between groups or within individuals. It could serve as a performance or health monitoring framework, with an individual characterizing his or her systemic mechanics and modeling new conditions or timepoints with a fixed effect (as demonstrated in Chapter 4). It could inform footwear choices and research, with the model being used to explore parameter adjustments in preferred or unfavorable shoes, which could then further be used to characterize mechanical relations to preference.

Moreover it could be a valuable tool to explore variability patterns within individuals. While much of this work has focused simply on the parameter estimations themselves, the assessment of the parameter variation may be a source of even greater insight. As discussed and explored in Chapter 5, variation among parameters may be indicative of varying levels of health and performance. NLR modeling of runners may be able to better explore the variability in their spring-mass parameters. For example, it may be warranted to ask: if a runner sees performance increase throughout a season, is there a corresponding change in his or her standard error on the stiffness estimate? If his or her steps are modeled as random effects, does their variance structure change for each parameter? What about periods of overreaching and overtraining? How do these parameter variabilities change? Could the model capture systemic changes related to injury? We saw in Chapter 4 that the fit of the model was indicative of greater impact peaks related to fatigue. It may yield further insights to capture more steps and investigate the specific spring-mass parameter variation patterns in that condition. The mixed-model framework is a powerful tool to facilitate and extend these systemic explorations.

The NLR method could also be used to study within-step dynamics. State-shift fixed effects could be employed to examine how system parameters adjust during loading and unloading. This would be similar to the shift modeled by Günther and Blickhan (Gunther & Blickhan, 2002), and it could reveal interesting insights into how the four parameters interact within a step. In a similar vein, it could also be used to model the spring-mass dynamics within Cavagna's "effective" ground contact of stance, which is the time in which the vGRF exceeds body weight (Cavagna, 2006). This may be a more sensitive and representative period of spring mass behavior, unbiased by early and late-stance deviations, and it could potentially provide more accurate spring-mass dynamic representations.

Finally, the NLR methodology may provide great utility in comparative biomechanics. As the spring-mass model is often used across the animal kingdom, the reduced assumptions and experimental overhead of this method may lend itself to non-human animal studies. In cases where measuring leg length or approximating angles in animals is spurious or in situations where kinematic capture is impracticable, this could provide a useful alternative to biomechanists, as it only requires a force plate. Simulation and model-experiment matching via optimization has been employed in avian runners (Birn-Jeffery et al., 2014). This methodology may be both operationally and computationally simpler with the further added value of its underlying statistical framework.

6.2.3 Elastic Similarity Measures

The elastic similarity metrics presented here could be of great value to clinicians and coaches. Each of the metrics was able to discriminate between the high-performance-capacity Kenyan runners and the lower-performance-capacity recreational runners and their distinct footwear conditions in Chapter 3, and the SM Fit proved discriminatory of race-induced fatigue in Chapter 4. The HV TD and BP:LU metrics could be of particular use, as they are computationally and operationally simple, requiring only a run over a force platform. These two metrics are indicative of a runner's energetic coordination, so the natural hypothesis to test would be if it is predicative of performance capacity. In our investigation, the groups were distinctly heterogenous between each other but quite homogenous within, preventing exploration of the patterns over a continuum of performances. Moore and her colleagues demonstrated that running economy improved as runners better aligned their leg axis to their horizontal and vertical GRF resultant vector (Moore et al., 2016). This captured a conceptually similar phenomenon but did not require kinematic equipment or its data processing. Furthermore, Legramandi and his colleagues observed a decline in the SB metric associated with age, suggesting a relation between spring-mass dissimilarity and the aging process (Legramandi et al., 2013). As described above, the NLR-derived SM fit metric was indicative of ultramarathon-induced fatigue. Together, this suite of spring-mass similarity measures may provide a comprehensive and informative analytical tool set to monitor health and performance as it relates to systemic gait behavior in runners.

6.2.4 Updates to Traditional Methods for Spring-Mass Analyses

The findings of this series of investigations can be used to provide updates to traditional spring-mass modeling methods and assumptions. For example, the leg-length modeling in Chapter 2 indicated that the effective spring leg length may be longer than the traditional hip-height approximation. This supported the use of the leg length correction factor proposed by Blum et al. (Blum et al., 2009). They used 1.05 for females and 1.10 for males, and work here suggested that 1.05 may be generally appropriate. Moreover, Chapters 2–4 demonstrated that the effective spring-mass contact time was shorter than the kinetic observation. This would also support the use of a correction factor of approximately 5-7% in the other direction. Finally, the length-angle approximation derived in Section 2.7 could provide more accurate touchdown and sweep angle approximations if flight time was to be incorporated. A comparison against simulations is warranted, but it would likely improve upon the underestimation of the traditional angle as approximated by Equation 8.

6.2.5 Field-based Studies of Spring-Mass Behavior

The experimental design and methods employed in Chapter 5 are readily extendable to field-based analyses for runners. The spring-mass metrics calculated there used Morin and his collegaues' "simple" method, requiring only the contact time, flight time, and speed for a runner (Morin et al., 2005). With the increasing availability and accuracy of accelerometer- and inertial-measurement unit-based gait-event detection and recording (Schutte et al., 2015), it is hoped that future studies will leverage this framework to characterize mechanical patterns in ecological settings. It was demonstrated that variabilities in stride length and frequency were related to expertise in the middle-distance runners. These measures can be recorded by common, commercially available sport watches via wrist accelerometry, and they have already been used to identify patterns in stride frequency variability within a race (Burns et al., 2019). These mixed-model designs could allow researchers and running enthusiasts alike to comprehensively characterize simple variability patterns across speeds and conditions in an operationally efficient research design.

6.2.6 Longitudinal Monitoring

Finally, these template-based approaches may yield their richest insights in longitudinal monitoring within runners. Given the highly individualized nature of the running gait – recall Fred Wilt's "fingerprint" likening (Wilt, 1959) – it is unlikely that there is any dogmatic characteristic of a spring-mass system that can be generalized as optimal for all. There may be trends, such as the stiffer systems observed in the elite middle distance runners, but the exact degree to which one moves in that direction is and likely will remain unknown. Chapter 5 demonstrated the nature by which these systemic parameters change within individuals within and across speeds. It is easy to assume that they will also systematically vary across days and across health and training statuses. Cavanagh and his colleagues recommended conducting repeated measures on elite runners for this very reason (Cavanagh et al., 1985). With a framework to assess global behaviors, these systemic changes can be brought into relief. Applying an NLR analysis, one could employ fixed effects for each time measure to test a parameter change hypothesis, or using the mixed-model approach, one could characterize the variance structures of simple measures across time. Approaching gait assessment with this framework can serve to help individuals better understand their own fingerprints.

6.3 Concluding Thoughts

In the aggregate, these integrated studies established and validated new methods with which to assess running gait and analyze it as a holistic, dynamic system. Using the canonical spring-mass template, an approach for system characterization via nonlinear regression was presented, and new metrics that compared the system-level dynamics of a runner against the template were presented. Finally, more comprehensive experimental designs were explored to more fully characterize the system-level behavior within runners. Along the way, each of the investigations explored traditional spring mass parameters in tandem, yielding new insights into the systemic mechanical patterns underlying competitive Kenyan runners, fatigued ultra-marathon runners, and elite middle distance runners. These template-based studies and mixed-model methods are distinct from the traditional approach of studying and manipulating individual factors in isolation and aggregating measures across observations that has traditionally characterized gait assessments. Shifting gait analysis away from component-level behaviors will drive a more function-based understanding of both pathology and health in running, and this shift may facilitate the design of programs and tools to mitigate injury and guide development. The NLR-based assessments and spring-mass methodologies explored in the current series of studies can be used to better characterize gait against a SLIP template. This enhanced systemic analysis brings the fundamental features of gait into relief and provides a unified framework to communicate and describe gait patterns. By formulating a means to assess gait with this template and demonstrating methods to apply it to population comparisons and within-subject studies of runners, a foundation has been laid to guide new efforts in gait research and to move towards fostering greater health and performance in runners.

In the aggregate, these investigations will add to our collective body of knowledge by providing researchers, clinicians, coaches, and athletes with methods and insights to better study and monitor an individual runner's system-level mechanical behavior. These methods and demonstrations may further promote template-based investigations and discussions, providing a framework and language to characterize global mechanical characteristics. The spring-mass, SLIP-based insights described and documented here can serve to broaden our understanding of these behaviors, to inspire new research questions, to advance the scientific exploration of those questions, and overarchingly, to facilitate more miles run.

…

Running is complex. Myriad mechanical, metabolic, and perhaps even metaphysical processes symphonically interact to produce its dynamic forward, monopodial, bouncing motion. Each individual across every species has a different suite of instruments to realize this common phenomenon, and each plays a slightly different tune. However, there are keys to which all adhere and melodies that are shared. The ultimate aim of this scholarly endeavor was to present means to better leverage those commonalities to assess the running motion.

Postface

"Is it possible, I wonder, to study a bird so closely, to observe and catalogue its peculiarities in such minute detail, that it becomes invisible? Is it possible that while fastidiously calibrating the span of its wings or the length of its tarsus, we somehow lose sight of its poetry? That in our pedestrian descriptions of marbled or vermiculated plumage we forfeit a glimpse of living canvases, cascades of carefully toned browns and golds that would shame Kandinsky, misty explosions of color to rival Monet? I believe that we do.

I believe that in approaching our subject with the sensibilities of statisticians and dissectionists, we distance ourselves increasingly from the marvelous and spell-binding planet of imagination whose gravity drew us to our studies in the first place.

This is not to say that we should cease to establish facts and to verify our information, but merely to suggest that unless those facts can be imbued with the flash of poetic insight then they remain dull gems; semi-precious stones scarcely worth the collecting"

…

A scientific understanding of the beautifully synchronized and articulated motion of an owl's individual feathers during flight does not impede a poetic appreciation of the same phenomenon. Rather, the two enhance each other, a more lyrical eye lending the cold data a romance from which it has long been divorced."

—Dr. Daniel Dreiberg, from Alan Moore's *Watchmen*, pp. 237-240 (Moore, Gibbons, & Higgins, 1987)

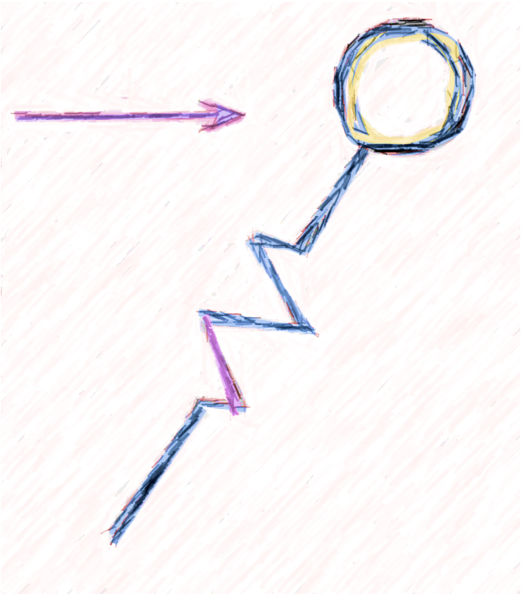

Bibliography

Aibast, H., Okutoyi, P., Sigei, T., Adero, W., Chemjor, D., Ongaro, N., . . . Pitsiladis, Y. (2017). Foot Structure and Function in Habitually Barefoot and Shod Adolescents in Kenya. *Current Sports Medicine Reports, 16*(6), 448-458.

Alexander, R. M. (1991a). Elastic mechanisms in primate locomotion. *Zeitschrift für Morphologie und Anthropologie, 78*(3), 315-320.

Alexander, R. M. (1991b). Energy-saving mechanisms in walking and running. *Journal of Experimental Biology, 160*, 55-69.

Alexander, R. M. (1995). Simple Models of Human Movement. *Applied Mechanics Reviews, 48*(8), 461-470.

Amar, J. (1916). Trottoir dynamographique. *Comptes Rendus de l'Académie des Sciences – Series I*(163), 130-132.

Anderson, T. (1996). Biomechanics and running economy. *Sports Med, 22*(2), 76-89.

Arampatzis, A., Brüggemann, G. P., & Metzler, V. (1999). The effect of speed on leg stiffness and joint kinetics in human running. *Journal of biomechanics, 32*(12), 1349-1353.

Bates, B. T., Osternig, L. R., Sawhill, J. A., & James, S. L. (1983). An assessment of subject variability, subject-shoe interaction, and the evaluation of running shoes using ground reaction force data. *Journal of biomechanics, 16*(3), 181-191.

Bates, D. M., & Watts, D. G. (1988). *Nonlinear Regression Analysis and Its Applications*.

Belli, A., Lacour, J. R., Komi, P. V., Candau, R., & Denis, C. (1995). Mechanical step variability during treadmill running. *European Journal of Applied Physiology and Occupational Physiology, 70*(6), 510-517.

Bencsik, L., & Zelei, A. (2017). Effects of human running cadence and experimental validation of the bouncing ball model. *Mechanical Systems and Signal Processing, 89*, 78-87.

Birn-Jeffery, A. V., Hubicki, C. M., Blum, Y., Renjewski, D., Hurst, J. W., & Daley, M. A. (2014). Don't break a leg: running birds from quail to ostrich prioritise leg safety and economy on uneven terrain. *Journal of Experimental Biology, 217*(Pt 21), 3786-3796.

Blickhan, R. (1989). The spring-mass model for running and hopping. *Journal of biomechanics, 22*(11-12), 1217-1227.

Blickhan, R., & Full, R. J. (1993). Similarity in Multilegged Locomotion - Bouncing Like a Monopode. *Journal of Comparative Physiology A. Neuroethology, Sensory, Neural, and Behavioral Physiology, 173*(5), 509-517.

Blum, Y., Lipfert, S. W., & Seyfarth, A. (2009). Effective leg stiffness in running. *Journal of biomechanics, 42*(14), 2400-2405.

Bobbert, M. F., Schamhardt, H. C., & Nigg, B. M. (1991). Calculation of vertical ground reaction force estimates during running from positional data. *Journal of biomechanics, 24*(12), 1095-1105.

Braun, W. A., & Dutto, D. J. (2003). The effects of a single bout of downhill running and ensuing delayed onset of muscle soreness on running economy performed 48 h later. *European Journal of Applied Physiology, 90*(1-2), 29-34.

Brughelli, M., & Cronin, J. (2008). A review of research on the mechanical stiffness in running and jumping: methodology and implications. *Scandinavian Journal of Medicine & Science in Sports, 18*(4), 417-426.

Bullimore, S. R., & Burn, J. F. (2006). Consequences of forward translation of the point of force application for the mechanics of running. *Journal of Theoretical Biology, 238*(1), 211-219.

Bullimore, S. R., & Burn, J. F. (2007). Ability of the planar spring-mass model to predict mechanical parameters in running humans. *Journal of Theoretical Biology, 248*(4), 686-695.

Burkett, L. N., Kohrt, W. M., & Buchbinder, R. (1985). Effects of shoes and foot orthotics on VO2 and selected frontal plane knee kinematics. *Medicine & Science in Sports & Exercise, 17*(1), 158-163.

Burns, G. T., Zendler, J. M., & Zernicke, R. F. (2019). Step frequency patterns of elite ultramarathon runners during a 100-km road race. *Journal of Applied Physiology, 126*(2), 462-468.

Candau, R., Belli, A., Millet, G. Y., Georges, D., Barbier, B., & Rouillon, J. D. (1998). Energy cost and running mechanics during a treadmill run to voluntary exhaustion in humans. *European Journal of Applied Physiology and Occupational Physiology, 77*(6), 479-485.

Carver, S. G., Cowan, N. J., & Guckenheimer, J. M. (2009). Lateral stability of the spring-mass hopper suggests a two-step control strategy for running. *Chaos, 19*(2), 026106.

Cavagna, G. A. (2006). The landing-take-off asymmetry in human running. *Journal of Experimental Biology, 209*(Pt 20), 4051-4060.

Cavagna, G. A. (2009). The two asymmetries of the bouncing step. *European Journal of Applied Physiology, 107*(6), 739-742.

Cavagna, G. A., Dusman, B., & Margaria, R. (1968). Positive work done by a previously stretched muscle. *Journal of Applied Physiology, 24*(1), 21-32.

Cavagna, G. A., Franzetti, P., Heglund, N. C., & Willems, P. (1988). The determinants of the step frequency in running, trotting and hopping in man and other vertebrates. *Journal of Physiology, 399*, 81-92.

Cavagna, G. A., Heglund, N. C., & Taylor, C. R. (1977). Mechanical work in terrestrial locomotion: two basic mechanisms for minimizing energy expenditure. *American Journal of Physiology, 233*(5), R243-261.

Cavagna, G. A., & Kaneko, M. (1977). Mechanical work and efficiency in level walking and running. *Journal of Physiology, 268*(2), 467--481.

Cavagna, G. A., & Legramandi, M. A. (2015). Running, hopping and trotting: tuning step frequency to the resonant frequency of the bouncing system favors larger animals. *Journal of Experimental Biology, 218*(Pt 20), 3276-3283.

Cavagna, G. A., Legramandi, M. A., & Peyre-Tartaruga, L. A. (2008a). The landing-take-off asymmetry of human running is enhanced in old age. *Journal of Experimental Biology, 211*(Pt 10), 1571-1578.

Cavagna, G. A., Legramandi, M. A., & Peyre-Tartaruga, L. A. (2008b). Old men running: mechanical work and elastic bounce. *Proceedings of the Royal Society B: Biological Sciences, 275*(1633), 411-418.

Cavagna, G. A., Saibene, F. P., & Margaria, R. (1964). Mechanical Work in Running. *Journal of Applied Physiology, 19*(2), 249-&.

Cavagna, G. A., Saibene, F. P., & Margaria, R. (1965). Effect of Negative Work on the Amount of Positive Work Performed by an Isolated Muscle. *Journal of Applied Physiology, 20*, 157-158.

Cavanagh, P. R., Andrew, G. C., Kram, R., Rodgers, M. M., Sanderson, D. J., & Hennig, E. M. (1985). An Approach to Biomechanical Profiling of Elite Distance Runners. *International Journal of Sport Biomechanics, 1*, 36-62.

Cavanagh, P. R., & Kram, R. (1989). Stride length in distance running: velocity, body dimensions, and added mass effects. *Medicine & Science in Sports & Exercise, 21*(4), 467-479.

Cavanagh, P. R., & Lafortune, M. A. (1980). Ground reaction forces in distance running. *Journal of biomechanics, 13*(5), 397-406.

Cavanagh, P. R., Pollock, M. L., & Landa, J. (1977). A biomechanical comparison of elite and good distance runners. *Annals of the New York Academy of Sciences, 301*, 328-345.

Chang, Y. H., & Kram, R. (1999). Metabolic cost of generating horizontal forces during human running. *Journal of Applied Physiology, 86*(5), 1657-1662.

Cheung, K., Hume, P., & Maxwell, L. (2003). Delayed onset muscle soreness : treatment strategies and performance factors. *Sports Medicine, 33*(2), 145-164.

Clark, K. P., Ryan, L. J., & Weyand, P. G. (2017). A general relationship links gait mechanics and running ground reaction forces. *Journal of Experimental Biology, 220*(Pt 2), 247-258.

Clauser, C. E., McConville, J. T., & Young, J. W. (1969). *Weight, volume, and center of mass of segments of the human body*. Retrieved from

Coleman, D. R., Cannavan, D., Horne, S., & Blazevich, A. J. (2012). Leg stiffness in human running: Comparison of estimates derived from previously published models to direct kinematic-kinetic measures. *Journal of biomechanics, 45*(11), 1987-1991.

Cross, R. (1999). Standing, walking, running, and jumping on a force plate. *American Journal of Physics, 67*(4), 304-309.

Crowell, H. P., & Davis, I. S. (2011). Gait retraining to reduce lower extremity loading in runners. *Clinical Biomechanics, 26*(1), 78-83.

da Rosa, R. G., Oliveira, H. B., Gomenuka, N. A., Masiero, M. P. B., da Silva, E. S., Zanardi, A. P. J., . . . Peyre-Tartaruga, L. A. (2019). Landing-Takeoff Asymmetries Applied to Running Mechanics: A New Perspective for Performance. *Frontiers in Physiology, 10*, 415.

Dalleau, G., Belli, A., Bourdin, M., & Lacour, J. R. (1998). The spring-mass model and the energy cost of treadmill running. *European Journal of Applied Physiology and Occupational Physiology, 77*(3), 257-263.

Daniels, J. (2014). *Daniels' Running Formula* (3rd ed.). Champaign, IL: Human Kinetics.

Daoud, A. I., Geissler, G. J., Wang, F., Saretsky, J., Daoud, Y. A., & Lieberman, D. E. (2012). Foot strike and injury rates in endurance runners: a retrospective study. *Medicine & Science in Sports & Exercise, 44*(7), 1325-1334.

Davis, I. S., Bowser, B. J., & Mullineaux, D. R. (2016). Greater vertical impact loading in female runners with medically diagnosed injuries: a prospective investigation. *British Journal of Sports Medicine, 50*(14), 887-892.

Davis, I. S., & Futrell, E. (2016). Gait Retraining: Altering the Fingerprint of Gait. *Physical Medicine and Rehabilitation Clinics of North America, 27*(1), 339-355.

de Ruiter, C. J., Verdijk, P. W., Werker, W., Zuidema, M. J., & de Haan, A. (2014). Stride frequency in relation to oxygen consumption in experienced and novice runners. *European Journal of Sport Science, 14*(3), 251-258.

Degache, F., Guex, K., Fourchet, F., Morin, J. B., Millet, G. P., Tomazin, K., & Millet, G. Y. (2013). Changes in running mechanics and spring-mass behaviour induced by a 5-hour hilly running bout. *Journal of Sports Sciences, 31*(3), 299-304.

Degache, F., Morin, J. B., Oehen, L., Guex, K., Giardini, G., Schena, F., . . . Millet, G. P. (2016). Running Mechanics During the World's Most Challenging Mountain Ultramarathon. *International Journal of Sports Physiology and Performance, 11*(5), 608-614.

Derrick, T. R., Dereu, D., & McLean, S. P. (2002). Impacts and kinematic adjustments during an exhaustive run. *Medicine & Science in Sports & Exercise, 34*(6), 998-1002.

Devita, P., & Bates, B. T. (1988). Intraday Reliability of Ground Reaction Force Data. *Human Movement Science, 7*(1), 73-85.

Dickinson, J. A., Cook, S. D., & Leinhardt, T. M. (1985). The Measurement of Shock-Waves Following Heel Strike While Running. *Journal of biomechanics, 18*(6), 415-422.

Dierks, T. A., Davis, I. S., & Hamill, J. (2010). The effects of running in an exerted state on lower extremity kinematics and joint timing. *Journal of biomechanics, 43*(15), 2993-2998.

Divert, C., Mornieux, G., Baur, H., Mayer, F., & Belli, A. (2005). Mechanical comparison of barefoot and shod running. *International Journal of Sports Medicine, 26*(7), 593-598.

Divert, C., Mornieux, G., Freychat, P., Baly, L., Mayer, F., & Belli, A. (2008). Barefoot-shod running differences: shoe or mass effect? *International Journal of Sports Medicine, 29*(6), 512-518.

Dos Santos, A. F., Nakagawa, T. H., Lessi, G. C., Luz, B. C., Matsuo, H. T. M., Nakashima, G. Y., . . . Serrao, F. V. (2019). Effects of three gait retraining techniques in runners with patellofemoral pain. *Physical Therapy in Sport, 36*, 92-100.

Dutto, D. J., & Smith, G. A. (2002). Changes in spring-mass characteristics during treadmill running to exhaustion. *Medicine & Science in Sports & Exercise, 34*(8), 1324-1331.

Edwards, W. B. (2018). Modeling Overuse Injuries in Sport as a Mechanical Fatigue Phenomenon. *Exercise and Sport Sciences Reviews, 46*(4), 224-231.

Farley, C. T., Glasheen, J., & McMahon, T. A. (1993). Running springs: speed and animal size. *Journal of Experimental Biology, 185*, 71-86.

Farley, C. T., & Gonzalez, O. (1996). Leg stiffness and stride frequency in human running. *Journal of biomechanics, 29*(2), 181-186.

Fenn, W. O. (1930a). Frictional and kinetic factors in the work of sprint running. *American Journal of Physiology, 92*(3), 583-611.

Fenn, W. O. (1930b). Work against gravity and work due to velocity changes in running: Movements of the center of gravity within the body and foot pressure on the ground. *American Journal of Physiology, 93*(2), 433-462.

Feodor Nielsen, S. (2000). The stochastic EM algorithm: estimation and asymptotic results. *Bernoulli, 6*(3), 457-489.

Ferber, R., Hreljac, A., & Kendall, K. D. (2009). Suspected mechanisms in the cause of overuse running injuries: a clinical review. *Sports Health, 1*(3), 242-246.

Ferber, R., Osis, S. T., Hicks, J. L., & Delp, S. L. (2016). Gait biomechanics in the era of data science. *Journal of biomechanics, 49*(16), 3759-3761.

Ferris, D. P., Louie, M., & Farley, C. T. (1998). Running in the real world: adjusting leg stiffness for different surfaces. *Proceedings of the Royal Society B: Biological Sciences, 265*(1400), 989-994.

Floria, P., Sanchez-Sixto, A., Ferber, R., & Harrison, A. J. (2018). Effects of running experience on coordination and its variability in runners. *Journal of Sports Sciences, 36*(3), 272-278.

Fokkema, T., Hartgens, F., Kluitenberg, B., Verhagen, E., Backx, F. J. G., van der Worp, H., . . . van Middelkoop, M. (2019). Reasons and predictors of discontinuation of running after a running program for novice runners. *Journal of Science and Medicine in Sport, 22*(1), 106-111.

Folland, J. P., Allen, S. J., Black, M. I., Handsaker, J. C., & Forrester, S. E. (2017). Running Technique is an Important Component of Running Economy and Performance. *Medicine & Science in Sports & Exercise, 49*(7), 1412-1423.

Fourchet, F., Girard, O., Kelly, L., Horobeanu, C., & Millet, G. P. (2015). Changes in leg spring behaviour, plantar loading and foot mobility magnitude induced by an exhaustive treadmill run in adolescent middle-distance runners. *Journal of Science and Medicine in Sport, 18*(2), 199-203.

Francis, P., Whatman, C., Sheerin, K., Hume, P., & Johnson, M. I. (2019). The Proportion of Lower Limb Running Injuries by Gender, Anatomical Location and Specific Pathology: A Systematic Review. *Journal of Science and Medicine in Sport, 18*(1), 21-31.

Friesenbichler, B., Stirling, L. M., Federolf, P., & Nigg, B. M. (2011). Tissue vibration in prolonged running. *Journal of biomechanics, 44*(1), 116-120.

Fukuchi, R. K., Fukuchi, C. A., & Duarte, M. (2017). A public dataset of running biomechanics and the effects of running speed on lower extremity kinematics and kinetics. *PeerJ, 5*, e3298.

Full, R. J., Farley, C. T., & Winters, J. M. (2000). Musculoskeletal dynamics in rhythmic systems: a comparative approach to legged locomotion. In *Biomechanics and Neural Control of Posture and Movement* (pp. 192-205): Springer.

Full, R. J., & Koditschek, D. E. (1999). Templates and anchors: neuromechanical hypotheses of legged locomotion on land. *Journal of Experimental Biology, 202*(Pt 23), 3325-3332.

Garcia-Pinillos, F., Garcia-Ramos, A., Ramirez-Campillo, R., Latorre-Roman, P. A., & Roche-Seruendo, L. E. (2019). How Do Spatiotemporal Parameters and Lower-Body Stiffness Change with Increased Running Velocity? A Comparison Between Novice and Elite Level Runners. *Journal of Human Kinetics, 70*(1), 25-38.

Gerlach, K. E., White, S. C., Burton, H. W., Dorn, J. M., Leddy, J. J., & Horvath, P. J. (2005). Kinetic changes with fatigue and relationship to injury in female runners. *Medicine & Science in Sports & Exercise, 37*(4), 657-663.

Geyer, H., Seyfarth, A., & Blickhan, R. (2005). Spring-mass running: simple approximate solution and application to gait stability. *Journal of Theoretical Biology, 232*(3), 315-328.

Giandolini, M., Gimenez, P., Temesi, J., Arnal, P. J., Martin, V., Rupp, T., . . . Millet, G. Y. (2016). Effect of the Fatigue Induced by a 110-km Ultramarathon on Tibial Impact Acceleration and Lower Leg Kinematics. *PLoS One, 11*(3), e0151687.

Giovanelli, N., Taboga, P., & Lazzer, S. (2017). Changes in Running Mechanics During a 6-Hour Running Race. *International Journal of Sports Physiology and Performance, 12*(5), 642-647.

Girard, O., Micallef, J. P., & Millet, G. P. (2011). Changes in spring-mass model characteristics during repeated running sprints. *European Journal of Applied Physiology, 111*(1), 125-134.

Grimston, S. K., & Zernicke, R. F. (1993). Exercise-Related Stress Responses in Bone. *Journal of Applied Biomechanics, 9*(1), 2-14.

Gunther, M., & Blickhan, R. (2002). Joint stiffness of the ankle and the knee in running. *Journal of biomechanics, 35*(11), 1459-1474.

Hafer, J. F., Freedman Silvernail, J., Hillstrom, H. J., & Boyer, K. A. (2016). Changes in coordination and its variability with an increase in running cadence. *Journal of Sports Sciences, 34*(15), 1388-1395.

Hamill, J., Palmer, C., & Van Emmerik, R. E. (2012). Coordinative variability and overuse injury. *Sports Medicine Arthroscopy Rehabilitation Therapy & Technology, 4*(1), 45.

Hamill, J., van Emmerik, R. E., Heiderscheit, B. C., & Li, L. (1999). A dynamical systems approach to lower extremity running injuries. *Clinical Biomechanics, 14*(5), 297-308.

Hanley, B., Stellingwerff, T., & Hettinga, F. J. (2019). Successful Pacing Profiles of Olympic and IAAF World Championship Middle-Distance Runners Across Qualifying Rounds and Finals. *International Journal of Sports Physiology and Performance, 14*(7), 894-901.

Hayes, P. R., & Caplan, N. (2014). Leg stiffness decreases during a run to exhaustion at the speed at VO2max. *European Journal of Sport Science, 14*(6), 556-562.

He, J. P., Kram, R., & McMahon, T. A. (1991). Mechanics of running under simulated low gravity. *Journal of Applied Physiology, 71*(3), 863-870.

Hecksteden, A., Skorski, S., Schwindling, S., Hammes, D., Pfeiffer, M., Kellmann, M., . . . Meyer, T. (2016). Blood-Borne Markers of Fatigue in Competitive Athletes - Results from Simulated Training Camps. *PLoS One, 11*(2).

Heiderscheit, B. C. (2011). Gait retraining for runners: in search of the ideal. *Journal of Orthopaedic & Sports Physical Therapy, 41*(12), 909-910.

Heise, G. D., & Martin, P. E. (1998). "Leg spring" characteristics and the aerobic demand of running. *Medicine & Science in Sports & Exercise, 30*(5), 750-754.

Hespanhol Junior, L. C., Pillay, J. D., van Mechelen, W., & Verhagen, E. (2015). Meta-Analyses of the Effects of Habitual Running on Indices of Health in Physically Inactive Adults. *Sports Medicine, 45*(10), 1455-1468.

Hiley, M. J., Zuevsky, V. V., & Yeadon, M. R. (2013). Is skilled technique characterized by high or low variability? An analysis of high bar giant circles. *Human Movement Science, 32*(1), 171-180.

Hough, J., Corney, R., Kouris, A., & Gleeson, M. (2013). Salivary cortisol and testosterone responses to high-intensity cycling before and after an 11-day intensified training period. *Journal of Sports Sciences, 31*(14), 1614-1623.

Hreljac, A. (2004). Impact and overuse injuries in runners. *Medicine & Science in Sports & Exercise, 36*(5), 845-849.

Hulme, A., Nielsen, R. O., Timpka, T., Verhagen, E., & Finch, C. (2017). Risk and Protective Factors for Middle- and Long-Distance Running-Related Injury. *Sports Medicine, 47*(5), 869-886.

Hunter, I. (2003). A new approach to modeling vertical stiffness in heel-toe distance runners. *Journal of Sports Science and Medicine, 2*(4), 139-143.

Hunter, I., & Smith, G. A. (2007). Preferred and optimal stride frequency, stiffness and economy: changes with fatigue during a 1-h high-intensity run. *European Journal of Applied Physiology, 100*(6), 653-661.

Ingle, S. (2018, October 1, 2018). How Parkrun's 13 became five million and changed weekends for ever. Retrieved from https://www.theguardian.com/sport/blog/2018/oct/01/parkrun-five-mlllion-runners

Jordan, K., Challis, J. H., & Newell, K. M. (2006). Long range correlations in the stride interval of running. *Gait & Posture, 24*(1), 120-125.

Julian, R., Meyer, T., Fullagar, H. H. K., Skorski, S., Pfeiffer, M., Kellmann, M., . . . Hecksteden, A. (2017). Individual Patterns in Blood-Borne Indicators of Fatigue-Trait or Chance. *Journal of Strength and Conditioning Research, 31*(3), 608-619.

Kenneally, M., Casado, A., & Santos-Concejero, J. (2018). The Effect of Periodization and Training Intensity Distribution on Middle- and Long-Distance Running Performance: A Systematic Review. *International Journal of Sports Physiology and Performance, 13*(9), 1114-1121.

Kim, W., Voloshin, A. S., & Johnson, S. H. (1994). Modeling of Heel Strike Transients during Running. *Human Movement Science, 13*(2), 221-244.

Kingma, I., Toussaint, H. M., Commissaris, D. A., Hoozemans, M. J., & Ober, M. J. (1995). Optimizing the determination of the body center of mass. *Journal of biomechanics, 28*(9), 1137-1142.

Kong, P. W., & de Heer, H. (2008). Anthropometric, gait and strength characteristics of kenyan distance runners. *Journal of Sports Science and Medicine, 7*(4), 499-504.

Kunimasa, Y., Sano, K., Oda, T., Nicol, C., Komi, P. V., Locatelli, E., . . . Ishikawa, M. (2014). Specific muscle-tendon architecture in elite Kenyan distance runners. *Scandinavian Journal of Medicine & Science in Sports, 24*(4), e269-274.

Lacour, J. R., & Bourdin, M. (2015). Factors affecting the energy cost of level running at submaximal speed. *European Journal of Applied Physiology, 115*(4), 651-673.

Lafond, D., Duarte, M., & Prince, F. (2004). Comparison of three methods to estimate the center of mass during balance assessment. *Journal of biomechanics, 37*(9), 1421-1426.

Lamberts, R. P., Lemmink, K. A., Durandt, J. J., & Lambert, M. I. (2004). Variation in heart rate during submaximal exercise: implications for monitoring training. *Journal of Strength and Conditioning Research, 18*(3), 641-645.

Lamberts, R. P., Maskell, S., Borresen, J., & Lambert, M. I. (2011). Adapting workload improves the measurement of heart rate recovery. *International Journal of Sports Medicine, 32*(9), 698-702.

Lamberts, R. P., Swart, J., Noakes, T. D., & Lambert, M. I. (2011). A novel submaximal cycle test to monitor fatigue and predict cycling performance. *British Journal of Sports Medicine, 45*(10), 797-804.

Larsen, H. B., Christensen, D. L., Nolan, T., & Sondergaard, H. (2004). Body dimensions, exercise capacity and physical activity level of adolescent Nandi boys in western Kenya. *Annals of Human Biology, 31*(2), 159-173.

Lavie, C. J., Lee, D. C., Sui, X., Arena, R., O'Keefe, J. H., Church, T. S., . . . Blair, S. N. (2015). Effects of Running on Chronic Diseases and Cardiovascular and All-Cause Mortality. *Mayo Clinic Proceedings, 90*(11), 1541-1552.

Lazzer, S., Salvadego, D., Taboga, P., Rejc, E., Giovanelli, N., & di Prampero, P. E. (2015). Effects of the Etna uphill ultramarathon on energy cost and mechanics of running. *International Journal of Sports Physiology and Performance, 10*(2), 238-247.

Lazzer, S., Taboga, P., Salvadego, D., Rejc, E., Simunic, B., Narici, M. V., . . . di Prampero, P. E. (2014). Factors affecting metabolic cost of transport during a multi-stage running race. *Journal of Experimental Biology, 217*(Pt 5), 787-795.

Lee, D. C., Brellenthin, A. G., Thompson, P. D., Sui, X., Lee, I. M., & Lavie, C. J. (2017). Running as a Key Lifestyle Medicine for Longevity. *Progress in Cardiovascular Diseases, 60*(1), 45-55.

Lee, M., Song, C., Lee, K., Shin, D., & Shin, S. (2014). Agreement between the spatio-temporal gait parameters from treadmill-based photoelectric cell and the instrumented treadmill system in healthy young adults and stroke patients. *Medical Science Monitor, 20.*

Legramandi, M. A., Schepens, B., & Cavagna, G. A. (2013). Running humans attain optimal elastic bounce in their teens. *Scientific Reports, 3*, 1310.

Leskinen, A., Hakkinen, K., Virmavirta, M., Isolehto, J., & Kyrolainen, H. (2009). Comparison of running kinematics between elite and national-standard 1500-m runners. *Sports Biomechanics, 8*(1), 1-9.

Lieberman, D. E., Castillo, E. R., Otarola-Castillo, E., Sang, M. K., Sigei, T. K., Ojiambo, R., . . . Pitsiladis, Y. (2015). Variation in Foot Strike Patterns among Habitually Barefoot and Shod Runners in Kenya. *PLoS One, 10*(7), e0131354.

Lieberman, D. E., Venkadesan, M., Werbel, W. A., Daoud, A. I., D'Andrea, S., Davis, I. S., . . . Pitsiladis, Y. (2010). Foot strike patterns and collision forces in habitually barefoot versus shod runners. *Nature, 463*(7280), 531-535.

Lipfert, S. W., Gunther, M., Renjewski, D., Grimmer, S., & Seyfarth, A. (2012). A model-experiment comparison of system dynamics for human walking and running. *Journal of Theoretical Biology, 292*, 11-17.

Liu, W., & Nigg, B. M. (2000). A mechanical model to determine the influence of masses and mass distribution on the impact force during running. *Journal of biomechanics, 33*(2), 219-224.

Lopes, A. D., Hespanhol Junior, L. C., Yeung, S. S., & Costa, L. O. (2012). What are the main running-related musculoskeletal injuries? A Systematic Review. *Sports Medicine, 42*(10), 891-905.

Ludwig, C., Grimmer, S., Seyfarth, A., & Maus, H. M. (2012). Multiple-step model-experiment matching allows precise definition of dynamical leg parameters in human running. *Journal of biomechanics, 45*(14), 2472-2475.

Lussiana, T., Patoz, A., Gindre, C., Mourot, L., & Hebert-Losier, K. (2019). The implications of time on the ground on running economy: less is not always better. *Journal of Experimental Biology, 222*(Pt 6).

Malisoux, L., Delattre, N., Urhausen, A., & Theisen, D. (2017). Shoe cushioning, body mass and running biomechanics as risk factors for running injury: a study protocol for a randomised controlled trial. *BMJ Open, 7*(8), e017379.

Mann, T. N., Platt, C. E., Lamberts, R. P., & Lambert, M. I. (2015). Faster Heart Rate Recovery with Increased Rpe: Paradoxical Responses after an 87-Km Ultramarathon. *Journal of Strength and Conditioning Research, 29*(12), 3343-3352.

Maus, H. M., Revzen, S., Guckenheimer, J., Ludwig, C., Reger, J., & Seyfarth, A. (2015). Constructing predictive models of human running. *Journal of The Royal Society Interface, 12*(103).

Maus, H. M., Seyfarth, A., & Grimmer, S. (2011). Combining forces and kinematics for calculating consistent centre of mass trajectories. *Journal of Experimental Biology, 214*(21), 3511-3517.

Maykranz, D., & Seyfarth, A. (2014). Compliant ankle function results in landing-take off asymmetry in legged locomotion. *Journal of Theoretical Biology, 349*, 44-49.

McMahon, T. A., & Cheng, G. C. (1990). The mechanics of running: how does stiffness couple with speed? *Journal of biomechanics, 23 Suppl 1*, 65-78.

McMahon, T. A., Valiant, G., & Frederick, E. C. (1987). Groucho running. *Journal of Applied Physiology, 62*(6), 2326-2337.

Millet, G. P., & Millet, G. Y. (2012). Ultramarathon is an outstanding model for the study of adaptive responses to extreme load and stress. *BMC Medicine, 10*, 77.

Millet, G. Y., Morin, J. B., Degache, F., Edouard, P., Feasson, L., Verney, J., & Oullion, R. (2009). Running from Paris to Beijing: biomechanical and physiological consequences. *European Journal of Applied Physiology, 107*(6), 731-738.

Milner, C. E., Ferber, R., Pollard, C. D., Hamill, J., & Davis, I. S. (2006). Biomechanical factors associated with tibial stress fracture in female runners. *Medicine & Science in Sports & Exercise, 38*(2), 323-328.

Mizrahi, J., Verbitsky, O., Isakov, E., & Daily, D. (2000). Effect of fatigue on leg kinematics and impact acceleration in long distance running. *Human Movement Science, 19*(2), 139-151.

Moore, A., Gibbons, D., & Higgins, J. (1987). *Watchmen*. New York: DC Comics, Inc.

Moore, I. S. (2016). Is There an Economical Running Technique? A Review of Modifiable Biomechanical Factors Affecting Running Economy. *Sports Medicine, 46*(6), 793-807.

Moore, I. S., Jones, A. M., & Dixon, S. J. (2012). Mechanisms for improved running economy in beginner runners. *Medicine & Science in Sports & Exercise, 44*(9), 1756-1763.

Moore, I. S., Jones, A. M., & Dixon, S. J. (2016). Reduced oxygen cost of running is related to alignment of the resultant GRF and leg axis vector: A pilot study. *Scandinavian Journal of Medicine & Science in Sports, 26*(7), 809-815.

Mooses, M., & Hackney, A. C. (2017). Anthropometrics and Body Composition in East African Runners: Potential Impact on Performance. *International Journal of Sports Physiology and Performance, 12*(4), 422-430.

Mooses, M., Mooses, K., Haile, D. W., Durussel, J., Kaasik, P., & Pitsiladis, Y. P. (2015). Dissociation between running economy and running performance in elite Kenyan distance runners. *Journal of Sports Sciences, 33*(2), 136-144.

Morgan, W. P., Brown, D. R., Raglin, J. S., O'Connor, P. J., & Ellickson, K. A. (1987). Psychological monitoring of overtraining and staleness. *British Journal of Sports Medicine, 21*(3), 107-114.

Morin, J. B., Dalleau, G., Kyrolainen, H., Jeannin, T., & Belli, A. (2005). A simple method for measuring stiffness during running. *Journal of Applied Biomechanics, 21*(2), 167-180.

Morin, J. B., Jeannin, T., Chevallier, B., & Belli, A. (2006). Spring-mass model characteristics during sprint running: correlation with performance and fatigue-induced changes. *International Journal of Sports Medicine, 27*(2), 158-165.

Morin, J. B., & Samozino, P. (2018). *Biomechanics of Training and Testing*: Springer.

Morin, J. B., Samozino, P., & Millet, G. Y. (2011). Changes in running kinematics, kinetics, and spring-mass behavior over a 24-h run. *Medicine & Science in Sports & Exercise, 43*(5), 829-836.

Morin, J. B., Tomazin, K., Edouard, P., & Millet, G. Y. (2011). Changes in running mechanics and spring-mass behavior induced by a mountain ultra-marathon race. *Journal of biomechanics, 44*(6), 1104-1107.

Morin, J. B., Tomazin, K., Samozino, P., Edouard, P., & Millet, G. Y. (2012). High-intensity sprint fatigue does not alter constant-submaximal velocity running mechanics and spring-mass behavior. *European Journal of Applied Physiology, 112*(4), 1419-1428.

Mousavi, S. H., Hijmans, J. M., Rajabi, R., Diercks, R., Zwerver, J., & van der Worp, H. (2019). Kinematic risk factors for lower limb tendinopathy in distance runners: A systematic review and meta-analysis. *Gait & Posture, 69*, 13-24.

Muybridge, E. (1887). *Animal Locomotion : an electro-photographic investigation of consecutive phases of animal movements, 1872-1885*. Philadelphia: University of Pennsylvania.

Mytton, G. J., Archer, D. T., Turner, L., Skorski, S., Renfree, A., Thompson, K. G., & Gibson, A. S. (2015). Increased Variability of Lap Speeds: Differentiating Medalists and Nonmedalists in Middle-Distance Running and Swimming Events. *International Journal of Sports Physiology and Performance, 10*(3), 369-373.

Naga, S. (2005). An Efficient Algorithm for Clinical Mass Center Location of Human Body.

Nakayama, Y., Kudo, K., & Ohtsuki, T. (2010). Variability and fluctuation in running gait cycle of trained runners and non-runners. *Gait & Posture, 31*(3), 331-335.

Napier, C., Cochrane, C. K., Taunton, J. E., & Hunt, M. A. (2015). Gait modifications to change lower extremity gait biomechanics in runners: a systematic review. *British Journal of Sports Medicine, 49*(21), 1382-1388.

Napier, C., MacLean, C. L., Maurer, J., Taunton, J. E., & Hunt, M. A. (2019). Real-Time Biofeedback of Performance to Reduce Braking Forces Associated With Running-Related Injury: An Exploratory Study. *Journal of Orthopedic and sports Physical Therapy, 49*(3), 136-144.

Nigg, B. M. (1997). Impact forces in running. *Current Opinion in Orthopaedics, 8*(6), 43-47.

Nigg, B. M., Baltich, J., Hoerzer, S., & Enders, H. (2015). Running shoes and running injuries: mythbusting and a proposal for two new paradigms: 'preferred movement path' and 'comfort filter'. *British Journal of Sports Medicine, 49*(20), 1290-1294.

Nigg, B. M., De Boer, R. W., & Fisher, V. (1995). A kinematic comparison of overground and treadmill running. *Medicine & Science in Sports & Exercise, 27*(1), 98-105.

Nikooyan, A. A., & Zadpoor, A. A. (2011). Mass-spring-damper modelling of the human body to study running and hopping--an overview. *Proceedings of the Institution of Mechanical Engineers, Part H: Journal of Engineering in Medicine, 225*(12), 1121-1135.

Nilsson, J., & Thorstensson, A. (1989). Ground reaction forces at different speeds of human walking and running. *Acta Physiologica Scandinavica, 136*(2), 217-227.

Noakes, T. (2003). *Lore of Running* (4th ed.). Champaign, IL: Human Kinetics.

Noehren, B., Scholz, J., & Davis, I. (2011). The effect of real-time gait retraining on hip kinematics, pain and function in subjects with patellofemoral pain syndrome. *British Journal of Sports Medicine, 45*(9), 691-696.

Novacheck, T. F. (1998). The biomechanics of running. *Gait & Posture, 7*(1), 77-95.

Nummela, A., Keranen, T., & Mikkelsson, L. O. (2007). Factors related to top running speed and economy. *International Journal of Sports Medicine, 28*(8), 655-661.

O'Connor, P. J., Morgan, W. P., Raglin, J. S., Barksdale, C. M., & Kalin, N. H. (1989). Mood state and salivary cortisol levels following overtraining in female swimmers. *Psychoneuroendocrinology, 14*(4), 303-310.

Oja, P., Titze, S., Kokko, S., Kujala, U. M., Heinonen, A., Kelly, P., . . . Foster, C. (2015). Health benefits of different sport disciplines for adults: systematic review of observational and intervention studies with meta-analysis. *British Journal of Sports Medicine, 49*(7), 434-440.

Otter, R. T., Brink, M. S., Lamberts, R. P., & Lemmink, K. A. (2015). A New Submaximal Rowing Test to Predict 2,000-m Rowing Ergometer Performance. *Journal of Strength and Conditioning Research, 29*(9), 2426-2433.

Outdoor Foundation. (2018). *Outdoor Participation Report 2018*. Retrieved from Online: https://outdoorindustry.org/resource/2018-outdoor-participation-report/

Padulo, J., Annino, G., Migliaccio, G. M., D'Ottavio, S., & Tihanyi, J. (2012). Kinematics of Running at Different Slopes and Speeds. *Journal of Strength and Conditioning Research, 26*(5), 1331-1339.

Pontzer, H. (2007). Effective limb length and the scaling of locomotor cost in terrestrial animals. *Journal of Experimental Biology, 210*(Pt 10), 1752-1761.

Preatoni, E., Hamill, J., Harrison, A. J., Hayes, K., Van Emmerik, R. E., Wilson, C., & Rodano, R. (2013). Movement variability and skills monitoring in sports. *Sports Biomechanics, 12*(2), 69-92.

Preatoni, E., La Torre, A., Santambrogio, G. C., & Rodano, R. (2010). Motion analysis in sports monitoring techniques: assessment protocols and application to racewalking. *Medicina Dello Sport, 63*(3), 327-342.

Rabita, G., Slawinski, J., Girard, O., Bignet, F., & Hausswirth, C. (2011). Spring-mass behavior during exhaustive run at constant velocity in elite triathletes. *Medicine & Science in Sports & Exercise, 43*(4), 685-692.

Robertson, G. E., Caldwell, G. E., Hamill, J., Kamen, G., & Whittlesey, S. (2018). *Research Methods in Biomechanics*: Human kinetics.

Robilliard, J. J., & Wilson, A. M. (2005). Prediction of kinetics and kinematics of running animals using an analytical approximation to the planar spring-mass system. *Journal of Experimental Biology, 208*(Pt 23), 4377-4389.

Robson-Ansley, P. J., Gleeson, M., & Ansley, L. (2009). Fatigue management in the preparation of Olympic athletes. *Journal of Sports Sciences, 27*(13), 1409-1420.

Rogers, S. A., Whatman, C. S., Pearson, S. N., & Kilding, A. E. (2017). Assessments of Mechanical Stiffness and Relationships to Performance Determinants in Middle-Distance Runners. *International Journal of Sports Physiology and Performance, 12*(10), 1329-1334.

Roper, J. L., Harding, E. M., Doerfler, D., Dexter, J. G., Kravitz, L., Dufek, J. S., & Mermier, C. M. (2016). The effects of gait retraining in runners with patellofemoral pain: A randomized trial. *Clinical Biomechanics, 35*, 14-22.

Runner. (1962). National Film Board of Canada.

Running USA. (2017). *2017 National Runner Survey*. Retrieved from Online: https://cdn.trustedpartner.com/docs/library/RunningUSA2012/RunningUSA_NRS_2017.pdf

Rushall, B. S. (1990). A tool for measuring stress tolerance in elite athletes. *Journal of Applied Sport Psychology, 2*(1), 51-66.

Saini, M., Kerrigan, D. C., Thirunarayan, M. A., & Duff-Raffaele, M. (1998). The vertical displacement of the center of mass during walking: a comparison of four measurement methods. *Journal of Biomechanical Engineering, 120*(1), 133-139.

Sandford, G. (2018). *Applications of the Anaerobic Speed Reserve to Elite 800m Running.* Auckland University of Technology,

Sandford, G. N., Day, B. T., & Rogers, S. A. (2019). Racing Fast and Slow: Defining the Tactical Behavior That Differentiates Medalists in Elite Men's 1,500 m Championship Racing. *Frontiers in Sports and Active Living, 1*(43).

Sandford, G. N., & Stellingwerff, T. (2019). “Question Your Categories”: the Misunderstood Complexity of Middle-Distance Running Profiles With Implications for Research Methods and Application. *Frontiers in Sports and Active Living, 1*(28).

Sano, K., Ishikawa, M., Nobue, A., Danno, Y., Akiyama, M., Oda, T., . . . Komi, P. V. (2013a). Muscle-tendon interaction and EMG profiles of world class endurance runners during hopping. *European Journal of Applied Physiology, 113*(6), 1395-1403.

Sano, K., Ishikawa, M., Nobue, A., Danno, Y., Akiyama, M., Oda, T., . . . Komi, P. V. (2013b). Muscle-tendon interaction and EMG profiles of world class endurance runners during hopping. *European Journal of Applied Physiology, 113*(6), 1395-1403.

Sano, K., Nicol, C., Akiyama, M., Kunimasa, Y., Oda, T., Ito, A., . . . Ishikawa, M. (2015). Can measures of muscle-tendon interaction improve our understanding of the superiority of Kenyan endurance runners? *European Journal of Applied Physiology, 115*(4), 849-859.

Santos-Concejero, J., Olivan, J., Mate-Munoz, J. L., Muniesa, C., Montil, M., Tucker, R., & Lucia, A. (2015). Gait-cycle characteristics and running economy in elite Eritrean and European runners. *International Journal of Sports Physiology and Performance, 10*(3), 381-387.

Santos-Concejero, J., Tam, N., Coetzee, D. R., Olivan, J., Noakes, T. D., & Tucker, R. (2017). Are gait characteristics and ground reaction forces related to energy cost of running in elite Kenyan runners? *Journal of Sports Sciences, 35*(6), 531-538.

Saragiotto, B. T., Yamato, T. P., Hespanhol Junior, L. C., Rainbow, M. J., Davis, I. S., & Lopes, A. D. (2014). What are the main risk factors for running-related injuries? *Sports Medicine, 44*(8), 1153-1163.

Saragiotto, B. T., Yamato, T. P., & Lopes, A. D. (2014). What do recreational runners think about risk factors for running injuries? A descriptive study of their beliefs and opinions. *Journal of Orthopaedic & Sports Physical Therapy, 44*(10), 733-738.

Sargent, R. M. (1926). The relation between oxygen requirement and speed in running. *Proceedings of the Royal Society B: Biological Sciences, 100*(700), 10-22.

Saunders, P. U., Pyne, D. B., Telford, R. D., & Hawley, J. A. (2004). Factors affecting running economy in trained distance runners. *Sports Med, 34*(7), 465-485.

Scheerder, J., & Breedveld, K. (2015). *Running across Europe : the rise and size of one of the largest sport markets*. New York: Palgrave Macmillan.

Schmitt, L., Regnard, J., Desmarets, M., Mauny, F., Mourot, L., Fouillot, J. P., . . . Millet, G. (2013). Fatigue shifts and scatters heart rate variability in elite endurance athletes. *PLoS One, 8*(8), e71588.

Schultz, G., & Mombaur, K. (2010). Modeling and Optimal Control of Human-Like Running. *IEEE/ASME Transactions on Mechatronics, 15*(5), 783-792.

Schutte, K. H., Maas, E. A., Exadaktylos, V., Berckmans, D., Venter, R. E., & Vanwanseele, B. (2015). Wireless Tri-Axial Trunk Accelerometry Detects Deviations in Dynamic Center of Mass Motion Due to Running-Induced Fatigue. *PLoS One, 10*(10), e0141957.

Schwind, W. J., & Koditschek, D. E. (2000). Approximating the stance map of a 2-DOF monoped runner. *Journal of Nonlinear Science, 10*(5), 533-568.

Seipel, J., & Holmes, P. (2007). A simple model for clock-actuated legged locomotion. *Regular & Chaotic Dynamics, 12*(5), 502-520.

Seipel, J. E., & Holmes, P. (2005). Running in three dimensions: Analysis of a point-mass sprung-leg model. *International Journal of Robotics Research, 24*(8), 657-674.

Serpell, B. G., Ball, N. B., Scarvell, J. M., & Smith, P. N. (2012). A review of models of vertical, leg, and knee stiffness in adults for running, jumping or hopping tasks. *Journal of Sports Sciences, 30*(13), 1347-1363.

Seyfarth, A., Geyer, H., Gunther, M., & Blickhan, R. (2002). A movement criterion for running. *Journal of biomechanics, 35*(5), 649-655.

Seyfarth, A., Geyer, H., & Herr, H. (2003). Swing-leg retraction: a simple control model for stable running. *Journal of Experimental Biology, 206*(Pt 15), 2547-2555.

Siegl, A., E, M. K., Tam, N., Koschnick, S., Langerak, N. G., Skorski, S., . . . Lamberts, R. P. (2017). Submaximal Markers of Fatigue and Overreaching; Implications for Monitoring Athletes. *International Journal of Sports Medicine, 38*(9), 675-682.

Slawinski, J., Demarle, A., Koralsztein, J. P., & Billat, V. (2001). Effect of supra-lactate threshold training on the relationship between mechanical stride descriptors and aerobic energy cost in trained runners. *Archives of Physiology and Biochemistry, 109*(2), 110-116.

Slawinski, J., Heubert, R., Quievre, J., Billat, V., & Hanon, C. (2008). Changes in spring-mass model parameters and energy cost during track running to exhaustion. *Journal of Strength and Conditioning Research, 22*(3), 930-936.

Slawinski, J. S., & Billat, V. L. (2004). Difference in mechanical and energy cost between highly, well, and nontrained runners. *Medicine & Science in Sports & Exercise, 36*(8), 1440-1446.

Spiriev, B., & Spiriev, A. (2017). *IAAF scoring tables of athletics*: International Association of Athletics Federations.

Srinivasan, M., & Ruina, A. (2006). Computer optimization of a minimal biped model discovers walking and running. *Nature, 439*(7072), 72-75.

Svedenhag, J., & Sjodin, B. (1994). Body-mass-modified running economy and step length in elite male middle- and long-distance runners. *International Journal of Sports Medicine, 15*(6), 305-310.

Tam, N., Astephen Wilson, J. L., Coetzee, D. R., van Pletsen, L., & Tucker, R. (2016). Loading rate increases during barefoot running in habitually shod runners: Individual responses to an unfamiliar condition. *Gait & Posture, 46*, 47-52.

Taylor, M. J., & Beneke, R. (2012). Spring mass characteristics of the fastest men on Earth. *International Journal of Sports Medicine, 33*(8), 667-670.

Tirosh, O., & Sparrow, W. A. T. (2003). Identifying heel contact and toe-off using forceplate thresholds with a range of digital-filter cutoff frequencies. *Journal of Applied Biomechanics, 19*(2), 178-184.

Trowell, D., Phillips, E., Saunders, P., & Bonacci, J. (2019). The relationship between performance and biomechanics in middle-distance runners. *Sports Biomechanics*.

Tucker, R., Onywera, V. O., & Santos-Concejero, J. (2015). Analysis of the Kenyan distance-running phenomenon. *International Journal of Sports Physiology and Performance, 10*(3), 285-291.

Van Belle, G. (2011). *Statistical rules of thumb* (Vol. 699): John Wiley & Sons.

van der Worp, H., Vrielink, J. W., & Bredeweg, S. W. (2016). Do runners who suffer injuries have higher vertical ground reaction forces than those who remain injury-free? A systematic review and meta-analysis. *British Journal of Sports Medicine, 50*(8), 450-457.

van der Worp, M. P., ten Haaf, D. S., van Cingel, R., de Wijer, A., Nijhuis-van der Sanden, M. W., & Staal, J. B. (2015). Injuries in runners; a systematic review on risk factors and sex differences. *PLoS One, 10*(2), e0114937.

van Gent, R. N., Siem, D., van Middelkoop, M., van Os, A. G., Bierma-Zeinstra, S. M., & Koes, B. W. (2007). Incidence and determinants of lower extremity running injuries in long distance runners: a systematic review. *British Journal of Sports Medicine, 41*(8), 469-480; discussion 480.

Verbitsky, O., Mizrahi, J., Voloshin, A., Treiger, J., & Isakov, E. (1998). Shock Transmission and Fatigue in Human Running. *Journal of Applied Biomechanics, 14*(3), 300-311.

Weyand, P. G., Sternlight, D. B., Bellizzi, M. J., & Wright, S. (2000). Faster top running speeds are achieved with greater ground forces not more rapid leg movements. *Journal of Applied Physiology, 89*(5), 1991-1999.

Williams, K. R., & Cavanagh, P. R. (1986). Biomechanical correlates with running economy in elite distance runners. *Proceedings of the North American Congress on Biomechanics, 2*, 287-288.

Williams, K. R., & Cavanagh, P. R. (1987). Relationship between distance running mechanics, running economy, and performance. *Journal of Applied Physiology, 63*(3), 1236-1245.

Williams, K. R., Cavanagh, P. R., & Ziff, J. L. (1987). Biomechanical studies of elite female distance runners. *International Journal of Sports Medicine, 8*, 107-118.

Williams, K. R., Snow, R., & Agruss, C. (1991). Changes in Distance Running Kinematics with Fatigue. *International Journal of Sport Biomechanics, 7*(2), 138-162.

Williams, P. T. (2012). Non-exchangeability of running vs. other exercise in their association with adiposity, and its implications for public health recommendations. *PLoS One, 7*(7), e36360.

Willy, R. W., Buchenic, L., Rogacki, K., Ackerman, J., Schmidt, A., & Willson, J. D. (2016). In-field gait retraining and mobile monitoring to address running biomechanics associated with tibial stress fracture. *Scandinavian Journal of Medicine & Science in Sports, 26*(2), 197-205.

Willy, R. W., Scholz, J. P., & Davis, I. S. (2012). Mirror gait retraining for the treatment of patellofemoral pain in female runners. *Clinical Biomechanics, 27*(10), 1045-1051.

Wilson, C., Simpson, S. E., van Emmerik, R. E., & Hamill, J. (2008). Coordination variability and skill development in expert triple jumpers. *Sports Biomechanics, 7*(1), 2-9.

Wilt, F. (1959). *How they train: Half mile to six mile*. Los Altos, CA: Track & Field News.

Winter, D. A. (1979). *Biomechanics of human movement*. New York: Wiley.

Winter, D. A. (1984). Kinematic and Kinetic Patterns in Human Gait - Variability and Compensating Effects. *Human Movement Science, 3*(1-2), 51-76.

Winter, D. A. (2005). *Biomechanics and motor control of human movement* (3rd ed.). Hoboken, N.J.: John Wiley & Sons.

Zadpoor, A. A., & Nikooyan, A. A. (2011). The relationship between lower-extremity stress fractures and the ground reaction force: a systematic review. *Clinical Biomechanics, 26*(1), 23-28.

Zadpoor, A. A., & Nikooyan, A. A. (2012). The effects of lower extremity muscle fatigue on the vertical ground reaction force: a meta-analysis. *Proceedings of the Institution of Mechanical Engineers, Part H: Journal of Engineering in Medicine, 226*(8), 579-588.